THE UNIVERSITY OF MICHIGAN

INDUSTRY PROGRAM OF THE COLLEGE OF ENGINEERING

TRANSIENT HEAT TRANSFER TO A LAMINAR TUBE FLOW OF A BINGHAM PLASTIC WITH INTERNAL ENERGY GENERATION

Carl D. Henning

A dissertation submitted in partial fulfillment
of the requirements for the degree of
Doctor of Philosophy in the
University of Michigan
Department of Mechanical Engineering
1965

July, 1965

IP-713

ACKNOWLEDGEMENTS

The author wishes to express his appreciation to all those individuals who aided in the completion of this investigation. The following are especially acknowledged:

Professor W. J. Yang, Chairman of Doctoral Committee, for his guidance throughout the course of the investigation. His criticism and suggestions were most helpful, and his encouragement aided greatly in the completion of the work.

Professor J. A. Clark for his interest and pertinent advice. Professor H. Merte, R. B. Keller, and F. G. Hammitt, members of the Doctoral Committee, for their assistance, interest, and cooperation throughout the entire work.

The Michigan Memorial Phoenix Project for providing financial aid.

The Department of Mechanical Engineering for providing funds for the experimental investigation.

The Computing Center, Dr. R. C. F. Bartels, Director, for providing computer time.

The Industry Program of the College of Engineering for aid in the preparation of the manuscript.

Finally, my wife for her sacrifices and understanding.

TABLE OF CONTENTS

TABLE OF CONTENTS CONT'D

LIST OF TABLES

LIST OF FIGURES

LIST OF FIGURES CONT'D

LIST OF FIGURES CONT'D

NOMENCLATURE

a	Bingham plastic constant defined in Equation (3.2)
A	Coefficient of $\mathrm{Sin}\,\Gamma\theta$ in the periodic part of the dimensionless temperature in the fluid
A_y	Area, as defined locally in Appendix B; A_{out}, area through which heat flows out of an element; A_{in}, area through which heat flows into an element; A_w, area of an element in the wall; A_f, area of an element in the fluid; ft^2.
AR	Amplitude ratio; $AR_f = \sqrt{A^2 + B^2}/\epsilon\psi_{sf}$; $AR_w = \sqrt{C^2 + D^2}/\epsilon\psi_{sw}$ dimensionless
B	Coefficient of $\mathrm{Cos}\,\Gamma\theta$ in the periodic part of the dimensionless temperature in the fluid
C	Coefficient of $\mathrm{Sin}\,\Gamma\theta$ in the periodic part of the dimensionless temperature in the wall
C_f	Fluid specific heat, BTU/lbm-^oF
C_w	Wall specific heat, BTU/lbm-^oF
D	Coefficient of $\mathrm{Cos}\,\Gamma\theta$ in the periodic part of the dimensionless temperature in the wall
d	Diameter of bob in Brookfield UL Adapter, cm
D_i	Inside tube diameter, ft
E	Test section voltage, volts
f	Friction factor, $h_f/(\frac{L}{Di}\,\frac{u_m^{*2}}{2g})$, dimensionless
g	Local acceleration of gravity, ft/sec^2
Gr	Grashof number, $\rho^2 g\beta_T\lvert T-T_\infty\rvert L^3/\mu^2$, dimensionless
h_f	Fluid velocity head, ft of water
I	Test section current, amperes
k	Thermal conductivity; k_f, fluid; k_l, liquid; k_s, solid; k_w, wall; k_{wire}, thermocouple wire

L_e	Hydrodynamic entrance length, ft
l	Length of bob in Brookfield UL Adapter, cm
N	Rotational speed, rev/min
n"	Slope of logarithmic plot of torque versus rotational speed, N, dimensionless
p	Pressure, lbf/ft^2
Pr	Prandtl number, $\mu C_f/k_f$, dimensionless
q"	Volumetric heat generation rate, BTU/ft^3-hr
q_o	Mean volumetric heat generation rate, BTU/ft^3-hr
$\dot{q}$	Surface heat flux, BTU/ft^2-hr
Q	Fluid flow rate, ft^3/sec
Q"	Dimensionless energy generation term defined following Equation (3.6)
R	A specific radius; R_f, radius of a specific point in the fluid; R_i, inside tube radius; R_o, outside tube radius; R_w, radius of a specific point in the wall; R_{wire}, radius of thermocouple wire, ft
Re	Reynolds number, $\frac{\rho u^* D_i}{\mu}$, dimensionless
r	Dimensionless radius, r^*/R_i
r*	Radius, ft
r_y	Radius at which yielding takes place in a Bingham plastic, ft
s	Ratio of bob to cylinder diameter of Brookfield UL Adapter
S_g	Specific gravity
T	Temperature; T_f, fluid temperature; T_i, initial temperature; T_o, entrance temperature; T_w, wall temperature; T_{mm}, mixed mean temperature, ^oF
t	Time, sec
u	Dimensionless fluid velocity, $u^*/2u^*_m$
u*	Fluid velocity, defined in Equation (3.3); u^*_m, average fluid velocity; u^*_{max} maximum fluid velocity; ft/sec

x	Dimensionless axial distance
x^*	Axial distance, ft
y	Dummy variable, dimensionless
z	Dummy variable, dimensionless
α_f	Fluid thermal diffusivity, ft^2/hr
α_w	Wall thermal diffusivity, ft^2/hr
β	Dimensionless parameter, $\rho_f C_f/\rho_w C_w$
β_T	Temperature coefficient of volume expansion, $1/^oF$
Γ	Dimensionless frequency, $\omega Ri^2/\alpha_f$
δ	Dimensionless wall thickness, $\frac{Ro}{Ri} - 1$
ϵ	Dimensionless maximum periodic heat generation amplitude, defined in Equation (A-1)
η	Volume fraction of solids in a suspension
θ	Dimensionless time, $t\,\alpha_f/Ri^2$
Λ	Dimensionless parameter, α_w/α_f
μ	Fluid viscosity lbm/ft-sec
μ_B	Bingham plastic viscosity, lbm/ft-sec
ξ	Dimensionless temperature $(T-T_i)/(T_o-T_i)$
π	3.14
ρ_f	Fluid density, lbm/ft^3
ρ_w	Wall density, lbm/ft^3
τ	Shear stress, τ_y, yield shear stress of Bingham plastic; τ_w, shear stress at wall, lb_f/ft^2
ϕ	Phase lag of temperature with respect to the heat generation function; ϕ_f, phase lag of the periodic dimensionless temperature in the fluid; ϕ_w, phase lag of the periodic dimensionless temperature in the wall; radians
ϕ_e	Potential function, ft^2/hr

ψ	Dimensionless temperature $\frac{(T-T_o)K_f}{q_o\ Ri^2}$
ψ_f	Dimensionless fluid temperature
ψ_{mm}	Dimensionless mixed mean temperature
ψ_w	Dimensionless wall temperature
ψ_{Pf}	Periodic part of ψ_f
ψ_{Pw}	Periodic part of ψ_w
ψ_{sf}	Steady part of ψ_f
ψ_{sw}	Steady part of ψ_w
ω	Frequency, radians/sec

CHAPTER I

INTRODUCTION

Interest in heat transfer to slurries has been stimulated by the increasing emergence of non-Newtonian fluids as important raw materials and products in a large variety of industrial processes. With the advent of the homogeneous nuclear reactor employing the suspensions of uranium oxide or thorium oxide in heavy or light water as a reactor fuel, there has been research activity in steady heat transfer to slurries with internal heat generation. Slurries containing high concentrations of oxide tend to behave as Bingham plastics. Since the velocity at which the transition from laminar to turbulent flow occurs is rather high and erosion and corrosion become serious problems at high velocity in a typical slurry[1], heat transfer to Bingham plastics in laminar flow is studied, despite the advantage of the high heat transfer coefficients realized in turbulent flow.

Poppendiek[2] has studied the fully-developed heat transfer both in laminar and turbulent flows of a Newtonian fluid through circular pipes with internal heat generation. Analytical solutions are given for the temperatures of liquid metals and ordinary fluids. Fluid temperature measurements, which are obtained in an experimental system with electrically generated internal heat sources, are compared with predicted values. Grigull[3] has analyzed the fully-developed laminar heat transfer to non-Newtonian fluids flowing through a circular tube. Sparrow and Siegel[4] have made an analysis to determine heat transfer

characteristics for the laminar flow of a heat generating fluid in a circular tube with heat transfer. Internal heat generation is permitted to vary in an arbitrary manner both longitudinally along the tube and radially across the section, and longitudinal variations in wall heat transfer are present. Tachibana and Morishita[5] have experimentally investigated heat transfer in a slurry (consisting of distilled water and alumina) flowing through a circular tube. The experimental data was correlated by an equation similar to Dittus-Boelter's equation for Newtonian fluids. Schechter and Wissler[1] have extended the work of Sparrow and Siegel to include Bingham plastics, but only the case of an insulated wall has been treated. Michiyoshi, et al.[6,7] have further extended Schechter and Wissler's analysis to the case in which the tube wall is subjected to a heat flux. Solutions are given for both the entrance region and the fully-developed region. Ayers[8] has investigated the transient heat transfer from the wall with timewisely sinusoidal internal heat generation to the laminar flow of a Newtonian fluid in a circular tube. The asymptotic solutions are obtained by means of numerical computations.

While steady heat transfer problems in slurries with internal heat generation have been fairly well treated, less is known about its transient behavior. This work investigates heat transfer to a laminar tube flow of a Bingham plastic with transient internal heat generation and inlet temperature. The nature of the disturbances is step and sinusoidal, with respect to time. An approximate solution is obtained by numerical methods using a set of finite difference equations derived

from the energy equations for the fluid and the wall. Both the fluid and the wall temperatures are functions of radial and axial distances as well as time. The experimental work includes the measurement of velocity and temperature distributions. The experimental results are in good agreement with theoretical predictions. The heat exchangers to which this analysis apply include the homogeneous nuclear reactor and a chemical reactor in which an exothermic reaction occurs.

CHAPTER II

BINGHAM-PLASTIC FLUIDS

Real fluids may be divided into two main classes: Newtonian and non-Newtonian fluids. According to Newton's law of viscosity a plot of shear-stress versus shear-rate for a given fluid is a straight line through the origin: i.e., the viscosity is a constant at a given temperature and pressure. Non-Newtonian fluids are those in which the viscosity at a given temperature and pressure is a function of the shear-rate. This classification includes quite a few industrially important materials such as colloidal suspensions.

Non-Newtonian fluids may be further classified according to the variation of the viscosity with the rate of shear. The shear-stress-shear-rate diagram is presented in Figure 1 for various non-Newtonian fluids. The Bingham plastic, or ideal plastic, has a linear relationship between shear-stress and rate of shear, once it has been deformed. The relation may be written as

$$\tau = \tau_y - \mu_B \frac{du^*}{dr^*} \tag{2.1}$$

where τ_y is the yield stress, the amount of shearing stress the Bingham plastic can withstand before deformation. The so called "real plastic" has a constant viscosity at fairly high shear rate. The flow of a pseudoplastic may be described as shear-thinning and that of a dilatant as shear-thickening.

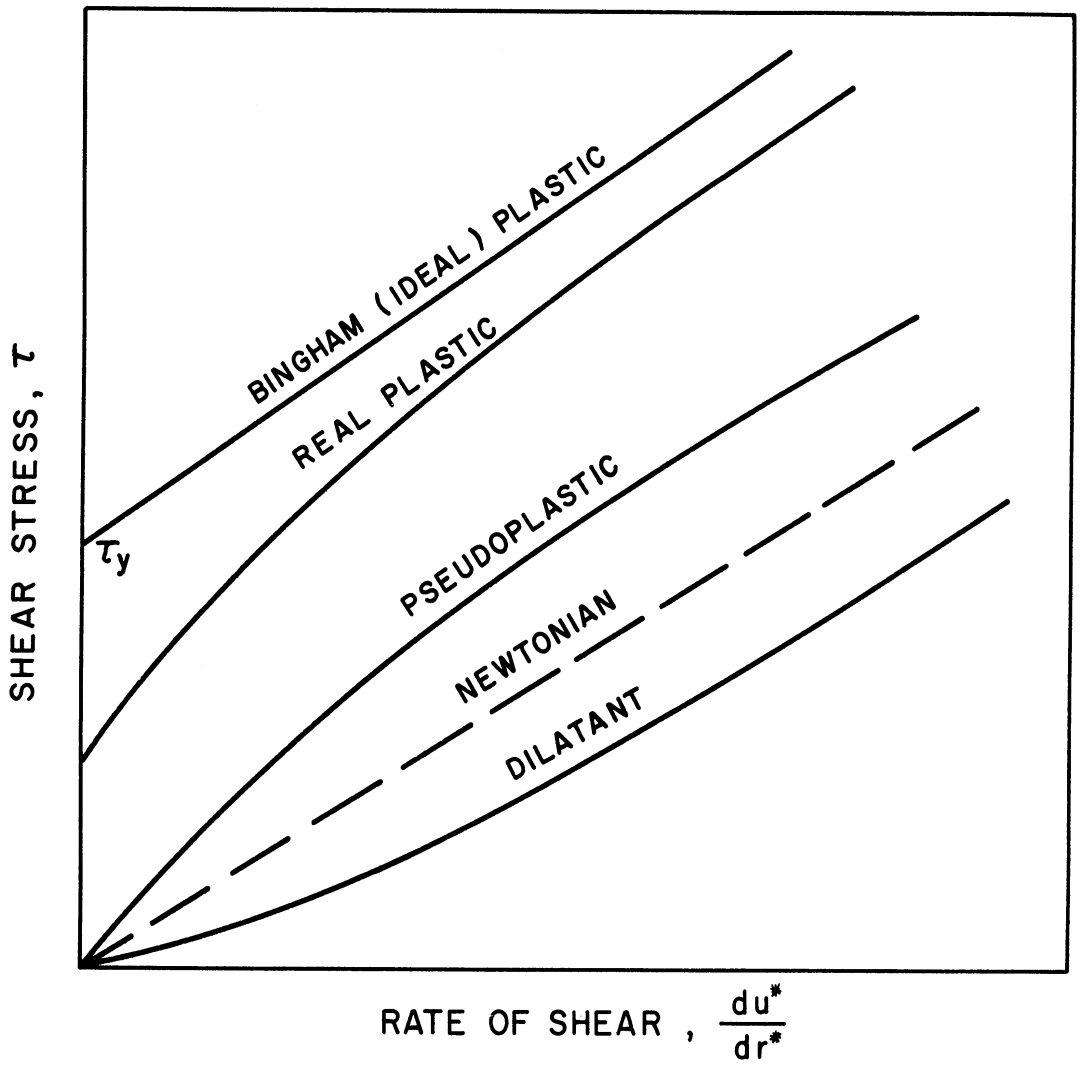

Figure 1. Various Non-Newtonian Fluids.

Colloidal slurries of solids in liquids have been found to be non-Newtonian by many investigators[19]. Through surface-attractive forces the finely divided particles dispersed in the liquid are able to exert a strong influence on the mechanical properties of the material as a whole, when the particles are sufficiently small or sufficiently close together. In aqueous slurries of uranium oxide and thorium oxide this colloidal behavior gives rise to a definite yield stress below which the fluid will not deform[28]. Thus, the Bingham plastic model has been used to describe its rheological behavior.

Experiments[25] show that for an aqueous slurry of UO_2

$$\tau_y = K_1 \eta^4 \qquad \mu_B = \mu e^{K_2 \eta}$$

and for ThO_2

$$\tau_y = K_3 \eta^3 \qquad \mu_B = \mu e^{K_4 \eta}$$

where η = volume fraction of solids in the suspension

μ = viscosity of water

K_1, K_2, K_3, K_4 = experimental constants which depend upon partical size.

For a 1.4 micron particle size of UO_2 or ThO_2

$K_1 = 150$ lb/ft^2 $\qquad K_2 = 1.8$

$K_3 = 60$ lb/ft^3 $\qquad K_4 = 0.8$

Sufficiently small solid particles will diffuse throughout the liquid due to their Brownian motion in a normal gravity field, and such dispersions are referred to as sols. For example, in aqueous solutions the ThO_2 particles in a sol are less than 0.05 microns, while particles whose specific gravity is near unity may be as large as 0.5 microns[25].

When small particles coalesce to form loose, relatively independent clusters of particles, they are referred to as flocs and may exhibit increased settling rates (although flocs of ThO_2 have hindered settling rates 10-50 times those expected for unflocculated slurries[28]). Either suspensions of flocs or particles which are large enough to settle are referred to as slurries and often exhibit colloidal properties[25].

The thermodynamically stable condition of lyophobic sols is a flocculated state, but electrostatic forces produced by ions which collect on the surface of the particles cause mutual replusion, inhibiting the formation of flocs and reducing settling rates. Flocs also can acquire an electrostatic charge which results in hindered settling[28]. This effect may be intensified by the addition of an electrolyte to the slurry as suggested by the reduced yield stresses in a ThO_2 slurry due to the addition of oxalic acid[29].

For a given liquid and solid phase the two most important variables which affect settling rates and fluid yield stress are concentration and particle size. Tests indicate that the settling rate decreases exponentially with increasing concentration[25] and yield stress is inversely proportional to the particle size[28]. Either increased concentration or decreased particle size will result in both reduced settling rates and higher yield stresses.

CHAPTER III

ANALYSIS

The physical system to be studied consists of an insulated horizontal tube through which a Bingham-plastic flows steadily with internal heat generation (see Figure 2). Heat generated in the fluid is uniform spatially but may vary in either a step-wise or sinusoidal manner with respect to time. Temperatures in both the fluid and wall are considered to be functions of radial distance, axial distance, and time. Since the steady solution has already been obtained by Michiyoshi, et al.[7] for both prescribed uniform wall heat flux and uniform wall temperature, and insulated outer tube wall is considered in the model. Due to the linearity in the differential equations of the system, the principle of super-position may be applied to obtain the solutions for the system with more complicated boundary conditions such as a specified wall heat flux.

Since the Bingham plastic has a yield stress "τ_y", the fully-developed laminar velocity distribution will exhibit a "plug" in the center in which the velocity will be a constant. If the radius of the plug is r_y

$$\frac{\tau}{\tau_w} = \frac{r^*}{R_i} \qquad \left(R_i \geq r^* \geq r_y \right) \tag{3.1}$$

and

$$\frac{\tau_y}{\tau_w} = \frac{r_y}{R_i} = a \tag{3.2}$$

Then Equations (2.1) and (3.2) yield the velocity distribution. For

$$0 \leq \frac{r^*}{Ri} \leq a$$

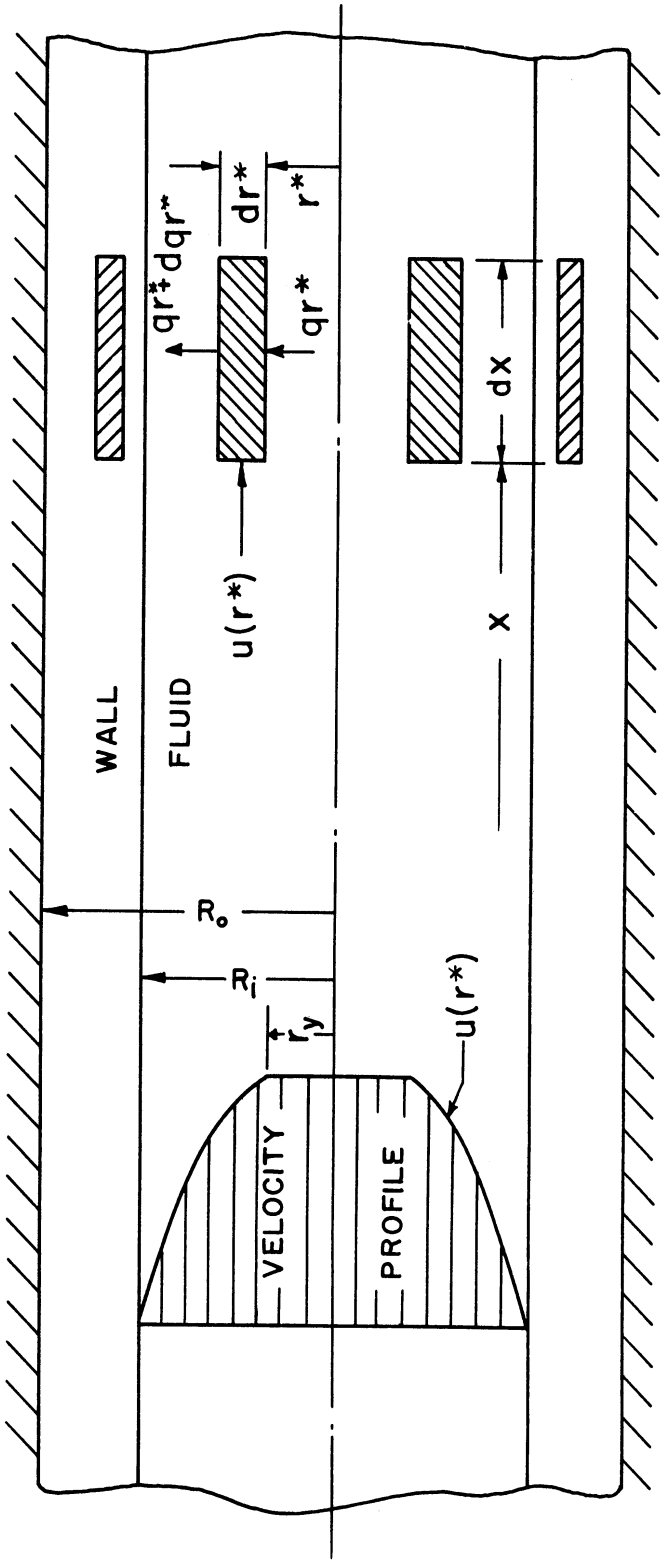

Figure 2. Physical Model Showing Velocity Distribution and Elements in the Fluid and Tube Wall.

$$u^*(r^*) = \frac{R_i \tau_y}{\mu_B} \frac{(1-a)^2}{2a} \qquad (3.3a)$$

and for $a \leq \frac{r^*}{Ri} \leq 1$

$$u^*(r^*) = \frac{R_i \tau_y}{\mu_B} \frac{1 - 2a + 2a\frac{r^*}{Ri} - \left(\frac{r^*}{Ri}\right)^2}{2a} \qquad (3.3b)$$

The velocity profiles are illustrated graphically in Figure 3 for several values of 'a'. Also, by defining the mean velocity to be

$$u_m^* = \frac{1}{\pi R_i^2} \int_0^{R_i} u^*(r^*)\, 2\pi r^*\, dr^*$$

and applying Equation (3.3), one finds

$$u_m^* = \frac{R_i \tau_y}{\mu_B} \frac{a^4 - 4a + 3}{12a} \qquad (3.4)$$

In the formulation of the problem the following assumptions are made:

a) The fluid is a Bingham plastic and flows in an incompressible, fully-developed, laminar, steady manner. This assumption is valid if an entrance length of the order $L_e \geq 0.035\ D\ Re$ is allowed,[20] $Re < 2300$, and there is no time variation of the axial pressure gradient in the fluid.

b) Axial conduction of heat in the fluid and wall are negligible. When the Peclet number (Re Pr), which represents the ratio of energy transport by enthalpy flux to that by heat conduction, is greater than 100 this assumption is valid.[24]

c) The physical properties of the fluid and wall are independent of temperature. Fluid viscosity, however, is known to be quite sensitive

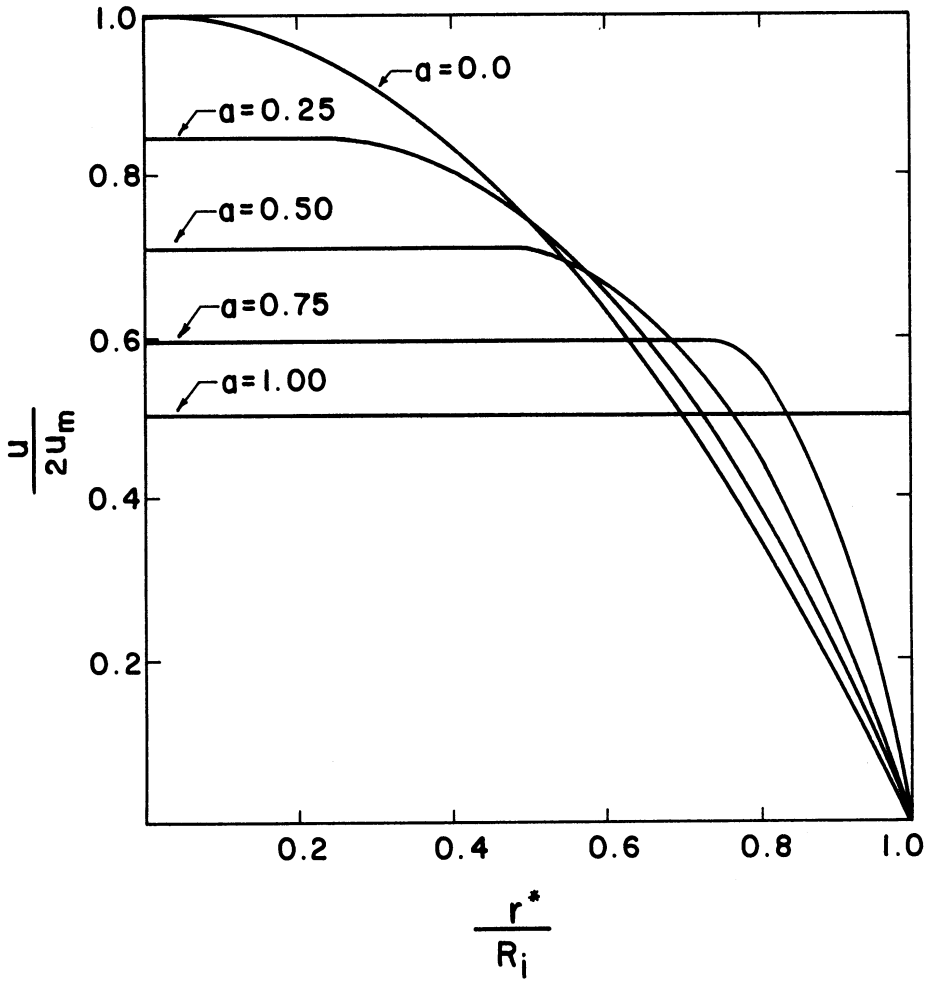

Figure 3. Velocity Profiles for Various Values of the Bingham Plastic Constant a .

to temperature. Thus, a large temperature gradient across the tube can lead to a considerable distortion of the velocity profile due to a radial viscosity gradient.

d) The velocity and temperature are symmetric about the axis of the tube. Free convection can invalidate this assumption at low Reynolds number when there is a large radial temperature gradient. The buoyant forces associated with free convection can cause a secondary flow which increases the temperature at the top of the tube and decreases it at the bottom of the tube. This secondary flow also may cause a mixing of the fluid which raises the centerline temperature above the predicted value while lowering the average wall temperature.

Any settling of solids suspended in the fluid will cause the velocity distribution to be distorted due to a viscosity gradient. The velocity will decrease at the bottom of the tube and increase at the top of the tube.

With the assumptions, the application of the first law of thermodynamics to the system shown in Figure 2 yields the following partial differential equations for temperature in the fluid and wall. The velocity distribution $u(r)$ is given by Equation (3.3). (Details of the derivation are given in Appendix A).

Fluid $(0 \leq r \leq 1)$

$$\frac{\partial \psi_f}{\partial \theta} + u(r)\frac{\partial \psi_f}{\partial x} = \frac{\partial^2 \psi_f}{\partial r^2} + \frac{1}{r}\frac{\partial \psi_f}{\partial r} + Q'' \qquad (3.5)$$

Wall $\left(1 \leq r \leq \frac{Ro}{Ri}\right)$

$$\frac{\partial \psi_w}{\partial \theta} = \Lambda\left(\frac{\partial^2 \psi_w}{\partial r^2} + \frac{1}{r}\frac{\partial \psi_w}{\partial r}\right) \qquad (3.6)$$

where $Q'' = \begin{cases} 0 & \text{for step disturbance in inlet fluid temperature} \\ 1 & \text{for step disturbance in internal heat generation} \\ \epsilon \sin \Gamma\theta & \text{for sinusoidal disturbance in internal heat generation} \end{cases}$

The boundary conditions to be satisfied are

$$\psi_f(X, 0, r) = 0 \qquad \text{(initial)}$$

$$\psi_f(0, \theta, r) = 0 \qquad \text{(entrance)}$$

$$\frac{\partial \psi_f}{\partial r}(X, \theta, r) = 0 \qquad \text{(symmetry)}$$

$$\psi_f(X, \theta, 1) = \psi_w(X, \theta, 1) \qquad \text{(fluid-wall interface)}$$

$$\frac{\partial \psi_w}{\partial r}(X, \theta, 1) = 0 \qquad \text{(adiabatic wall)}$$

A. Step-Response to Inlet Fluid Temperature and Internal Heat Generation

The step response in fluid and wall temperatures is studied for two cases:

Case 1. The inlet fluid temperature remains constant, and energy generation is suddenly started in the fluid.

Case 2. The fluid has no energy generation, but the inlet fluid temperature is suddenly raised to a new level and maintained there.

For a step disturbance in inlet fluid temperature the dimensionless temperature symbol ψ_f is replaced by $\xi_f = \frac{T - T_i}{T_o - T_i}$. The equation for the fluid then becomes

$$\frac{\partial \xi_f}{\partial \theta} + u(r) \frac{\partial \xi_f}{\partial X} = \frac{\partial^2 \xi_f}{\partial r^2} + \frac{1}{r} \frac{\partial \xi_f}{\partial r} \qquad (3.7)$$

The equation for the wall remains the same, but the entrance boundary condition is changed to

$$\xi_f(0,\theta,r) = 1$$

These changes are so minor that it is unnecessary to treat Case 1 and Case 2 as two distinct problems. Instead, Case 1 is considered below, and important differences between Case 1 and Case 2 are noted.

1. Finite Difference Equations

To solve the wall and fluid equations a radially and axially divided grid is constructed as shown in Figure 4. All derivatives in Equations (3.5) and (3.6) are approximated by finite differences involving the variables of surrounding points. The resulting equations are solved using numerical methods on the IBM 7090 digital computer.

The finite difference approximations to Equations (3.5) and (3.6) appear in Table I. (Full details are given in Appendix B). Because the coefficients of the variables in the finite difference equations of Table I form a square $3(M + N + 1)$ tridiagonal matrix, where M and N are the fluid and wall divisions, respectively, the method of Gaussian Elimination can be used for their solution. Thus, an explicit method is used in the axial direction, while an implicit method is used in the radial and time directions. This is implemented by solving for the variables at the first axial location with Gaussian Elimination. The axial dimension is incremented and the process continued until the desired axial distance is reached.

2. Computer Solution

Computer program A, presented in Appendix E, is used to solve the finite difference equations of Table I on the IBM 7090 digital

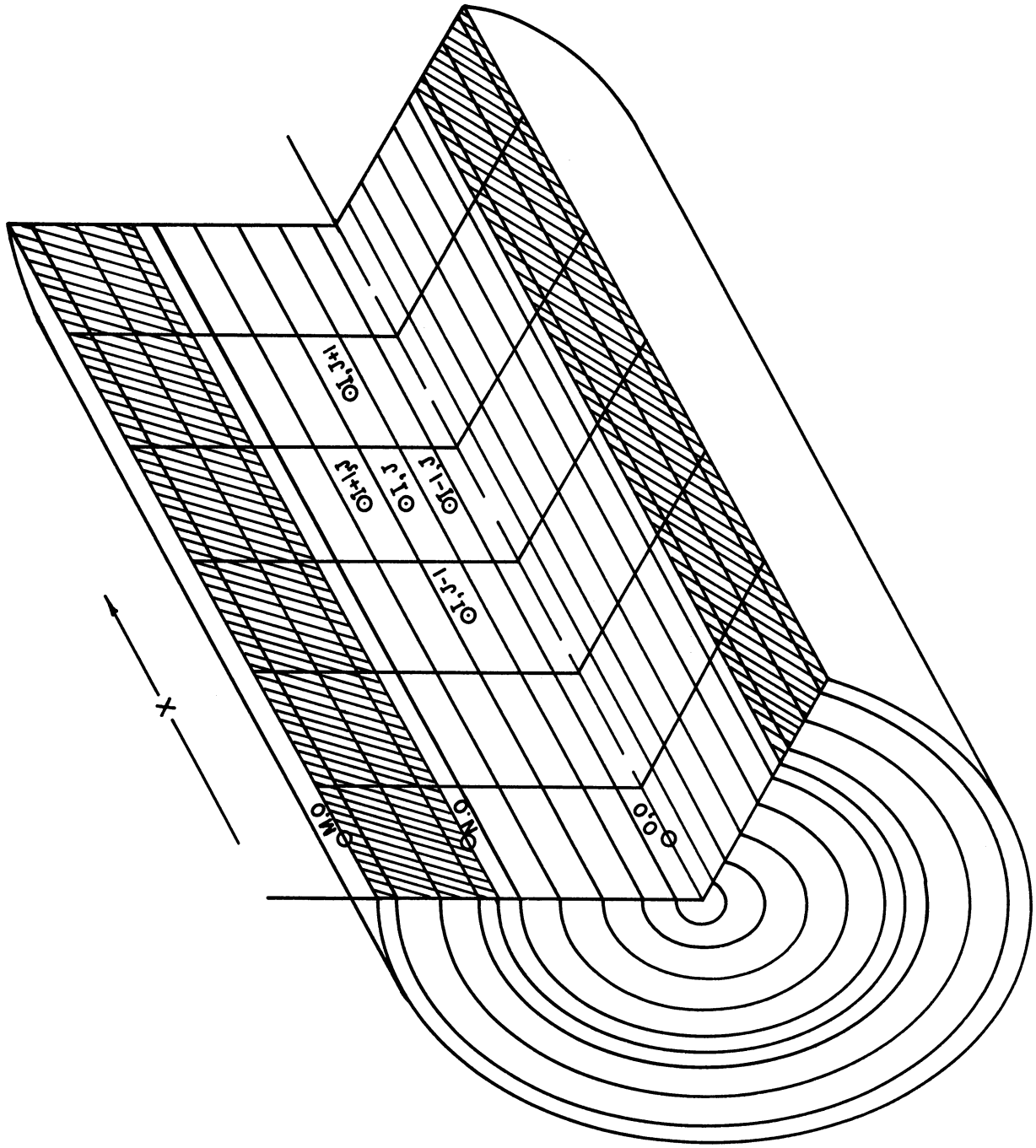

Figure 4. Radial and Axial Grid Used in Finite Difference Equations.

TABLE I

INTERNAL ENERGY GENERATION STEP RESPONSE FINITE DIFFERENCE EQUATIONS *

Eqn.	Funct.	Computer Notation	Location	Difference Equation
a.	$\psi_f(0,J)$	S(0)	Centerline	$(\frac{1}{\Delta\theta} + \text{VMAX}\,\frac{P}{L} + 4N^2)\,S(0) - 4N^2\,S(1) = \frac{F(0)}{\Delta\theta} + \frac{P}{L}\,\text{VMAX}\,U(0) + 1$
b.	$\psi_f(I,J)$	S(I)	General Fluid	$-N^2\,(1 - \frac{1}{2I})\,S(I-1) + (\frac{1}{\Delta\theta} + \frac{P}{L}\,\text{VEL}(I) + 2N^2)\,S(I) - N^2(1 + \frac{1}{2I})\,S(I+1) = \frac{F(I)}{\Delta\theta} + \frac{P}{L}\,\text{VEL}(I)\,U(I) + 1$
c.	$\psi_f(N,J)$ $\psi_w(0,J)$	S(N) V(0)	Fluid-Wall Interface	$-(N - \frac{1}{2})\,S(N-1) + \left[\frac{1}{2\Delta\theta}\,(\frac{\delta}{BM} + \frac{1}{N}) + (N - \frac{1}{2}) + \frac{\Lambda}{B}(\frac{M}{B} + \frac{1}{2})\right] S(N) - \frac{\Lambda}{B}\,(\frac{M}{B} + \frac{1}{2})\,V(1) = \frac{Q}{2N} + \frac{1}{2\Delta\theta}\,(\frac{\delta}{BM} + \frac{1}{N})\,F(N)$
d.	$\psi_w(K,J)$	V(K)	General Wall	$-\Lambda\,\frac{M^2}{\delta^2} - \left[\frac{M}{2\delta(1 + \frac{K\delta}{M})}\right] V(K-1) + (\frac{1}{\Delta\theta} + 2\,\frac{\Lambda M^2}{\delta^2})\,V(K) - \Lambda\left[\frac{M^2}{\delta^2} + \frac{M}{2\delta(1 + \frac{K\delta}{M})}\right] V(K+1) = \frac{W(K)}{\Delta\theta}$
e.	$\psi_w(M,J)$	V(M)	Outside Wall	$-\Lambda\,(\frac{M}{\delta} + M - \frac{1}{2})\,V(M-1) + \left[\frac{\delta(1+\delta)}{2\Delta\theta M} + \Lambda(\frac{M}{\delta} + M - \frac{1}{2})\right] V(M) = \frac{\delta(1+\delta)}{2\Delta\theta M}\,W(M)$

* Dimensionless computer program nomenclature used in table is given in Appendix E.

computer. The Program is written in the Michigan Algorithm Decoder Language. The Gaussian Elimination method used in the radial and time directions applies only to the solution of a tridiagonal matrix as would be produced by the set of equations below; where a_n, b_n, and c_n are coefficients of the variables y_n, and d_n is a constant.

$$
\begin{aligned}
b_1 y_1 + c_1 y_2 &= d_1 \\
a_2 y_1 + b_2 y_2 + c_3 y_3 &= d_2 \qquad (3.8) \\
a_3 y_2 + b_3 y_3 + c_3 y_4 &= d_3 \\
&\vdots \\
a_M y_{M-1} + b_M y_M &= d_M
\end{aligned}
$$

The variables, y_n, of the above system of equations can be found directly. Multiply the first equation by $-a_2/b_1$ and add it to the second equation. The second equation is replaced by this resulting equation in which the coefficient of y_1 is zero. Next, the third equation is replaced by the result of adding to it the second equation multiplied by $-a_3/b_2$. This manipulation eliminates the variable y_2 from the third equation. The process is continued until every equation, except the last, contains only two unknowns. The last equation will contain only one unknown, making the value of y_M directly available. By back substituting the value of y_M into the M-1 equation, whose only unknowns are y_M and y_{M-1}, the value of y_{M-1} can be found. Thus, by continuing the back substitution process the entire system of

equations is resolved. When made suitable for automatic machines, the algorithm for Gaussian Elimination is given by[26]

$$y_M = \gamma_M$$

$$y_i = \gamma_i - \frac{c_i y_{i+1}}{\beta_i} \qquad i = M-1, M-2, \ldots 1 \tag{3.9}$$

where γ and β are determined by

$$\beta_1 = b_1 \quad , \quad \gamma_1 = \frac{d_1}{\beta_1}$$

$$\beta_i = b_i - \frac{a_i c_{i-1}}{\beta_{i-1}} \qquad i = 2, 3, \ldots M$$

$$\gamma_i = \frac{d_i - a_i \gamma_{i-1}}{\beta_i} \qquad i = 2, 3, \ldots M$$

This method is unconditionally stable if the equations are consistent. In practical applications this will always be the case, since each equation will contain a unique set of unknowns not repeated in any other equation. However, considerable roundoff error can accumulate because of the large number of arithmetic operations involved. Therefore, it is necessary to check the final result. The transient solution should converge to the same steady-state solution already obtained by Michiyoshi[7] in closed form. If it converges to the correct steady-state value, the solution can be assumed to be accurate at all values of time.

B. Steady and Steady-Periodic Solutions to Internal Heat Generation

The term "steady-periodic" means that although the temperature varies periodically with time, the effects of an initial time condition

are no longer present. Thus, if a disturbance in the system varies periodically with respect to time, so the temperature will also vary periodically with a frequency equal to that of the disturbance.

Because the governing equations and associated boundary conditions are linear, the solution may be divided into two portions: one a steady solution and the other a steady-periodic solution. The method of handling the steady-periodic solution is similar to that used by Ayers[8].

Fluid

$$\Psi_f(X,\theta,r) = \Psi_{sf}(X,r) + \Psi_{Pf}(X,\theta,r) \tag{3.10}$$

Wall

$$\Psi_w(X,\theta,r) = \Psi_{sw}(X,r) + \Psi_{Pw}(X,\theta,r) \tag{3.11}$$

Substitution of Equations (3.10) and (3.11) into (3.8) and (3.9), respectively, and separating the steady and steady-periodic portions yields the following equations.

Fluid

$$u(r)\frac{\partial \Psi_{sf}}{\partial X} = \frac{\partial^2 \Psi_{sf}}{\partial r^2} + \frac{1}{r}\frac{\partial \Psi_{sf}}{\partial r} + 1 \tag{3.12}$$

$$\frac{\partial \Psi_{Pf}}{\partial \theta} + u(r)\frac{\partial \Psi_{Pf}}{\partial X} = \frac{\partial^2 \Psi_{Pf}}{\partial r^2} + \frac{1}{r}\frac{\partial \Psi_{Pf}}{\partial r} + \epsilon \sin\Gamma\theta \tag{3.13}$$

Wall

$$\frac{\partial^2 \Psi_{sw}}{\partial r^2} + \frac{1}{r}\frac{\partial \Psi_{sw}}{\partial r} = 0 \tag{3.14}$$

$$\frac{\partial^2 \Psi_{pw}}{\partial \theta} = \Lambda \left(\frac{\partial^2 \Psi_{pw}}{\partial r^2} + \frac{1}{r} \frac{\partial \Psi_{pw}}{\partial r} \right) \tag{3.15}$$

The boundary conditions are

$$\Psi_{sf}(0,r) = -\Psi_{pf}(0,\theta,r) = 0$$

$$\frac{\partial \Psi_{sf}(X,0)}{\partial r} = -\frac{\partial \Psi_{pf}(X,\theta,0)}{\partial r} = 0$$

$$\Psi_{sf}(X,1) - \Psi_{sw}(X,1) = \Psi_{pf}(X,\theta,1) - \Psi_{pw}(X,\theta,1) = 0$$

$$\frac{\partial \Psi_{sw}(X,\theta,R_o/R_i)}{\partial r} = -\frac{\partial \Psi_{pw}(X,\theta,R_o/R_i)}{\partial r} = 0$$

Because a steady-periodic solution is being sought, valid as θ approaches infinity, and because the energy generation rate is sinusoidal, $q_o(1 + \epsilon \operatorname{Sin} \Gamma\theta)$, it can be assumed that the fluid and wall temperatures will also be sinusoidal. Thus it is assumed

$$\Psi_{pf} = \left[A^2(X,r) + B^2(X,r) \right]^{1/2} \operatorname{Sin}(\Gamma\theta - \phi_f) \tag{3.16}$$

and

$$\Psi_{pw} = \left[C^2(X,r) + D^2(X,r) \right]^{1/2} \operatorname{Sin}(\Gamma\theta - \phi_w) \tag{3.17}$$

where

$$\phi_f = \operatorname{Tan}^{-1}\left(\frac{-B}{A}\right) \quad ; \quad \phi_w = \operatorname{Tan}^{-1}\left(\frac{-D}{C}\right)$$

By defining the amplitude ratio as the amplitude of the steady periodic temperature divided by the temperature resulting from an infinitely long period $(\Gamma \to 0)$, the following definitions are derived.

$$AR_f = \frac{\sqrt{A^2 + B^2}}{\epsilon \, \Psi_{sf}} \tag{3.18}$$

$$AR_w = \frac{\sqrt{C^2 + D^2}}{\epsilon \, \Psi_{sw}} \tag{3.19}$$

Then, the temperature response for the fluid and wall can be expressed as follows:

$$\Psi_f = \Psi_{sf}\left(1 + \epsilon \, AR_f \, \sin\left(\Gamma\theta - \phi_f\right)\right) \tag{3.20}$$

$$\Psi_w = \Psi_{sw}\left(1 + \epsilon \, AR_w \, \sin\left(\Gamma\theta - \phi_w\right)\right) \tag{3.21}$$

It may be noted that the functions AR_f, AR_w, ϕ_f and ϕ_w are functions of x and r.

1. Finite difference equations

The solution for the steady temperature distribution is obtained by applying finite differences to Equations (3.12) and (3.14) and solving the resulting equations on the IBM 7090 digital computer. Similarly, the steady-periodic temperature distribution is obtained. Equations (3.16) and (3.17) are applied to Equations (3.13) and (3.15), respectively, before they are written in finite difference form. For example, substituting Equation (3.16) into (3.13) results in

$$A\Gamma \cos\Gamma\theta - B\Gamma \sin\Gamma\theta + u(r)\left(\frac{\partial A}{\partial x}\sin\Gamma\theta + \frac{\partial B}{\partial x}\cos\Gamma\theta\right)$$

$$= \left(\frac{\partial^2 A}{\partial r^2} + \frac{1}{r}\frac{\partial A}{\partial r}\right)\sin\Gamma\theta + \left(\frac{\partial^2 B}{\partial r^2} + \frac{1}{r}\frac{\partial B}{\partial r}\right)\cos\Gamma\theta + \epsilon \sin\Gamma\theta \tag{3.22}$$

Because Equation (3.22) is valid for all values of time, it can be divided into two equations. One equation corresponds to the sum of all the terms with $\sin\Gamma\theta$ coefficients, and the other corresponds to the sum of all the terms with $\cos\Gamma\theta$ coefficients. In this way the following equations are obtained.

$$A\Gamma + u(r)\frac{\partial B}{\partial x} = \frac{\partial^2 B}{\partial r^2} + \frac{1}{r}\frac{\partial B}{\partial r} \tag{3.23}$$

$$-B\Gamma + u(r)\frac{\partial A}{\partial x} = \frac{\partial^2 A}{\partial r^2} + \frac{1}{r}\frac{\partial A}{\partial r} + \epsilon \tag{3.24}$$

Similarly the equations for the wall coefficients C and D can be obtained by combining Equations (3.15) and (3.17) and separating the result into its $\sin\Gamma\theta$ and $\cos\Gamma\theta$ components. The process yields

$$\Gamma C = \Lambda\left(\frac{\partial^2 D}{\partial r^2} + \frac{1}{r}\frac{\partial D}{\partial r}\right) \tag{3.25}$$

$$-\Gamma D = \Lambda\left(\frac{\partial^2 C}{\partial r^2} + \frac{1}{r}\frac{\partial C}{\partial r}\right) \tag{3.26}$$

To solve the wall and fluid equations all derivatives are approximated by finite differences involving the variables of surrounding points. The finite difference equations for the fluid and wall are presented in Appendix B and the results given in Table II. These finite

difference equations compose a set of simultaneous linear algebraic equations whose coefficients form a square $3(M + N + 1)$ matrix, where M and N are the wall and fluid grid divisions, respectively.

An implicit method of solution is used in the radial direction, while an explicit method is employed in the axial direction. This permits use of an iterative technique by reducing the number of variables to be solved for at any one time to those present at one axial location. Starting at the first axial location, all variables are solved for by means of the Gauss-Seidel iterative method until convergence is achieved. Then the axial dimension is incremented and the variables solved for at the new axial location. This process is continued as far down the tube as desired.

2. Computer solution

The computer program used to solve the set of equations in Table II is presented in Appendix E, and is based on one developed by Ayers[8]. This program is written in the Michigan Algorithm Decoder Language for use on the IBM 7090 digital computer. The flow diagram also given in Appendix E schematically describes the order of computation used.

Stability tests are automatically made to insure convergence for a particular set of data. If stability is not assured, the data is rejected and the next set of data is read. For the Gauss-Seidel iterative method, a sufficient condition for convergence requires that the absolute value of the element on the main-diagonal of the matrix, constructed by the coefficients of the variables, be greater than or equal

TABLE II

STEADY-PERIODIC FINITE DIFFERENCE EQUATIONS*

Eqn.	Function	Computer Notation	Location	Difference Equation
a.	ψ_{sf}	S(0)	Centerline	$S(0) = \dfrac{4N^2\ S(1) + P/L\ VMAX\ U(0) + 1}{P/L\ VMAX + 4N^2}$
b.	A(0,J)	A(0)	Centerline	$A(0) = \dfrac{4N^2\ A(1) + P/L\ VMAX\ E(0) + \Gamma\ B(0) + \epsilon}{4N^2 + P/L\ VMAX}$
c.	B(0,J)	B(0)	Centerline	$B(0) = \dfrac{4N^2\ B(1) + P/L\ VMAX\ F(0) - \Gamma\ A(0)}{4N^2 + P/L\ VMAX}$
d.	ψ_{sf}(I,J)	S(I)	General Fluid	$S(I) = \dfrac{N^2(1+\frac{1}{2I})\ S(I+1) + N^2(1-\frac{1}{2I})\ S(I-1) + \frac{P}{L}\ VEL(I) + 1}{2N^2 + P/L\ VEL(I)}$
e.	A(I,J)	A(I)	General Fluid	$A(I) = \dfrac{N^2(1+\frac{1}{2I})\ A(I+1) + N^2(1-\frac{1}{2I})\ A(I-1) + \frac{P}{L}\ VEL(I)\ E(I) + \Gamma B(I) + \epsilon}{2N^2 + P/L\ VEL(I)}$
f.	B(I,J)	B(I)	General Fluid	$B(I) = \dfrac{N^2(1+\frac{1}{2I})\ B(I+1) + N^2(1-\frac{1}{2I})\ B(I-1) + \frac{P}{L}\ VEL(I)\ F(I) - \Gamma A(I)}{2N^2 + P/L\ VEL(I)}$
g.	ψ_{sf}(N,J) ψ_{sw}(O,J)	S(N) V(O)	Fluid-Wall Interface	$S(I) = V(0) = \dfrac{N^2(1+\frac{1}{2I})\ S(I+1) + N^2(1-\frac{1}{2I})\ S(I-1) + \frac{P}{L}\ VEL(I) + 1}{2N^2 + P/L\ VEL(I)}$
h.	A(N,J) C(O,J)	A(N) C(O)	Fluid-Wall Interface	$A(N) = C(0) = \dfrac{-(N-\frac{1}{2})(B(N)-B(N-1)) + \frac{\Lambda}{B}(\frac{M}{\delta}+\frac{1}{2})(D(1)-D(0))}{\Gamma(\frac{\delta}{2BM}+\frac{1}{2N})}$
i.	B(N,J) D(O,J)	B(N) D(O)	Fluid-Wall Interface	$B(N) = D(0) = \dfrac{-\Lambda/B\ (M/\delta + 1/2)\ [C(1)-C(0)] + (N-1/2)\ [A(N)-A(N-1)] - \epsilon/2N}{\Gamma(\delta/2BM + 1/2N)}$
j.	ψ_{sw}(K,J)	S(N)	General Wall	$\psi_{sw} = S(N)$
k.	C(K,J)	C(K)	General Wall	$C(K) = \dfrac{\Lambda}{\Gamma}\left[\dfrac{M^2}{\delta^2} + \dfrac{M}{2\delta(1+\frac{K\delta}{M})}\right]D(K+1) - \dfrac{2\Lambda}{\Gamma}\dfrac{M^2}{\delta^2}D(K) + \dfrac{\Lambda}{\Gamma}\left[\dfrac{M^2}{\delta^2} + \dfrac{M}{2\delta(1+\frac{K\delta}{M})}\right]D(K-1)$
l.	D(K,J)	D(K)	General Wall	$D(K) = -\dfrac{\Lambda}{\Gamma}\left[\dfrac{M}{\delta^2} + \dfrac{M}{2\delta(1+\frac{K\delta}{M})}\right]C(K+1) + \dfrac{2\Lambda}{\Gamma}\dfrac{M}{\delta^2}C(K) - \dfrac{\Lambda}{\Gamma}\left\{\dfrac{M^2}{\delta^2} - \dfrac{M}{2\delta(1+\frac{K\delta}{M})}\right\}C(K-1)$
m.	C(M,J)	C(M)	Outer Wall	$C(M) = \dfrac{-\Lambda(M/\delta + M - 0.5)(D(M) - D(M-1))}{\Gamma\frac{\delta}{2M}(1+\delta)}$
n.	D(M,J)	D(M)	Outer Wall	$D(M) = \dfrac{\Lambda(M/\delta + M - 0.5)(C(M) - C(M-1))}{\Gamma\frac{\delta}{2M}(1+\delta)}$

*Dimensionless computer program nomenclature used in table is given in Appendix E.

to the sum of the absolute values of all the other elements in the same row[26]. Thus, for the i-th row:

$$\left| a_{ii} \right| \geq \sum_{\substack{j=1 \\ j \neq i}}^{3(M+N+1)} \left| a_{ij} \right| \qquad (3.27)$$

The strict inequality must hold for at least one row. The stability requirements given in Table III can be determined directly from the equations in Table II. Inspection reveals that the equations corresponding to the steady solution are always stable. Inequalities d, e, and f are the most strict and are tested by the computer program. First, inequality d is tested at location N-1 where it is most severe. If it is not satisfied, the quantity P/L is increased until convergence is assured. An upper limit is put on P/L so that excessive computer time will not be required. Second, inequalities e and f are tested. If they are not satisfied, the data is rejected and the next set of data is read.

Once stability is assured and iteration of the difference equations has begun, it is necessary to test for convergence after each iteration. Each variable is tested to see how rapidly it is changing with each successive iteration. For example, the variable S(I) is stored in location E(I) prior to each iteration. After each iteration of the wall and fluid difference equations, the following test is made.

$$\left| \frac{S(I) - E(I)}{S(I)} \right| < \text{ALPHA} \qquad (3.28)$$

TABLE III

STEADY-PERIODIC STABILITY REQUIREMENTS*

Inequality	Equation	Requirement
a.	Steady Centerline	$1 \geq \dfrac{4N^2}{4N^2 + \frac{P}{L}\,VMAX}$
b.	Periodic Centerline	$1 \geq \dfrac{4N^2 + \Gamma}{4N^2 + \frac{P}{L}\,VMAX}$
c.	Steady General Fluid	$1 \geq \dfrac{2N^2}{2N^2 + \frac{P}{L}\,VMAX}$
d.	Periodic General Fluid	$1 \geq \dfrac{2N^2 + \Gamma}{2N^2 + \frac{P}{L}\,VEL(I)}$
e.	Periodic Fluid-Wall Interface	$1 \geq \dfrac{2(N - \frac{1}{2}) + 2\frac{\Lambda}{B}(\frac{M}{\delta} + \frac{1}{2})}{\Gamma(\frac{1}{B}\frac{\delta}{2M} + \frac{1}{2N})}$
f.	Periodic General Wall	$1 \geq \dfrac{4\Lambda M^2}{\Gamma\delta^2}$
g.	Periodic Outer Wall	$1 \geq \dfrac{2\Lambda(\frac{M}{\delta} + M - \frac{1}{2})}{\Gamma\frac{\delta}{2M}(1 + \delta)}$

* Dimensionless computer program nomenclature used in table is given in Appendix E.

The size of the parameter ALPHA controls the degree of convergence attained during the iteration process at each axial location. Errors resulting from incomplete convergence of the solution will influence the accuracy of the solution at the next axial location. Although the error may be small at the first axial location, the error will propagate in the axial direction and may become excessive. By varying the magnitude of ALPHA, it was found that a value of 0.001 was quite satisfactory. Decreasing ALPHA to 0.0001 resulted in a maximum change in the solution of 0.0025 per cent after 150 axial nodal points.

When the convergence test similar to that given in Equation (3.28) is passed for all variables, the iteration process is ended. The program then continues to do other calculations before going on to the next axial location. The closer the initial guess is to the true value of the variables, and the further the inequalities (Table III) are from being equal, the faster the solution will converge. An upper limit of 100 is placed on the number of iterations, so that unnecessary computer time will not be used.

C. Heat Transfer Computations

The temperature gradient in the fluid or wall at the fluid-wall interface is important to any heat transfer problem. For the steady periodic solution, the wall gradient is evaluated at $\pi/6$ time intervals according to the equation

$$\left.\frac{\partial \Psi_f}{\partial r}\right|_{r=1} = N\left[\left(A(N)-A(N-1)\right)\sin\Gamma\theta + \left(B(N)-B(N-1)\right)\cos\Gamma\theta\right] \qquad (3.29)$$

In the step response solution both the fluid and wall gradients were evaluated according to Equations (3.30) and (3.31) respectively.

$$\left.\frac{\partial \Psi_f}{\partial r}\right|_{r=1} = N\left(S(N) - S(N-1)\right) \tag{3.30}$$

$$\left.\frac{\partial \Psi_w}{\partial r}\right|_{r=1} = \frac{M}{\delta}\left(V(1) - V(0)\right) \tag{3.31}$$

To achieve accurate values for the temperature gradients at the wall, a very fine grid was necessary. This is often the case when using a finite difference technique, because the fluid and wall temperatures change very rapidly near the fluid-wall interface.

The mixed mean temperature as defined by Equation (3.32) is also evaluated.

$$T_{mm} = \frac{2\pi \int_0^{R_i} \rho_f C_f T_f u^*(r^*)\, r^*\, dr^*}{2\pi \int_0^{R_i} \rho_f C_f u^*(r^*)\, dr^*} \tag{3.32}$$

Using dimensionless parameters and expressing the integrals over the two velocity regimes of a Bingham plastic yields the following result for the steady-periodic solution.

$$\Psi_{mm} = \frac{\int_0^a (1-a)^2 \Psi_f\, r\, dr + \int_a^1 (1-2a+2ar-r^2)\Psi_f\, r\, dr}{\int_0^a (1-a)^2\, r\, dr + \int_a^1 (1-2a+2ar-r^2)\, r\, dr} \tag{3.33}$$

Using finite differences this becomes

$$\psi_{mm} = \left[(1-a)^2 \frac{1}{8N^2} \left(S(0) + A(0) \sin\Gamma\theta + B(0) \cos\Gamma\theta \right) \right.$$

$$+ \sum_{I=1}^{I=[aN]} (1-a)^2 \frac{I}{N^2} \left(S(I) + A(I) \sin\Gamma\theta + B(I) \cos\Gamma\theta \right)$$

$$+ \sum_{I=[aN]+1}^{N-1} \left((1-2a) \frac{I}{N^2} + 2a \frac{I^2}{N^2} - \frac{I^3}{N^4} \right) \left(S(I) + A(I) \sin\Gamma\theta \right.$$

$$\left. \left. + B(I) \cos\Gamma\theta \right) \right] \Big/ \left(\frac{a^4 - 4a + 3}{12} \right) \qquad (3.33)$$

The equation for the mixed mean temperature, as it applies to the step response, can be obtained by dropping all terms in Equation (3.33) which have a $\sin\Gamma\theta$ or $\cos\Gamma\theta$ coefficient.

CHAPTER IV

NUMERICAL RESULTS

The IBM 7090 digital computer, located at the University of Michigan Computing Center, was used to run the computer programs given in Appendix E. In order to conserve computer time, most runs were made using the physical constants β , Λ and δ which applied to a 25 per cent sulfuric acid solution, with and without fine alumina particles, flowing through a polyvinylchloride tube of the size used in the experiment described in Chapter IV. The parameter 'a' defined in Equation (3.2), which describes the velocity profile of a Bingham plastic, was varied over the range $0. \backsim 1.$ to study the effect of a Bingham plastic on the temperature distribution. The numerical results are presented in four parts: steady, internal energy generation step response, inlet temperature step response, and steady periodic response. The truncation error inherent to the finite difference technique is discussed in Appendix B.

A. Steady Solution

The steady solution gives the temperature distribution in the fluid as a function of x, r, and a. Volumetrically uniform energy is generated in the fluid, and the outer tube wall is insulated. Because the temperature is time-steady and the outer wall is insulated, the tube wall has a uniform radial temperature equal to the temperature of the fluid-wall interface.

Figure 5 gives the steady temperature distribution in the fluid as a function of radial distance for various values of x ; the Bingham plastic constant 'a' equals 0.25. It can be seen that the radial temperature profiles are continuing to develop at $x = .01$. Michiyoshi[7] has shown that this development will continue until $x = .30$, after which both the centerline and wall temperatures will increase linearly with respect to x .

Figure 6 gives the steady-wall and centerline temperatures as a function of axial distance for various values of the Bingham plastic constant 'a'. Even for very small values of x the centerline temperature increases linearly with respect to x. However, the wall temperature still is increasing non-linearly at $x = .01$.

Figure 7 illustrates how decreasing the value of 'a' increases the centerline-to-wall temperature difference. This increase is due to the higher velocity present at the center of the tube when 'a' is small. The effect of an increase in 'a' is much more pronounced at large values of the parameter. For example, there is a considerably greater difference between the lines $a = 0.50$ and $a = 0.75$ than there is between the lines $a = 0.0$ and $a = 0.25$. The radius of the plug portion in the fluid velocity profile is proportional to 'a', making the area of the plug proportional to a^2. This squared relation accounts for the increased effect of 'a' on the temperature profile as the parameter becomes larger.

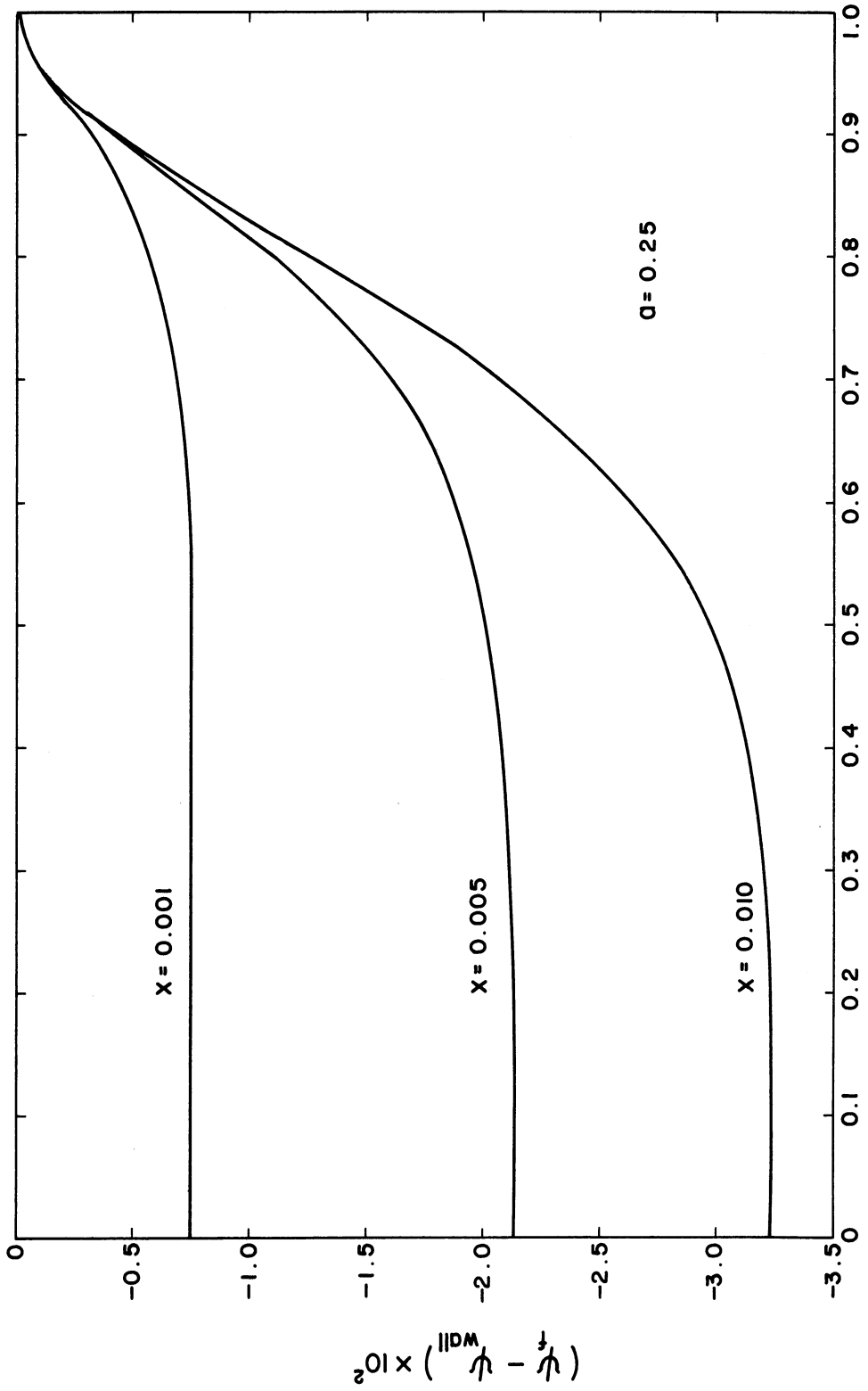

Figure 5. Steady Fluid-Wall Temperature Difference versus Radius for Various Axial Distances.

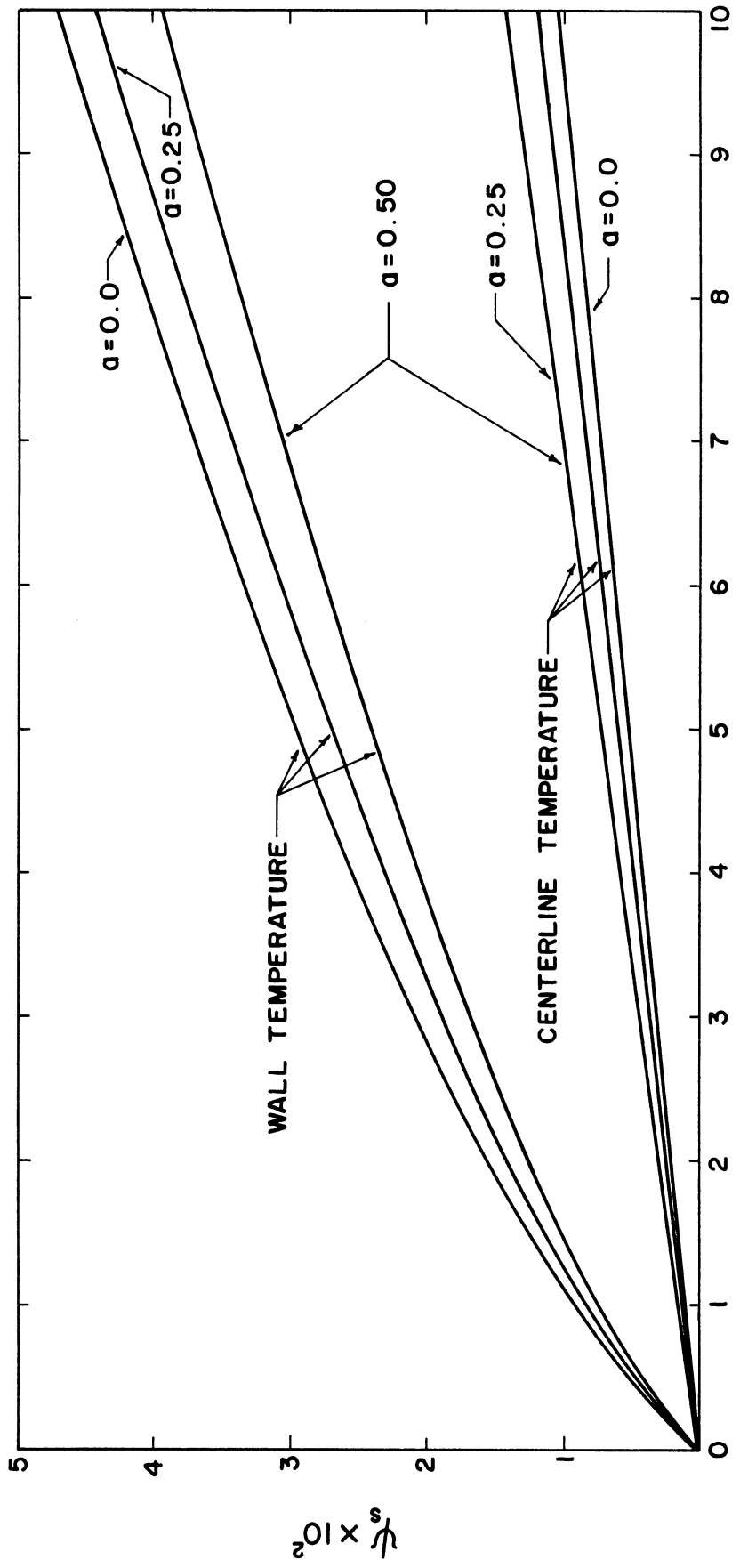

Figure 6. Steady Centerline and Wall Temperatures versus Axial Distance as a Function of 'a'.

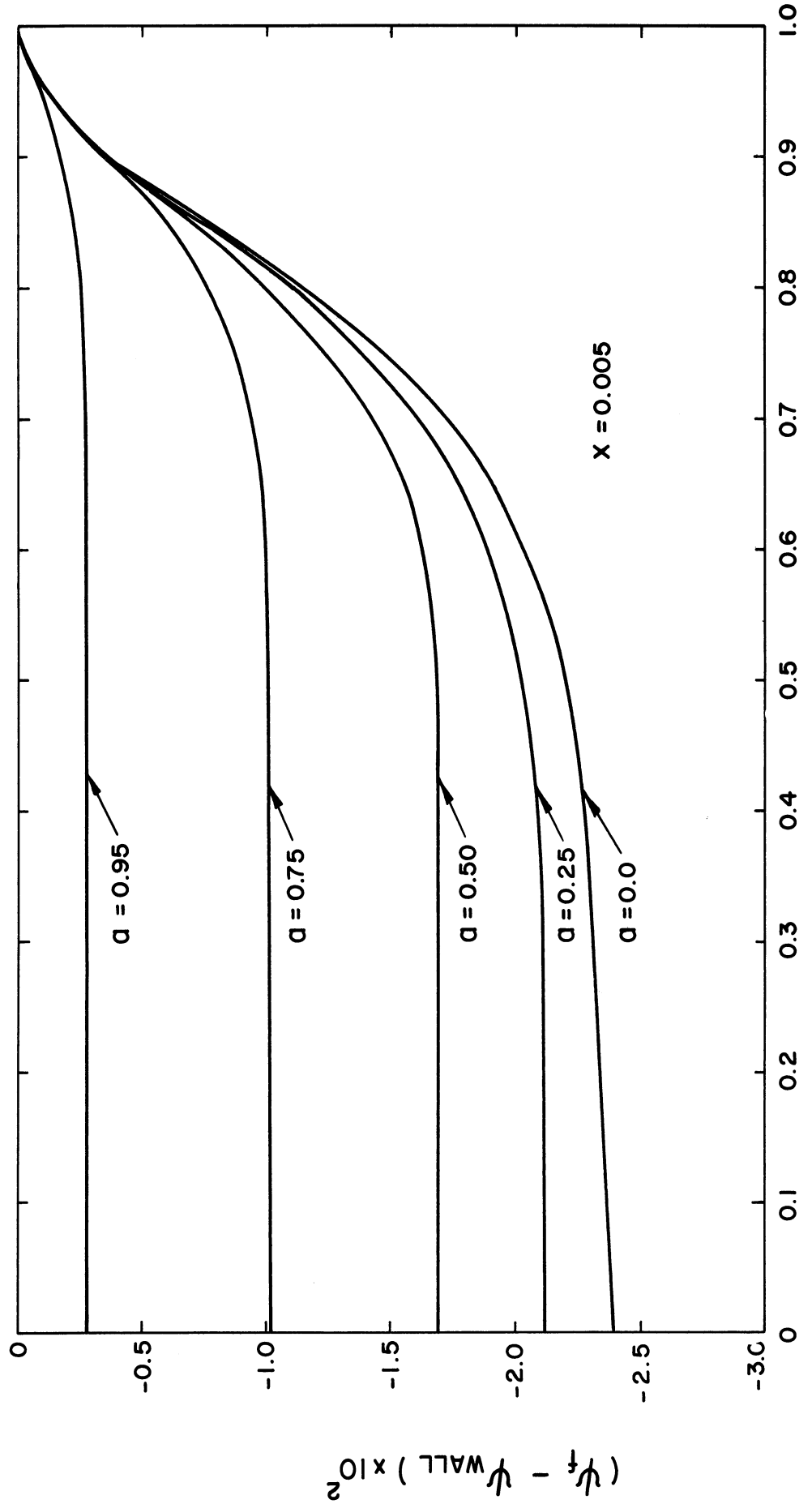

Figure 7. Steady Fluid-Wall Temperature Difference versus Radius as Function of 'a'.

B. Internal Energy Generation Step Response

Program A, shown in Appendix E, was used to evaluate the transient temperature response of the fluid-tube system due to the sudden starting of internal energy generation in the fluid. The fluid and wall temperatures are functions of δ, χ, β, Λ, a, and r. At large values of time, the solutions obtained from the step response were found to agree with those obtained from the steady portion of the steady-periodic solution, and the analytical solution given by Michiyoshi[7].

Figure 8 gives the transient centerline fluid temperature as a function of axial distance and time. At small values of time and large values of x, there is no x-direction temperature variation. This is because the enthalpy flux, which started at location $x = 0$ when $\theta = 0$, has not yet traveled sufficiently far down the tube. The characteristic time required for the enthalpy flux to reach a given location is x/u.

The development with time of the radial temperature profiles in the fluid and tube wall can be seen in Figure 9. The equality of heat fluxes at the fluid-wall interface requires that the slopes of fluid and wall temperatures at the interface be of the same sign and is expressed as

$$\frac{\partial \Psi_f}{\partial r} = \frac{\Lambda}{\beta} \frac{\partial \Psi_w}{\partial r} \tag{4.1}$$

Inspection of the curves in Figure 9 reveals that the derivative of the fluid temperature, with respect to radius, experiences a very rapid change near the interface. This change of derivative appears

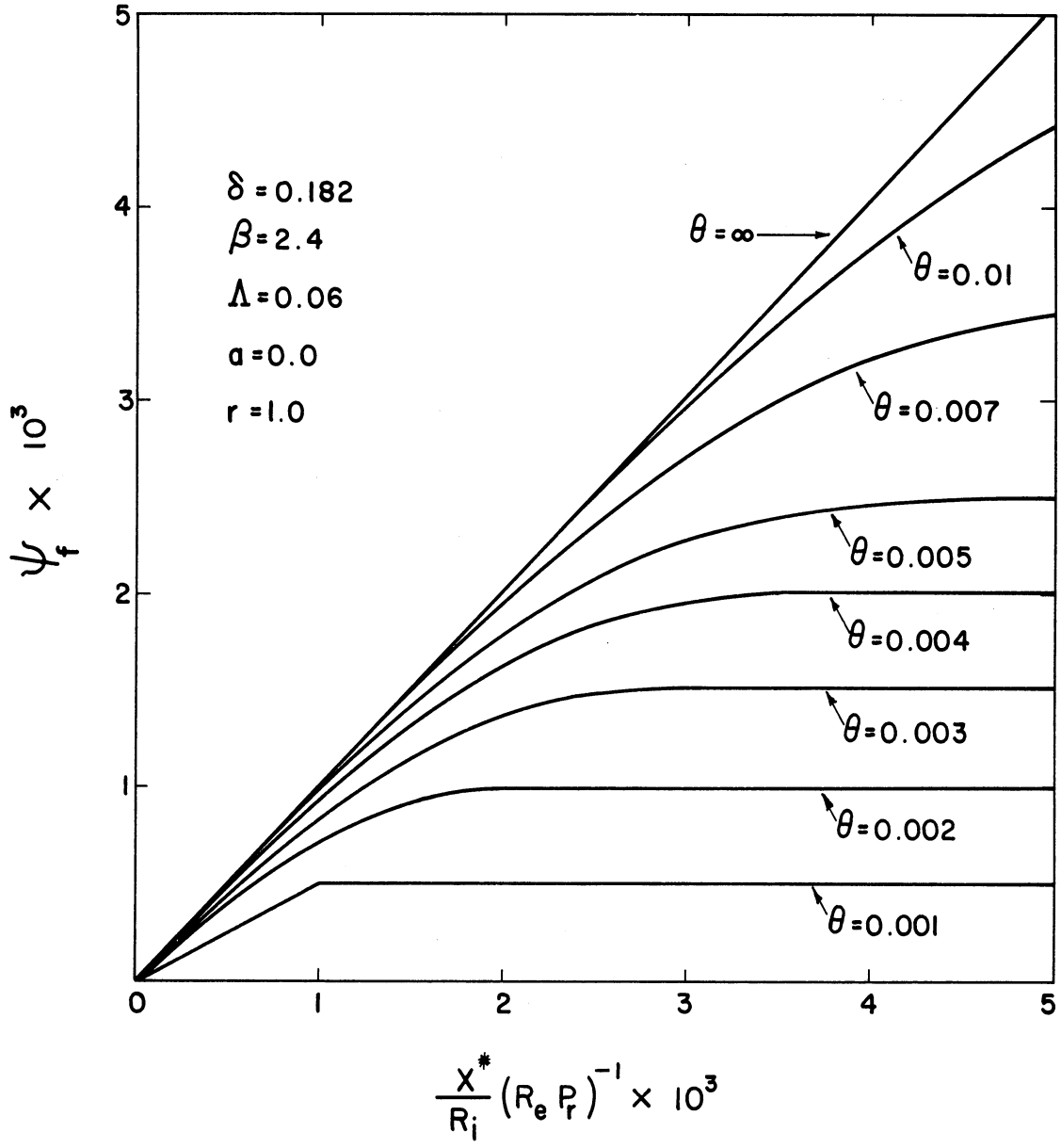

Figure 8. Step Response of Centerline Fluid Temperature versus Axial Distance.

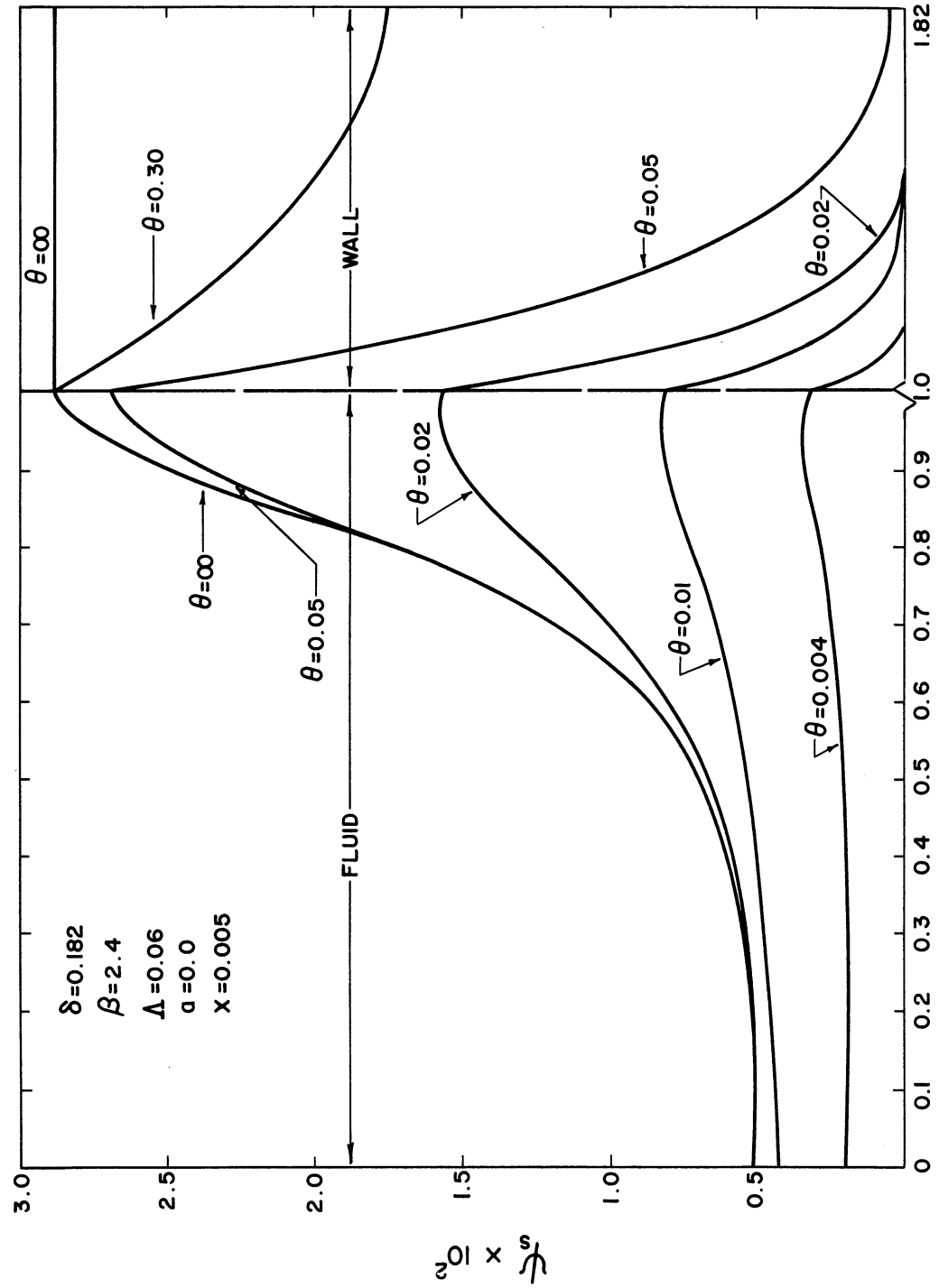

Figure 9. Step Response of Fluid and Wall Temperatures versus Radius.

to be less drastic at smaller values of time. Evaluation of the radial temperature gradient of the fluid at the wall would require an extremely small grid size. Therefore, it was found more practical to evaluate the radial gradient of the wall temperature and relate it to the fluid gradient by means of Equation (4.1).

An increase in the Bingham plastic constant, 'a', yields a faster transient response of the fluid-tube system. Figure 10 indicates that the fluid-wall interface would reach steady state nearly twice as fast for plug flow (a = 1.0) as for parabolic flow (a = 0.0). This is due to the greater velocity present near the tube wall associated with an increase in 'a' for a constant mass flow rate.

The radial fluid temperature gradient as a function of time is displayed in Figure 11. At zero time, it is equal to zero since the fluid and wall are the same initial temperature. As time increases, the temperature gradient goes through a maximum before decreasing again towards zero as steady state is approached. At infinite time, a zero fluid-wall temperature gradient is required because of the insulated outer tube wall.

A few computer runs were made to determine the effect of the fluid and wall material properties upon the transient temperature response of the fluid-tube system. The increasing importance of the wall to fluid thermal diffusivity ratio, Λ, as the fluid-wall heat capacity ratio, M , is decreased is apparent in Figure 12. A high thermal diffusivity in the tube wall, large Λ, has a greater retarding effect on the fluid-wall interface temperature as the wall thickness is increased, M decreased. Heat conduction in the tube

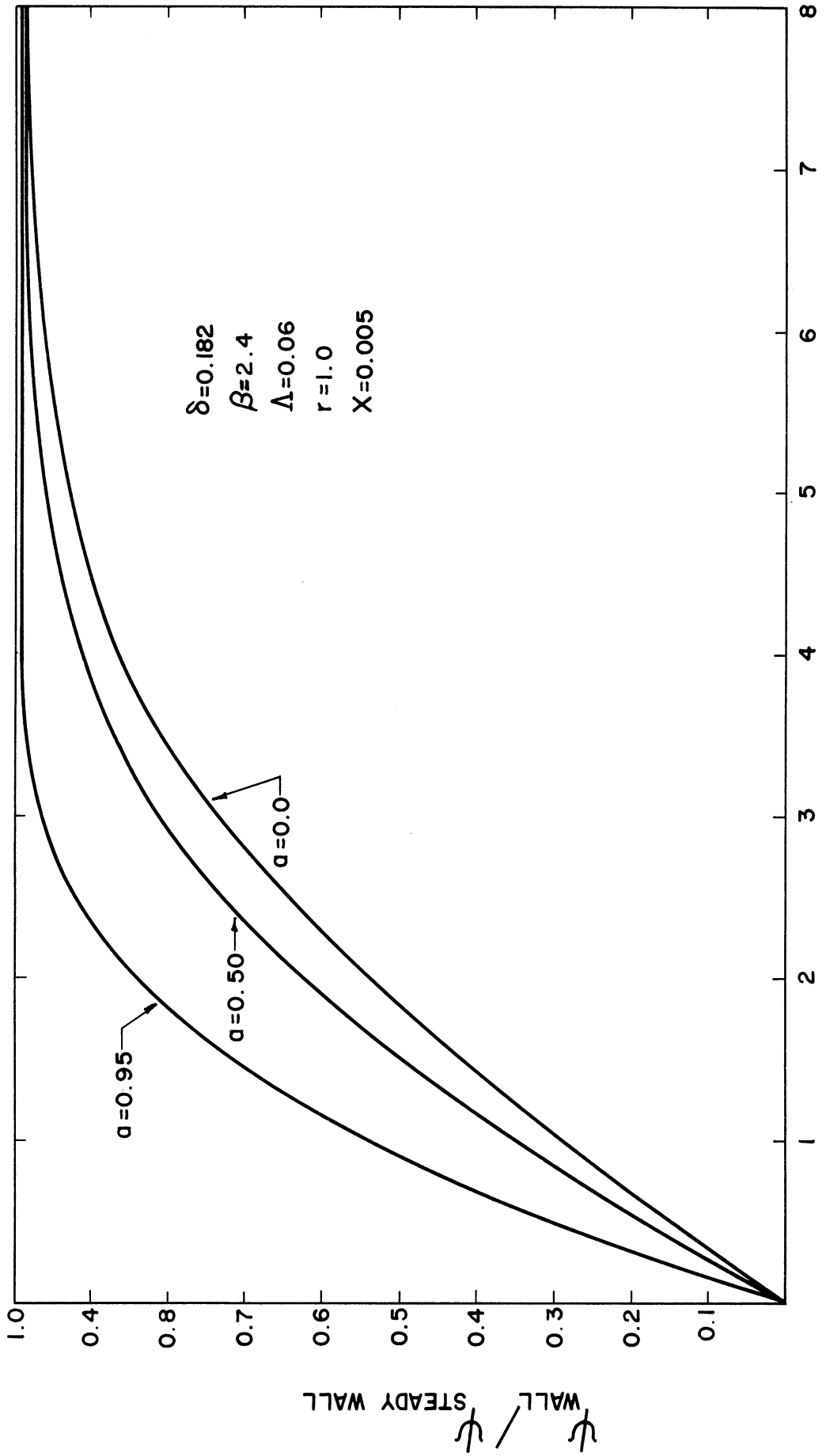

Figure 10. Step Response of Fluid-Wall Interface Temperature as Function of 'a'.

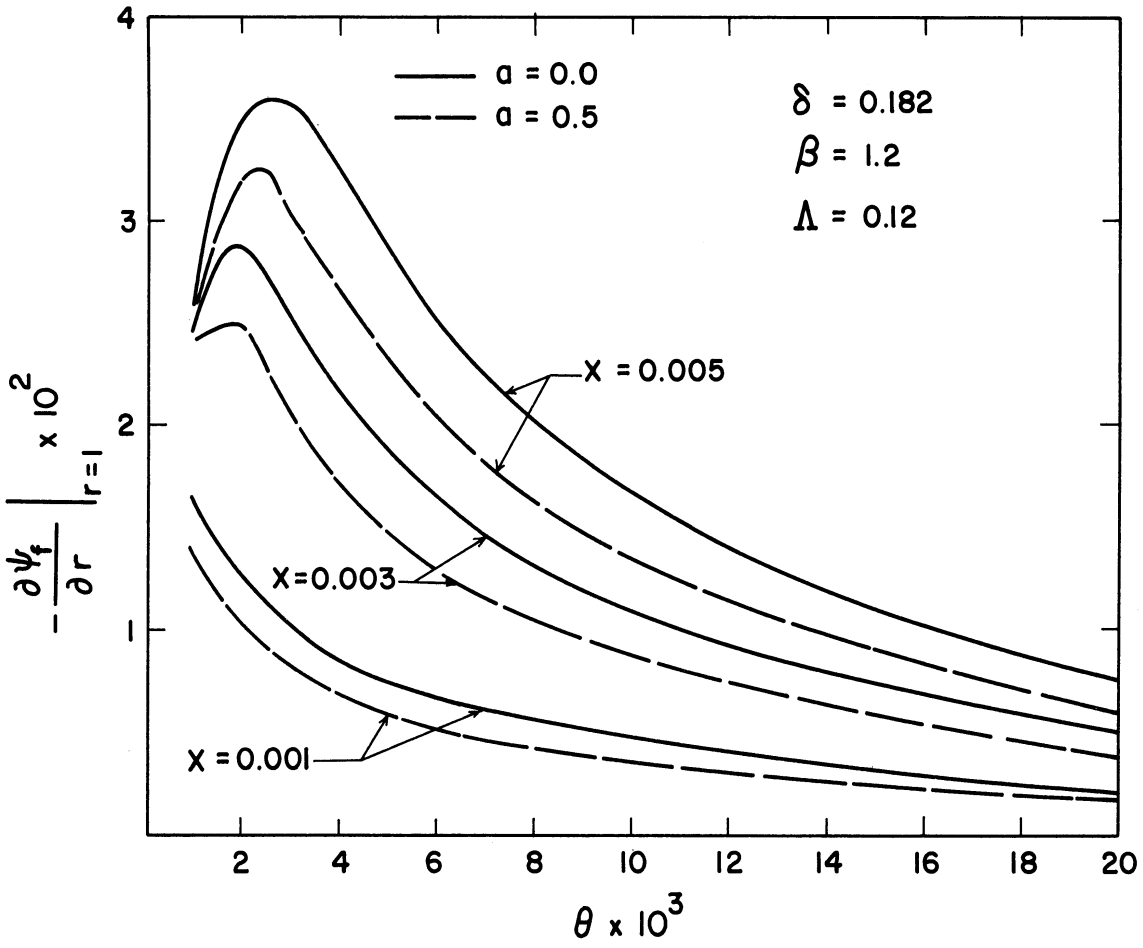

Figure 11. Response of Fluid Temperature Gradient at Fluid-Wall Interface Due to Step in Energy Generation.

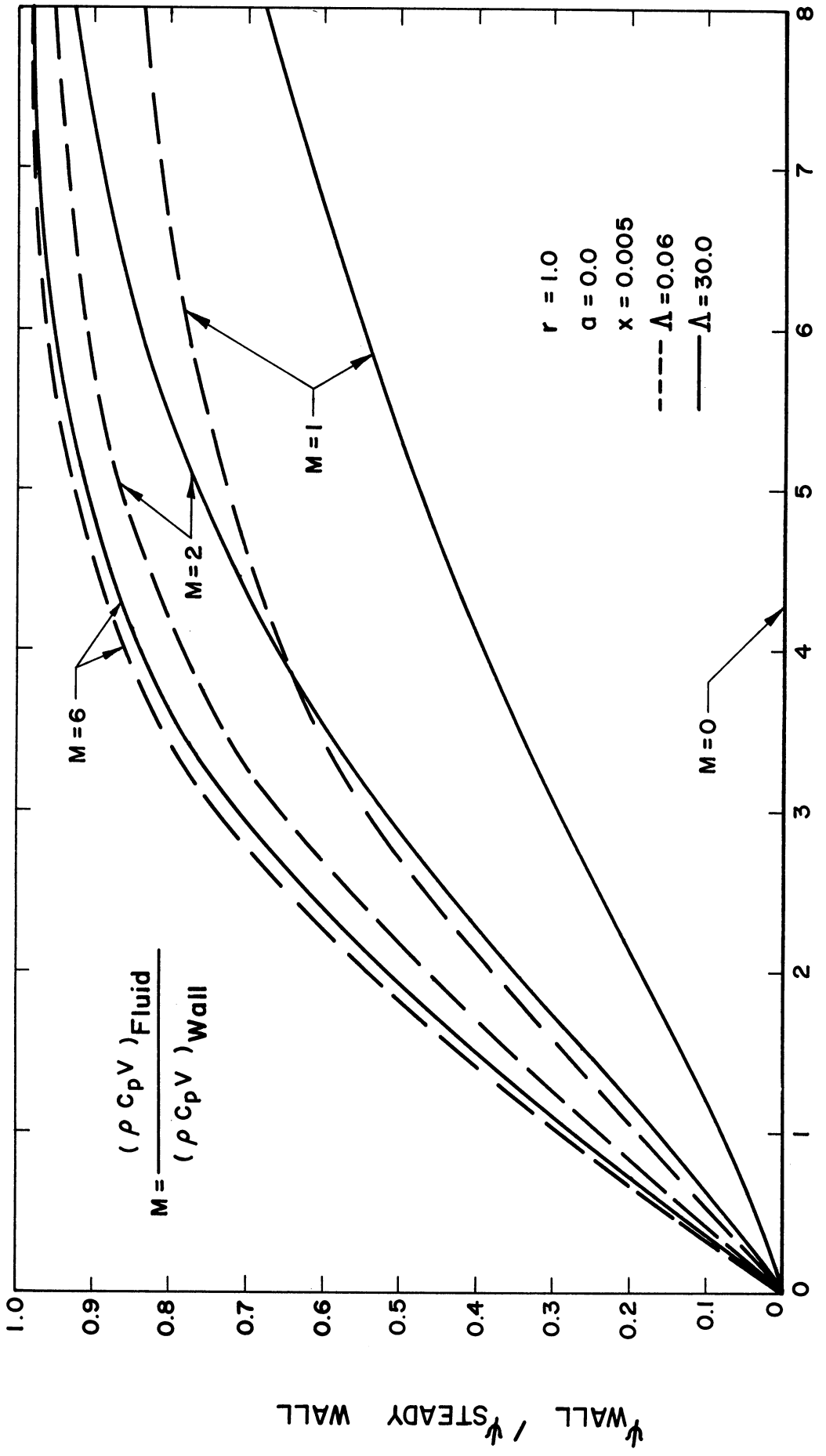

Figure 12. Step Response of Fluid-Wall Interface Temperature as Function of Λ and Fluid-Wall Heat Capacity Ratio M.

wall results in a more uniform wall temperature response, retarding the fluid-wall interface response and increasing the outer-wall response. Greatly reducing the fluid volume or increasing the wall thickness, M approaches zero, would result in an infinitely long response time.

C. Inlet Temperature Step Response

A slight change in the data used in Computer Program A in Appendix E will enable the program to be used for the temperature response of a fluid-tube system in which there is no internal energy generation, but whose fluid inlet temperature is suddenly raised to some new value and held there. If, in the input data, Q is put equal to 0.0 and INLET is put equal to 1.0, the inlet-temperature step response may be studied. The fluid and wall temperatures are functions of δ, X, β, Λ, a, and r.

The temperature response resulting from a step increase in the inlet fluid temperature is displayed in Figures 13 and 14. As noted from Figure 14, for a = 0.5, the centerline response lags that for a = 0.0, while the wall response leads. This difference results from the change in enthalpy flux due to the decreased centerline velocity and increased velocity near the wall as 'a' is increased.

The radial fluid-temperature gradient evaluated at the tube wall is displayed in Figure 15. Initially the gradient is zero because the fluid-tube system is at a uniform temperature. When the enthalpy flux resulting from the increase in inlet temperature reaches a given axial location, the gradient increases, goes through a maximum, and

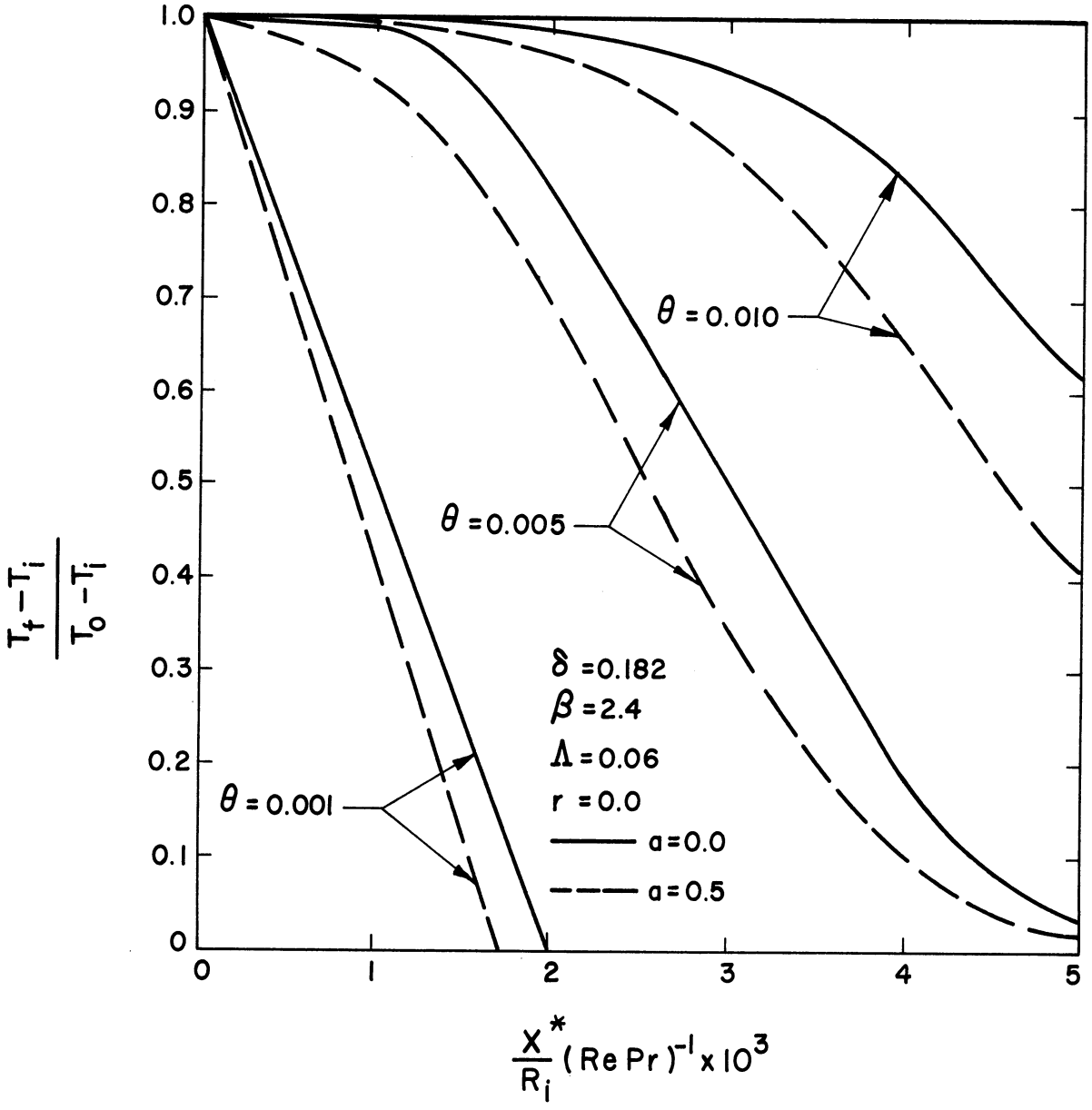

Figure 13. Centerline Fluid Temperature Response Due to Inlet Temperature Step.

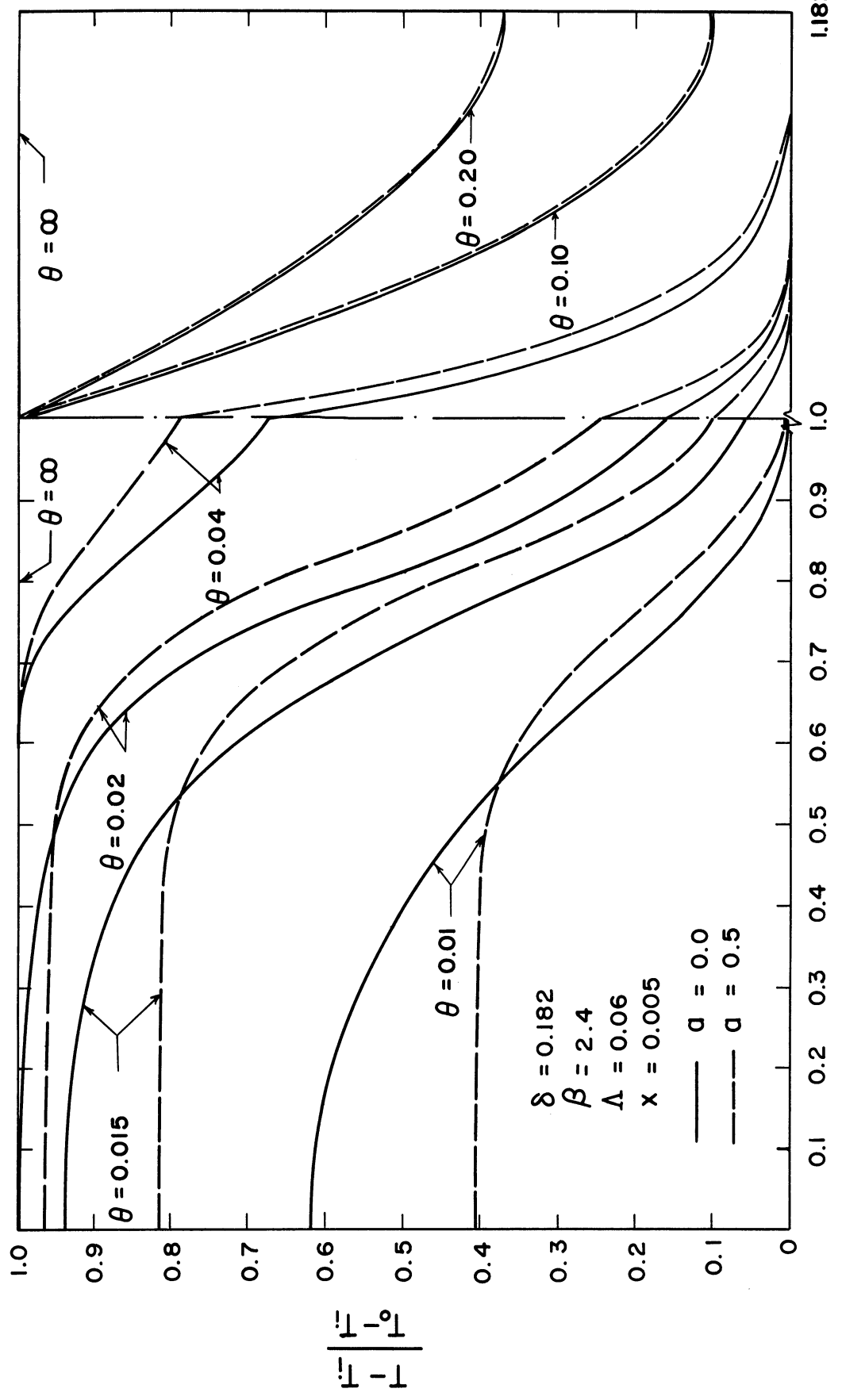

Figure 14. Fluid and Wall Temperature Response Due to Inlet Temperature Step.

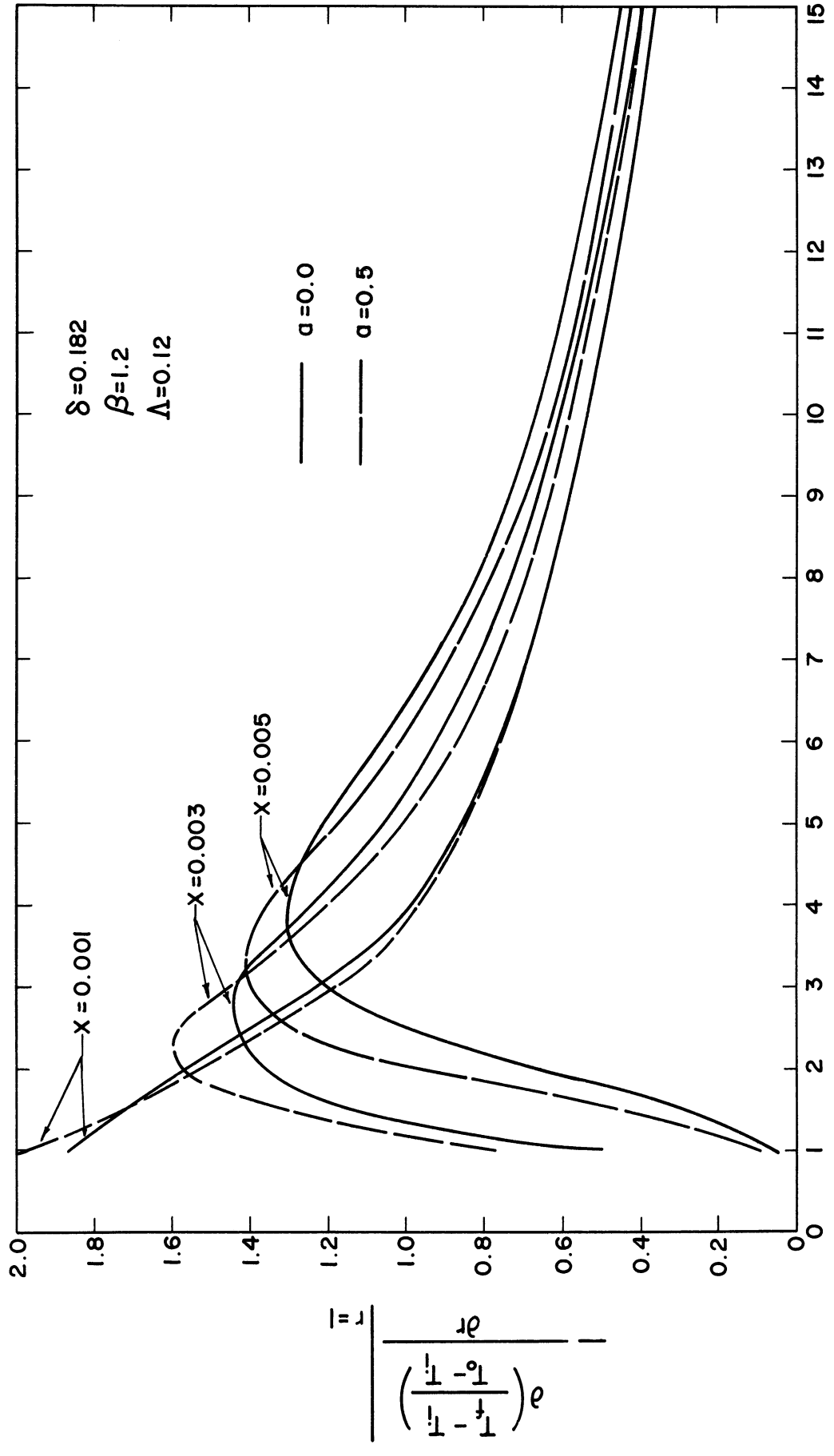

Figure 15. Response of Fluid Temperature Gradient at Fluid-Wall Interface Due to Inlet Temperature Response.

decreases towards zero as steady state is approached. The peak value of the temperature gradient decreases with axial distance because some cooling of the fluid has taken place due to heat transfer from the fluid to the tube wall. An increase in the Bingham plastic constant raises the peak value of the fluid-temperature gradient. The greater heat flux due to the increased gradient is the factor which causes the more rapid temperature rise of the fluid-wall interface for larger values of 'a', as shown in Figure 16.

D. Steady-Periodic Solution to Internal Heat Generation

The steady-periodic solution gives the temperature distribution in the fluid and wall due to sinusoidal internal energy generation, $q_o \in \mathrm{Sin}\Gamma\theta$, in the fluid. Quantities considered are the amplitude ratio, $AR = \frac{\sqrt{A^2+B^2}}{\epsilon\, \Psi_{sf}}$, and the phase angel, ϕ. The steady-periodic solution is a function of $\delta, \Gamma\chi, \epsilon, \beta, \Lambda$, a, and r.

A resonance phenomenon is evident in Figures 17 and 18 which display the amplitude ratio and phase shift, respectively, versus axial distance times frequency. This resonance phenomenon is known to be characteristic of distributed parameter systems under distributed disturbances[12]. As $\Gamma\chi$ increases, the amplitude ratio decreases; and the phase lag tends toward $\pi/2$.

Consideration of a simplified form of Equation (3.13), which assumes plug flow and neglects the effect of the tube wall, reveals some interesting results. The simplified equation becomes

$$\frac{\partial \Psi_f}{\partial \theta} + \frac{1}{2}\frac{\partial \Psi_f}{\partial \chi} = \epsilon\, \mathrm{Sin}\,\Gamma\theta \qquad (4.2)$$

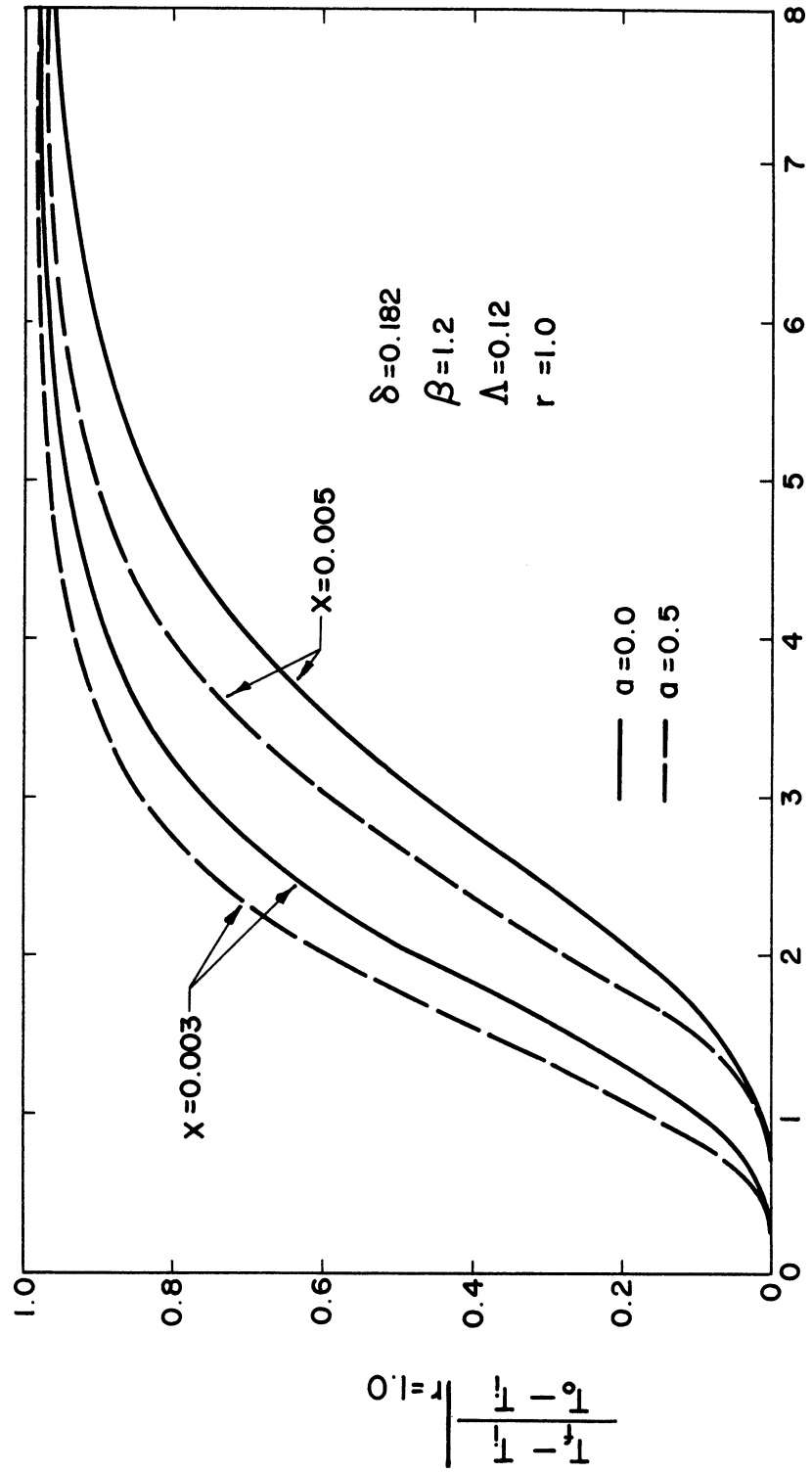

Figure 16. Response of Fluid-Wall Interface Temperature Due to Inlet Temperature Step.

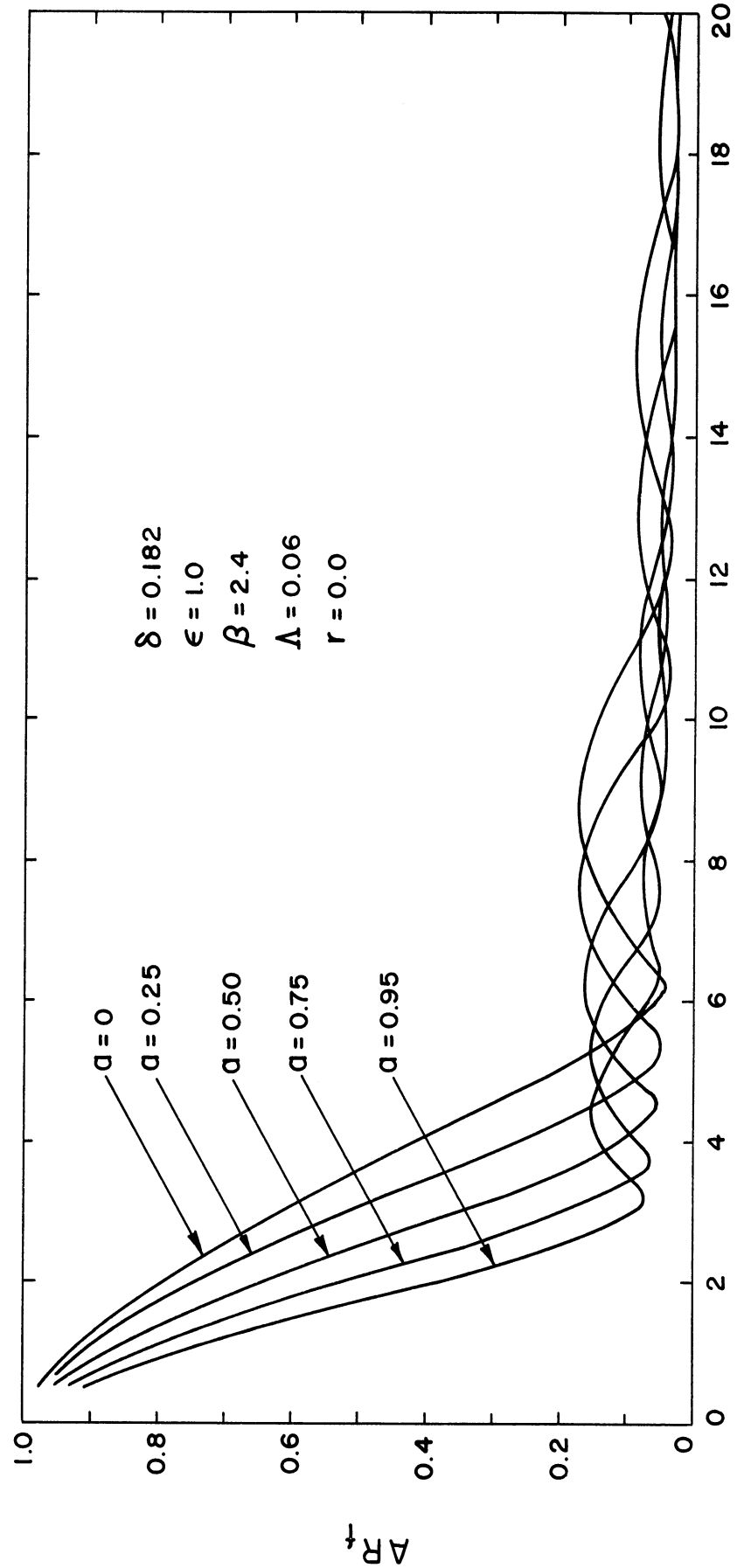

Figure 17. Amplitude-Ratio Response of Centerline Fluid Temperature as Function of 'a'.

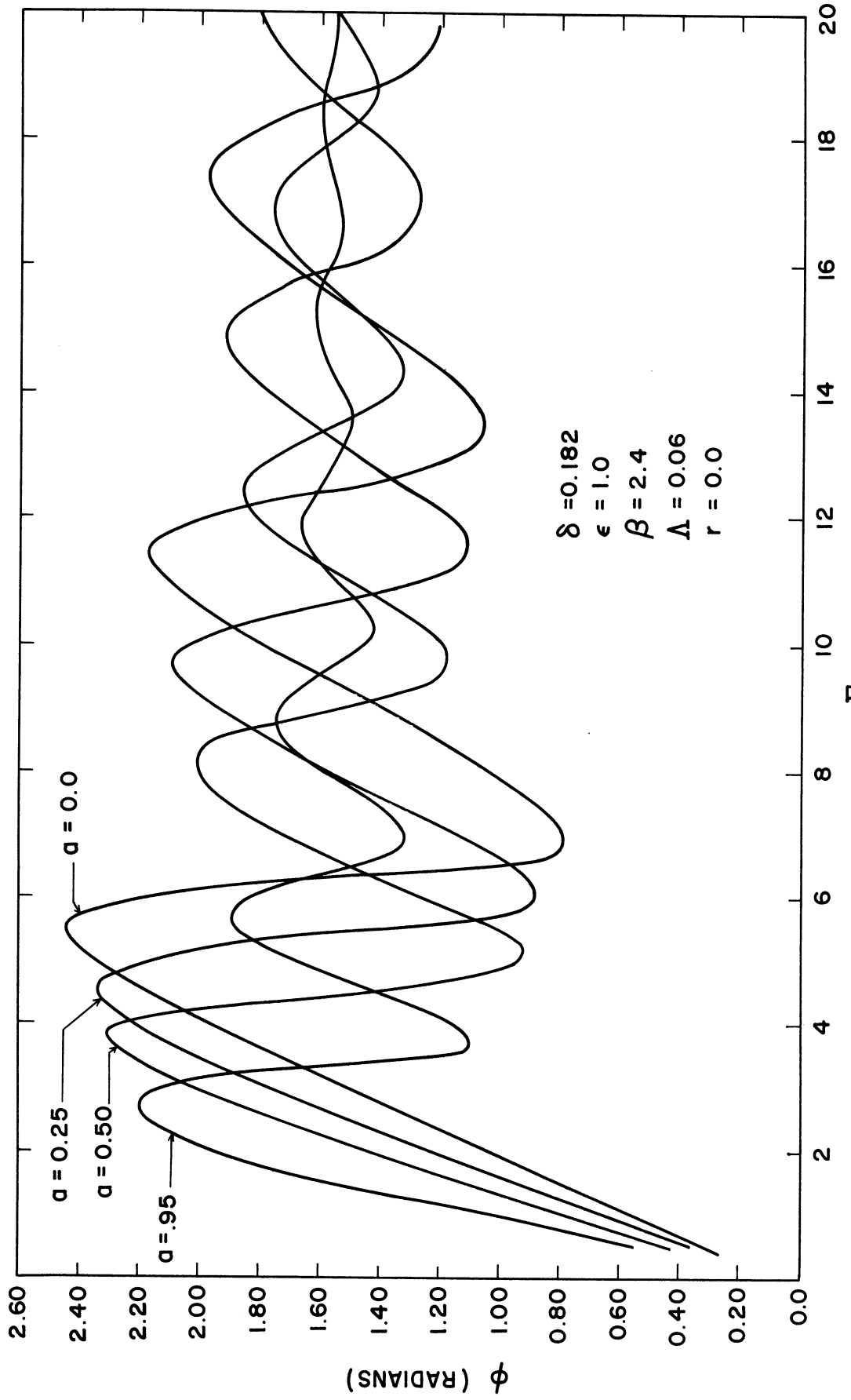

Figure 18. Phase Lag Response of Centerline Fluid Temperature as Function of 'a'.

The boundary conditions are

$$\psi_f(X,0) = 0 \qquad \text{(initial)}$$

$$\psi_f(0,\theta) = 0 \qquad \text{(entrance)}$$

After solving Equation (4.2) and considering only that portion of the result which corresponds to the steady-periodic solution ($\theta > \frac{X}{u}$), the following result is obtained.

$$\psi_f = \frac{\epsilon}{\Gamma}\left[\left(1-\cos 2\Gamma X\right)\cos\Gamma\theta + \sin 2\Gamma X \sin\Gamma\theta\right] \qquad (4.3)$$

Now for the case of $\Gamma = 0$

$$\psi_{f\,\Gamma=0} = \epsilon\frac{X}{u} \qquad (4.4)$$

The ratio of the steady-periodic temperature to the temperature when $\Gamma = 0$ can be written

$$\frac{\psi_f}{\psi_{f\,\Gamma=0}} = \frac{\left(1-\cos 2\Gamma X\right)\cos\Gamma\theta + \sin 2\Gamma X \sin\Gamma\theta}{2\Gamma X}$$

$$= \frac{\sqrt{2\left(1-\cos 2\Gamma X\right)}}{2\Gamma X}\sin\left[\Gamma\theta + \tan^{-1}\left(\frac{1-\cos 2\Gamma X}{\sin 2\Gamma X}\right)\right] \qquad (4.5)$$

Equation (4.5) and Figures 17 and 18 show that for the case of plug flow ($a = 1.0$) there is a resonance phenomenon of period $\Gamma X = \pi$. As seen from Figures 17 and 18, decreasing the value of 'a' increases the period of resonance until at $a = 0.0$, (Newtonian fluid) the period is about 2π. The quantity ΓX used for the abscissa in Figures 17 and 18 was shown to be meaningful by the natural occurrance of ΓX in Equation (4.5). Also the plots of AR versus ΓX from numerical

solutions obtained for various values of Γ fell on the same line.

The resonance phenomenon can best be explained physically by considering a single fluid particle as it travels through the tube. If the fluid particle passes the location $x = 0$, where heat generation is assumed to begin, with some inlet lag $\Gamma\theta'$ (see Figure 19), a simplified equation can be obtained for an observer located on the particle by eliminating the space derivative of Equation (4.2).

$$\frac{\partial \psi_f}{\partial \theta} = \epsilon \sin\left(\Gamma\theta + \Gamma\theta'\right) \tag{4.6}$$

Integrating Equation (4.6) subject to the boundary condition $\psi_f(0) = 0$ yields

$$\psi_f = \frac{\epsilon}{\Gamma}\left[\left(1 - \cos\Gamma\theta\right)\cos\Gamma\theta' + \sin\Gamma\theta\,\sin\Gamma\theta'\right]$$

The ratio of the steady periodic temperature to the temperature when $\Gamma = 0$ can be written

$$\frac{\psi_f}{\psi_{f\,\Gamma=0}} = \frac{\sqrt{2\left|1-\cos\Gamma\theta\right|}}{\Gamma\theta}\sin\left[\Gamma\theta' + \tan^{-1}\left(\frac{1-\cos\Gamma\theta}{\sin\Gamma\theta}\right)\right] \tag{4.7}$$

From Equation (4.7) it can be seen that the resonance phenomenon which appears in Figures 17 and 18 is due to the inlet phase lag shown in Figure 11. At $\Gamma\theta = 2\pi,\ 4\pi,\ \ldots\ 2n\pi$, the total energy generated in the fluid is equal to the energy which would be generated by steady state energy generation ($\Gamma = 0$). The transient component of the particle temperature would be expected to be zero. However, the effect of the wall causes some transient component of the temperature to remain even at $\Gamma\theta = 2\pi,\ 4\pi,\ \ldots\ 2n\pi$. For plug flow the time θ can be replaced by the physical time $\frac{x}{u} = 2x$. Again it is shown that resonance occurs for plug flow with a period of $\Gamma\theta = 2\pi$ or $\Gamma X = \pi$.

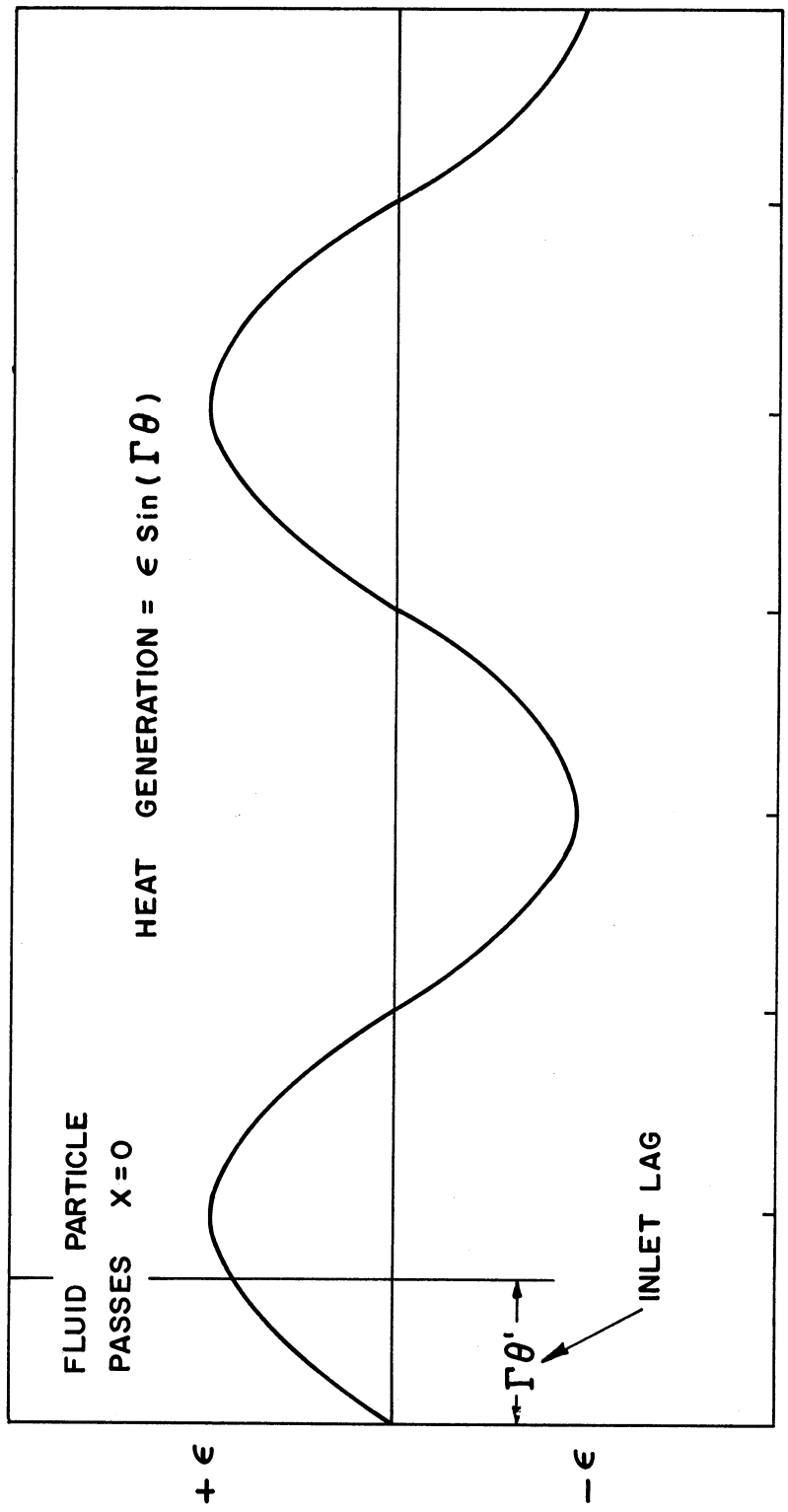

Figure 19. Relationship between Sinusoidal Energy Generation and the Time at which a Fluid Particle Passes Location X = 0.0.

Figures 20 and 21 display the effect of radius upon the amplitude ratio and phase angle respectively. As the wall is approached ($r \to 1$), the damping effect due to the wall increases. This causes the amplitude ratio to decrease and the phase angle to approach $\pi/2$.

The amplitude ratio and phase-angle lag versus radius are given in Figures 22 and 23, respectively. A non-monotonic nature of the curves for larger values of ΓX is illustrated.

Figure 24 presents the temperature gradient in the fluid at the fluid-wall interface as a function of time. The time-average of the wall gradient was evaluated numerically and found to be less than 10^{-9}. A zero average wall gradient is necessary because the outer wall of the tube is insulated.

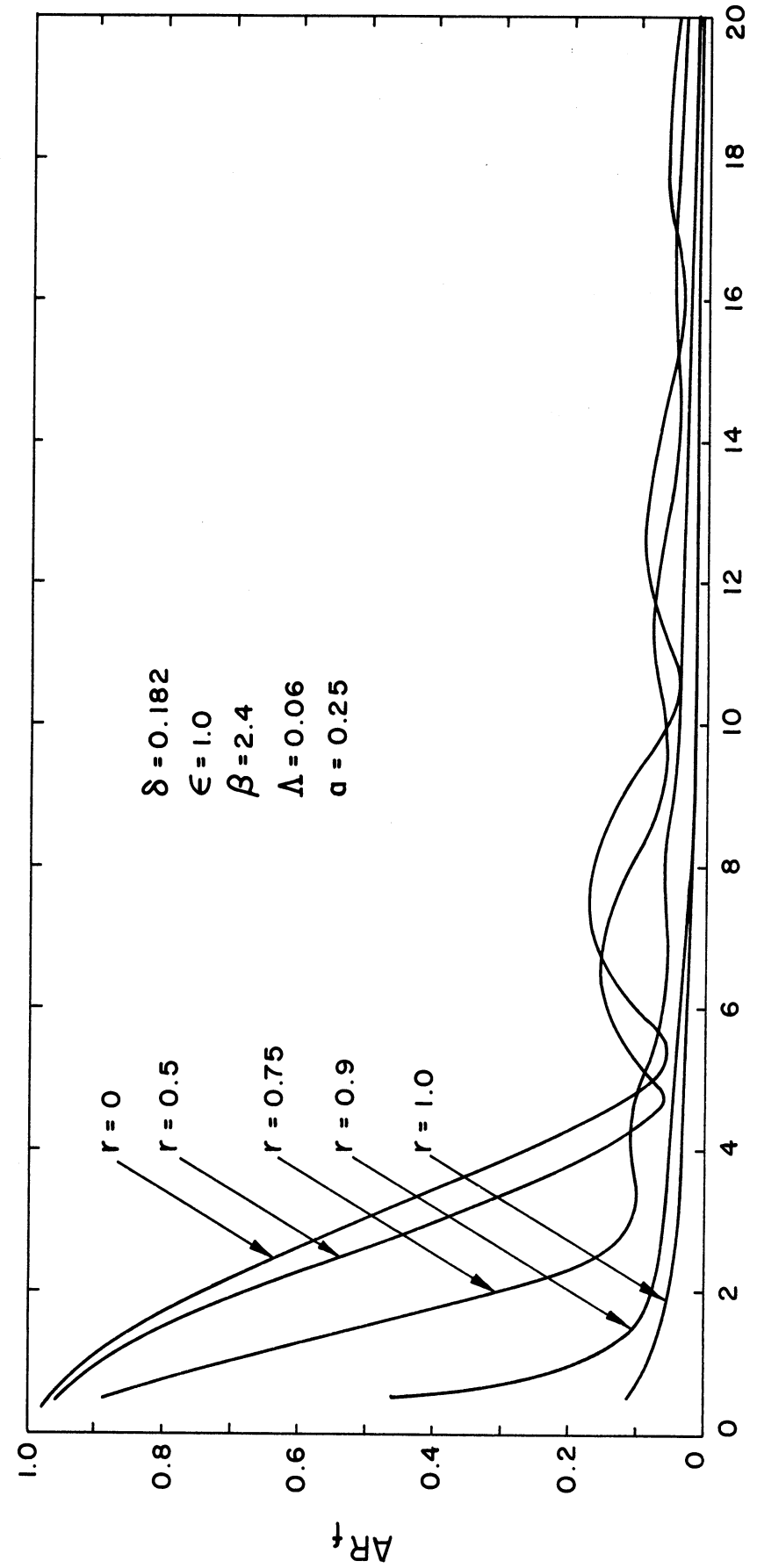

Figure 20. Fluid Amplitude Ratio versus Axial Distance Times Frequency for Various Radii.

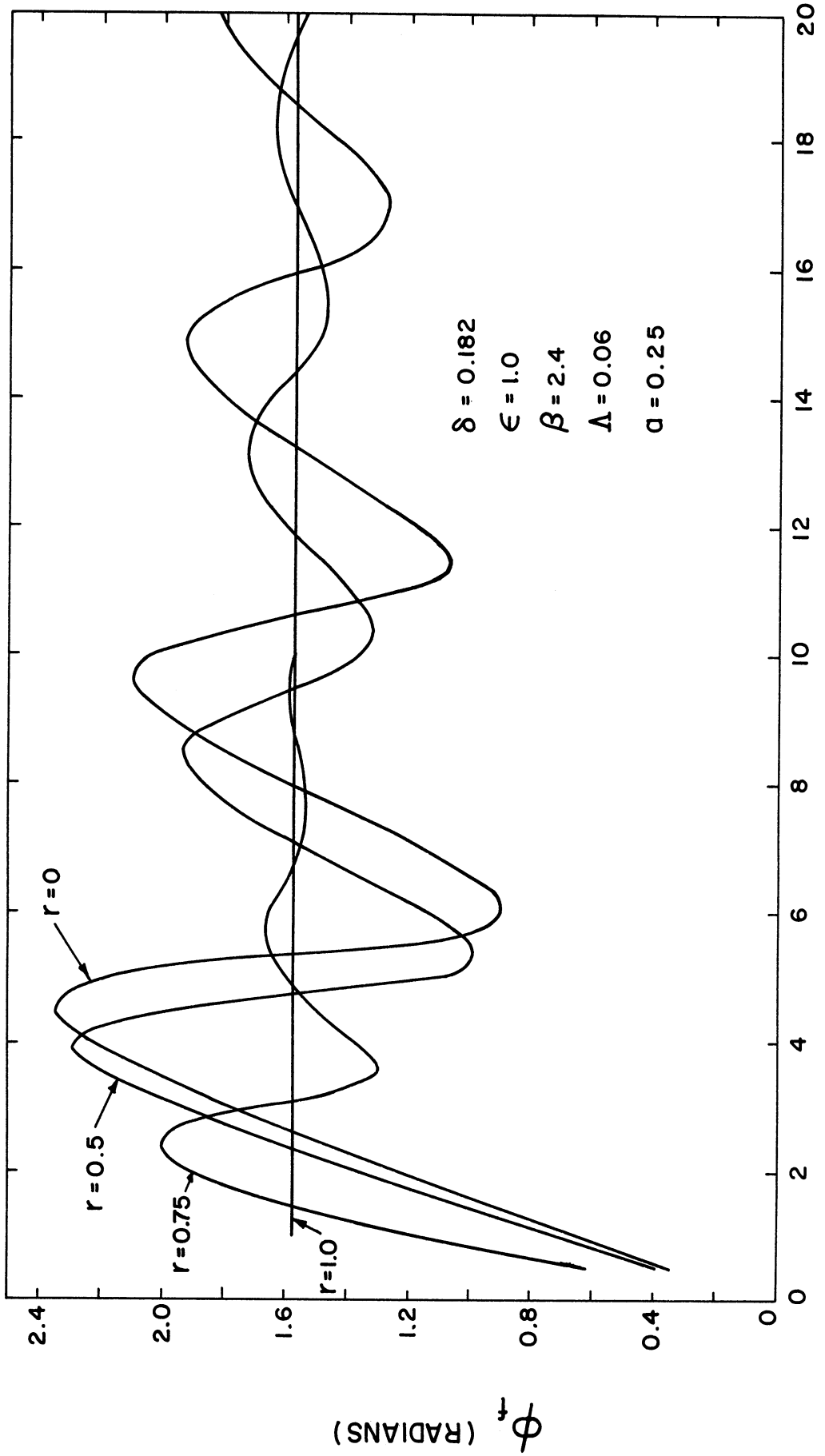

Figure 21. Fluid Phase Angle Lag versus Axial Distance times Frequency for Various Radii.

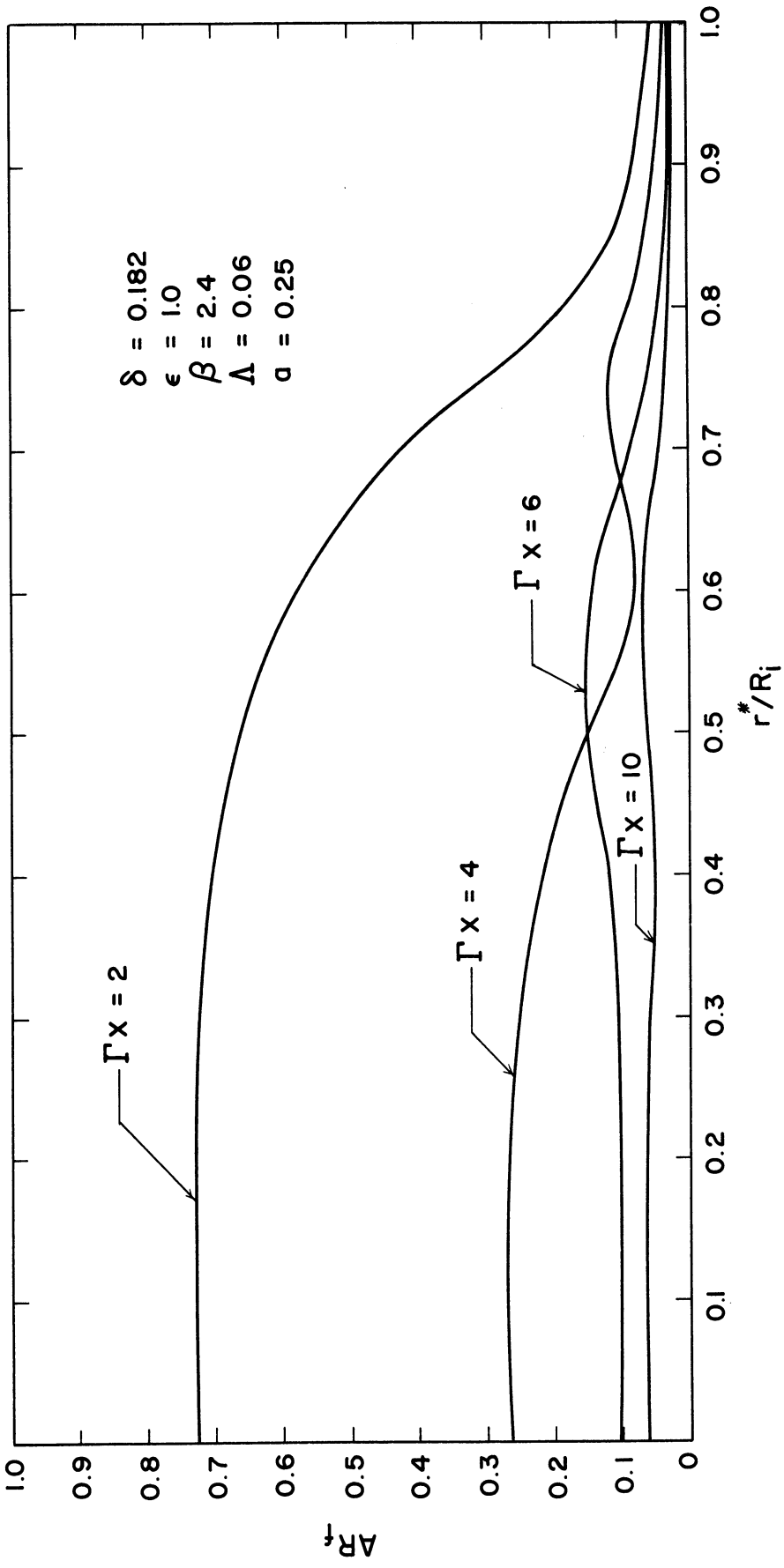

Figure 22. Fluid Amplitude Ratio versus Radius for Various Values of ΓX.

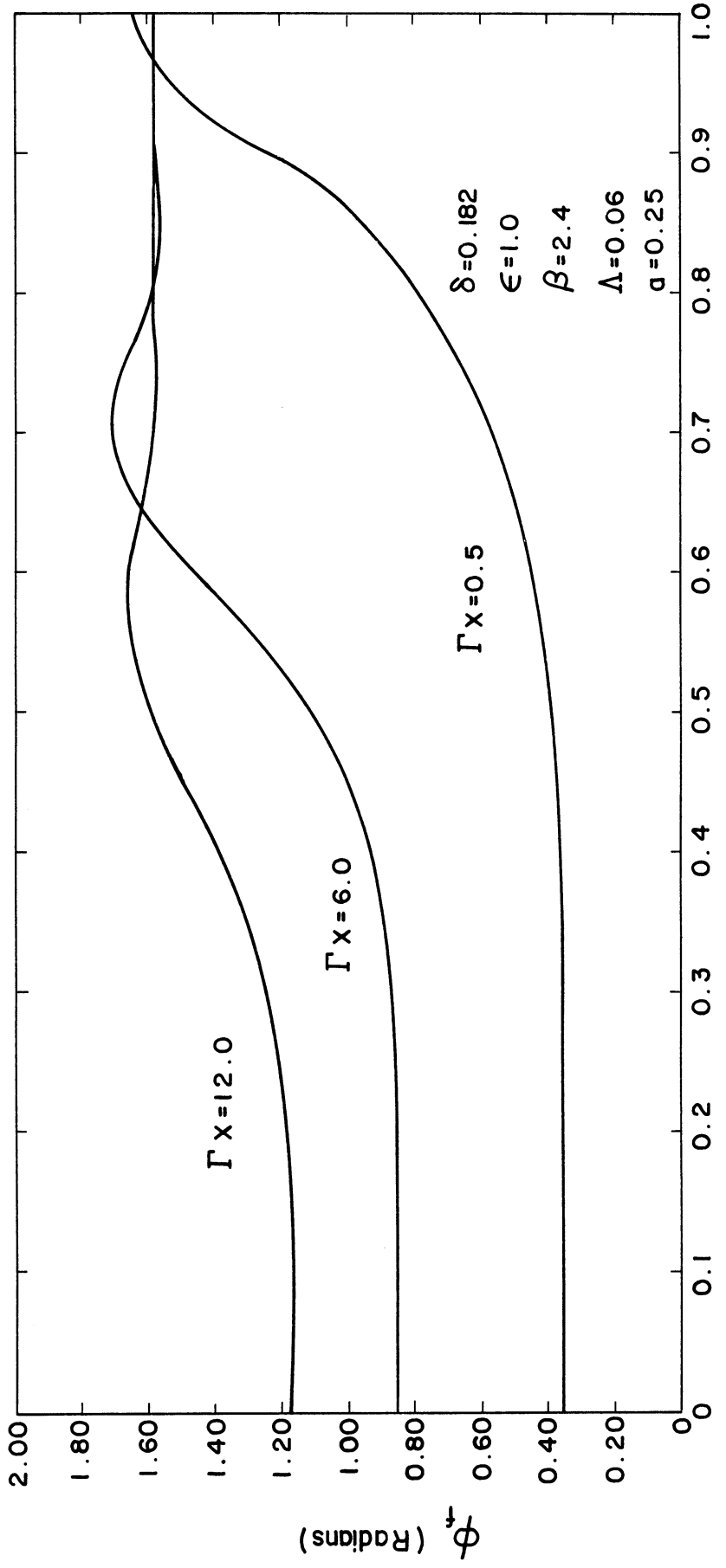

Figure 23. Fluid Phase Angle Lag versus Radius for Various Values of ΓX .

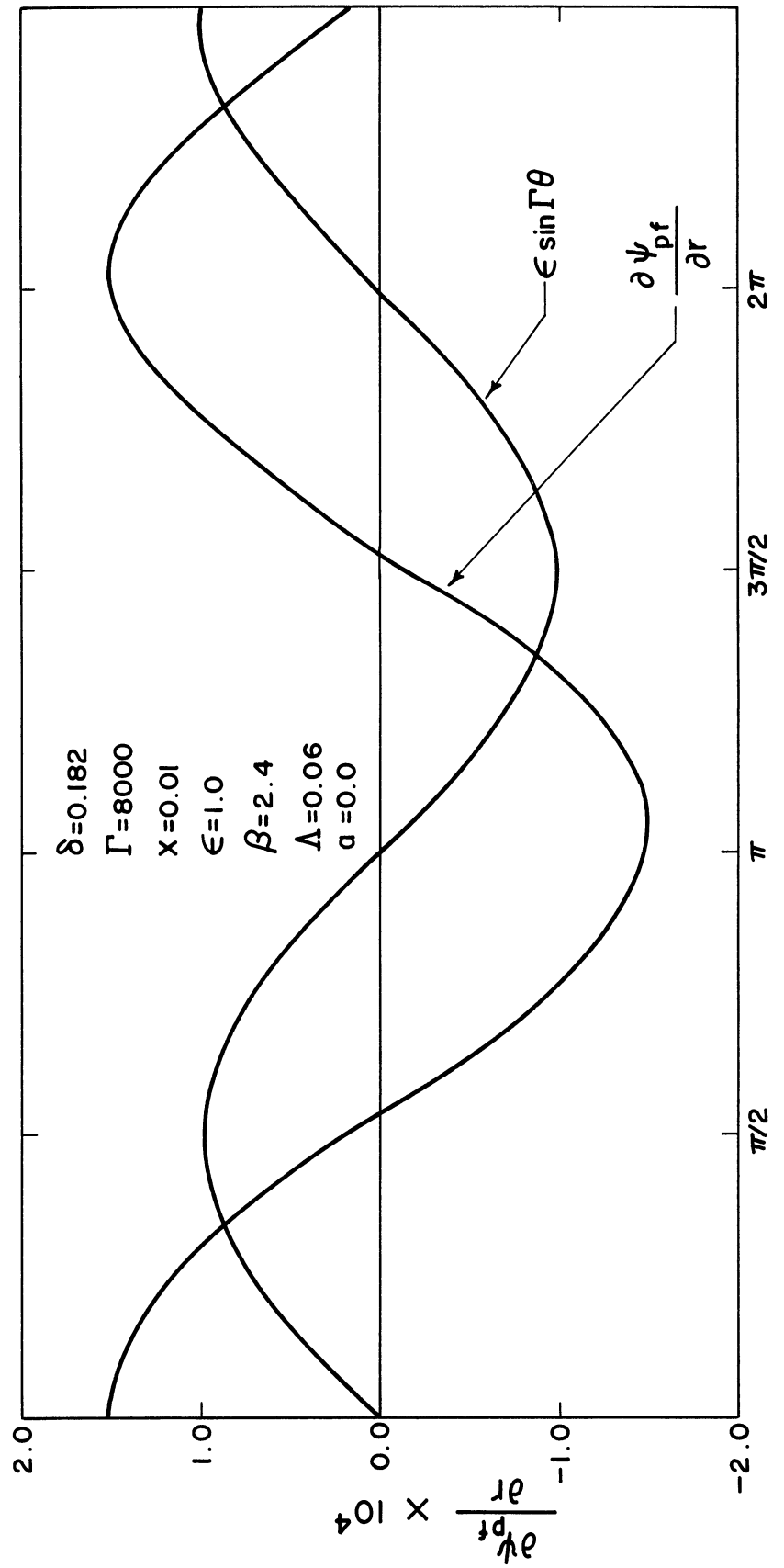

Figure 24. Periodic Temperature Gradient in Fluid at Fluid-Wall Interface.

CHAPTER V

EXPERIMENTS

An experimental program was conducted in order to determine the validity of the assumptions made in the analytical model, to ascertain under what conditions the analytical solution can be used, and to provide a confirmation of the numerical results.

A. Experimental Apparatus

The physical system to be experimentally investigated consists of an insulated horizontal tube through which a fluid, with and without solid suspension, flows steadily with electrically-produced internal heat generation. A schematic diagram of the system is shown in Figure 25. Temperatures were measured radially in the fluid and at the fluid-wall interface at the top, bottom, and sides of the horizontal test section. Mass flow rate, energy generation rate, and inlet and exit temperatures were simultaneously measured. The experiments were performed in the Heat Transfer Laboratory, Department of Mechanical Engineering, the University of Michigan.

As illustrated in Figures 25 and 26, the component parts of the apparatus are; test section, fluid supply, heat exchanger, direct current power supply, and appropriate instrumentation.

1. Test section

The test section is a 3/4" I.D., 7/8" O.D., polyvinyl-chloride tube, 1 foot in length. The fluid flowing through the tube is 25 per cent sulfuric acid, a good electrolyte, through which an

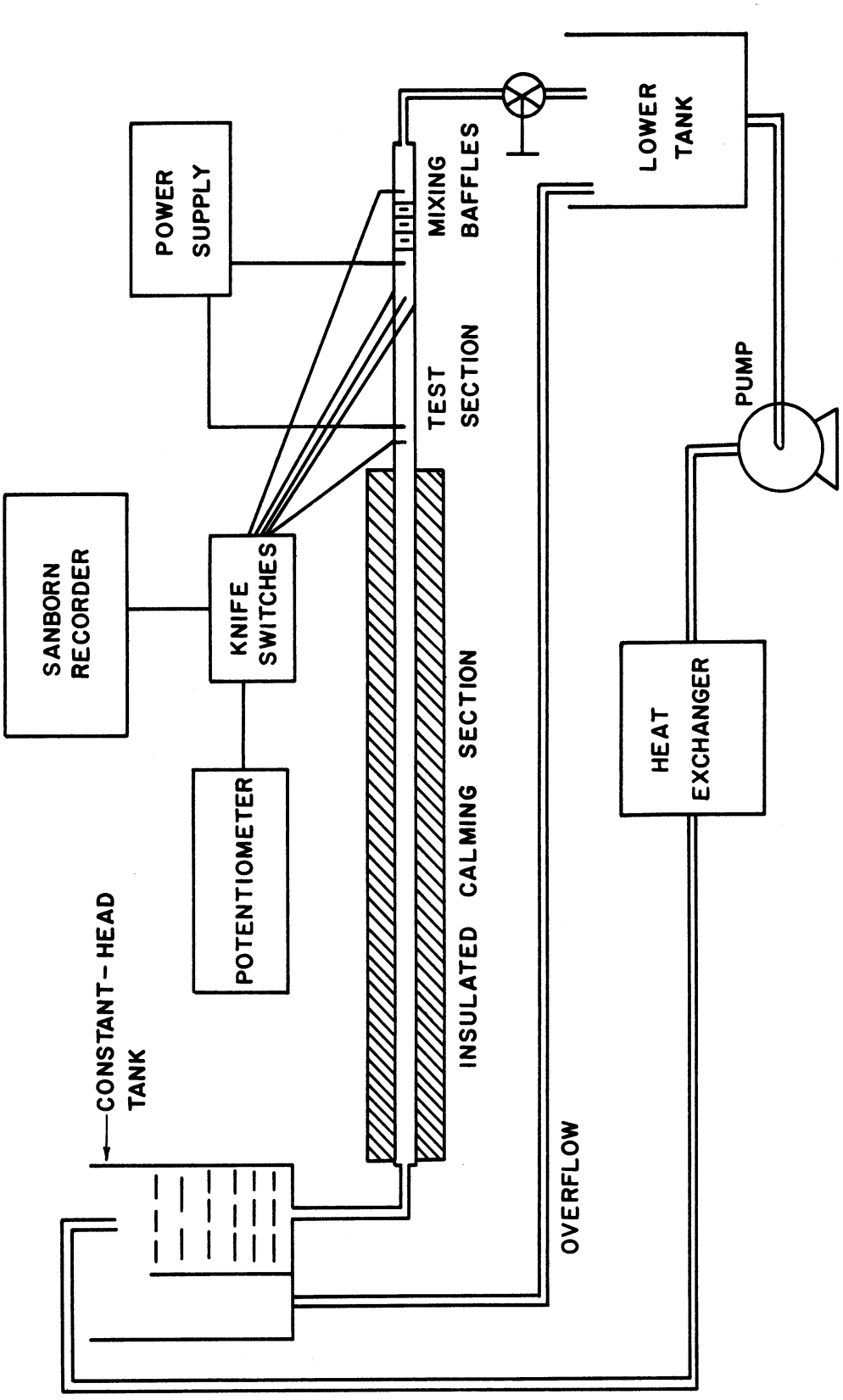

Figure 25. Schematic Diagram of Experimental Equipment.

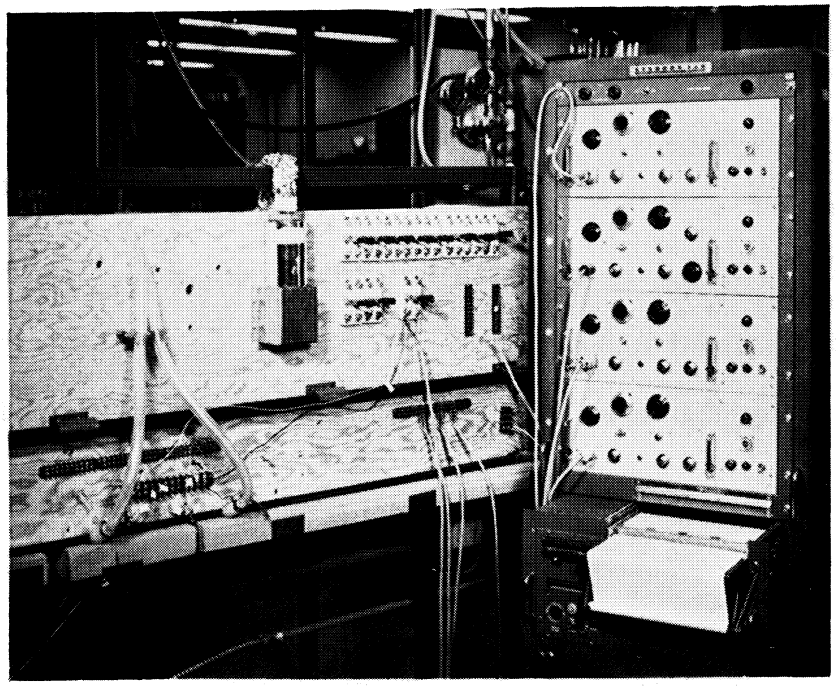

Figure 26. Experimental Apparatus Showing Test Section, Knife Switches, and Four Channel Sanborn Recorder.

electric current is passed from two platinum electrodes to produce internal heat generation. The polyvinylchloride tube was selected because of its corrosive resistance against the acid, besides being an electrical and thermal insulator. Preceding the test section was a 5 feet length of tubing encased in styrofoam insulation. This served the double purpose of establishing a fully-developed hydrodynamic condition as well as eliminating any influence on the inlet fluid temperature resulting from radial conduction of heat.

Following the test section, mixing baffles were installed in the tube just upstream from the outlet fluid thermocouple as shown in Figure 27. This thermocouple read the mixed mean temperature of the fluid leaving the test section. The baffles are made of 0.1 inch thick polyethylene disks of negligible heat capacity with alternately spaced holes.

2. Fluid supply and heat exchanger

A steady-state flow of test fluid was established by a constant-head tank located about 15 inches above the test section. The flow rate was measured using the discharge from the test section which was pumped continuously from a lower collection tank by a 1/15 horsepower stainless steel pump. Before returning to the constant-head tank, the fluid was passed through a heat exchanger consisting of a 50 foot coil of 3/8 I.D. polyvinylchloride tubing submerged in a constant-temperature water bath. Heat generated within the fluid in the test section was removed by the low temperature coolant in the heat exchanger.

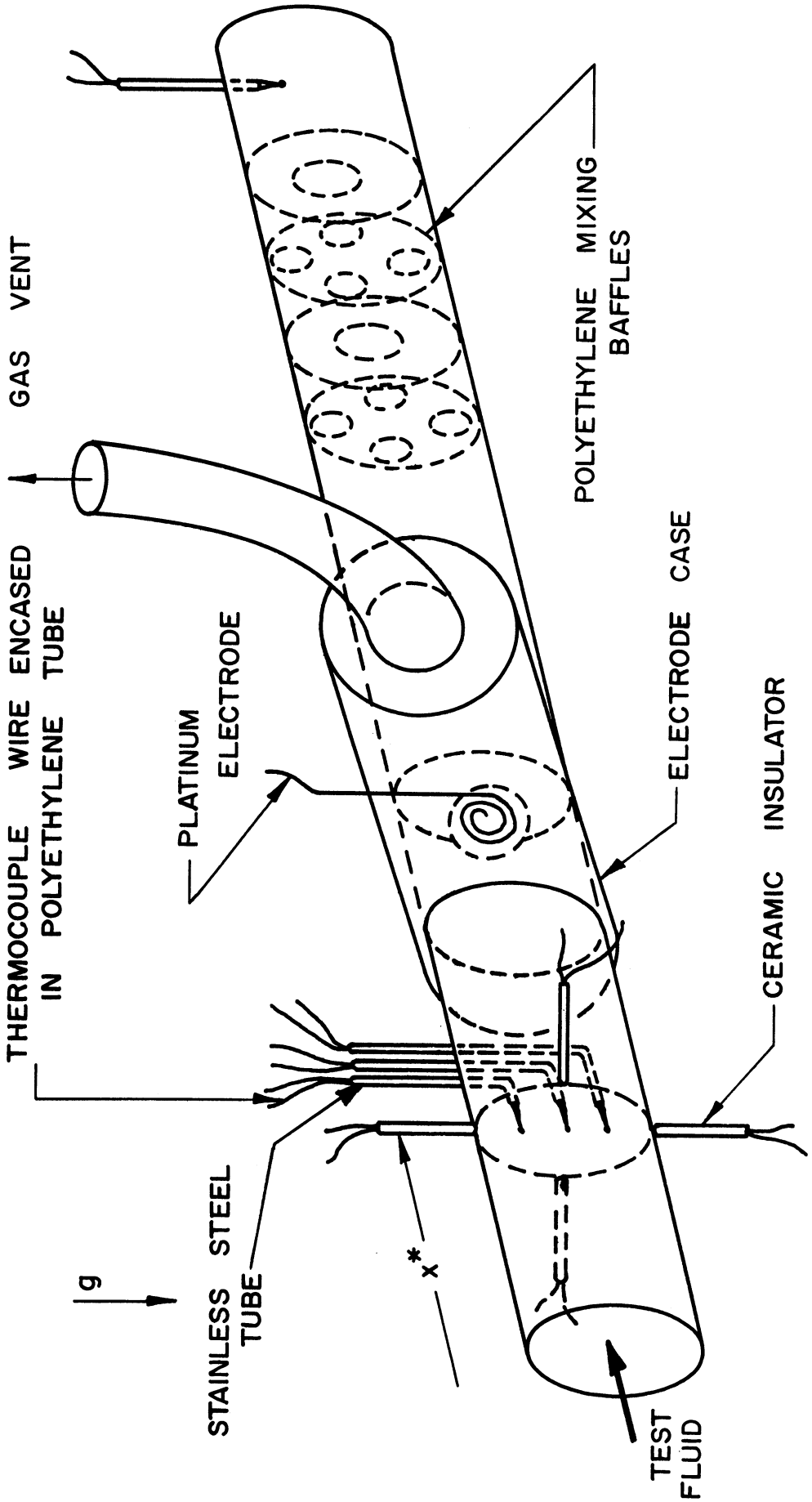

Figure 27. Detail of Test Section and Mixing Baffles.

3. Thermocouples

The locations of the wall and fluid thermocouples, all made from 0.002" diameter copper and constantan wires, are shown in Figures 25 and 27. One fluid thermocouple was located upstream of the leading electrode, one immediately after the mixing baffle, and three at a distance of 7.8" from the leading electrode. The last three thermocouples were placed radially at the centerline and at distances halfway between the centerline and the inner surface, respectively. They were encased in 0.011" I.D. polyethylene tubes and placed in an 0.050" I.D. stainless steel tube, as shown in Figure 27. It was necessary to coat all thermocouples which extended into the fluid with General Electric 1201 Enamel. This coating protected the thermocouples from the corrosive effects of the sulfuric acid and eliminated any direct current voltage from being superimposed on the thermocouple emf. The final diameter of the coated thermocouple junction was estimated at .005 inch.

Four wall thermocouples were installed at a distance of 7.8 inches from the leading electrode at the top, bottom, and both sides of the inner surface. Holes were made in the tube wall. Then the thermocouples were placed as near as possible to the fluid-wall interface and the holes filled with a solvent mixture of the wall material. Care was taken to electrically insulate the thermocouple wire from the fluid by an estimated .005 inch of the wall material.

The inherent lag of the coated thermocouple made from 0.002" diameter copper constantan thermocouple wires was found to be less than 0.1 second by monitoring the transient thermocouple response with

a Sanborn recorder when energy generation was suddenly started in the test section while the fluid was stationary.

By considering the thermal resistance of the air outside the tube, the tube wall, and the fluid inside the tube, the calculated heat loss from the tube was about 1 BTU/hr-ft^2 for a 10°F temperature difference. This heat loss amounts to less than 0.1 per cent of the heat being generated in the tube. However, when considering the thermal resistance of the fluid and a 0.005 inch covering of wall material on the thermocouple, a 0.45°F error in temperature measurement results.

Embedding a thermocouple wire of high thermal conductivity in a low conductivity material can cause an error resulting from increased heat conduction along the wire. J. V. Beck[30] considered the problem of a cylinder embedded in a semi-infinite solid perpendicular to a surface subjected to a heat flux. The equation for the disturbance is given below, where evaluation of the factor F was done numerically and presented in graphical form.[30]

$$\Delta T = F \frac{\dot{q} R_{wire} k_{wire}}{k_w^2} \qquad (5.1)$$

For a copper wire embedded a distance of two wire diameters below the surface of a semi-infinite polyethylene solid whose surface receives a heat flux of 1 BTU/hr-ft^2, an upper limit on F may be obtained by extrapolating the graphs presented by Beck. Substitution of the appropriate values into Equation (5.1) results in a temperature disturbance of 0.25°F due to the presence of a wall thermocouple being embedded in the test section tube wall.

4. Heat generation device

Two platinum electrodes placed 11 inches apart at the sides of the tube were made of spirals of 36 gage platinum wire and enclosed in a polyethylene chamber as shown in Figure 27. A 3/8 inch hole was made in the tube wall next to the electrodes to allow electrical contact with the circulating fluid. The polyethylene chambers were located at a place where all gas generated at the electrodes due to electrolysis was caught and vented through a vertical tube. Thus, gas bubbles were prevented from entering the fluid flowing through the test section.

The location of the electrodes at the side of the tube caused a non-uniform energy generation across the tube section, especially near the region of the electrodes. It is estimated in Appendix C that the electrical entrance length, defined as the one per cent variation of the potential across the channel cross-section, is about 1.3 diameters. This is not totally insignificant since the test section thermocouples were located roughly 10 diameters from the leading electrode. However, temperature measurements given in section C disclosed no consistent asymmetry in the fluid temperature resulting from the nonsymmetrical location of the electrodes.

Because the electrodes were of finite size and the electrical potential was non-uniform near them, an effective length between the electrodes was taken as 10.5 inches. This length is subject to an uncertainty of $\pm$ 0.5 inches.

For an experimental fluid, a good electrolyte was necessary in order to electrically produce internal energy generation. A sulfuric

acid solution (25% by weight) was chosen because of its high electrical conductivity[2].

It is possible to eliminate electrolysis of the fluid at an electrode by using an alternating current power source of about 400 cycles per second[31]. However, when transient temperature measurements are to be made the resolution of the recording instrument is often reduced by the superimposing of an alternating voltage upon the thermocouple emf due to inductance between the power source and temperature-sensing instrumentation.

Attempts to use both a 60 cycles per second alternating current power source and a full wave rectifier resulted in an a.c. pickup which was not eliminated by extensive electrical shielding. Finally, several 12 volt automobile batteries were used either in parallel or series for the power source. The voltage applied to the electrodes ranged between 24 and 48 volts.

For the electrolysis of a strong acidic solution the reactions at the electrodes are given by[32]

cathode reaction

$$2\,H^{+} + 2\,e^{-} \longrightarrow 2\,H_2\uparrow$$

anode reaction

$$4\,OH^{-} \longrightarrow O_2\uparrow + 2\,H_2O + 4\,e^{-}$$

then the net reaction is

$$4\,H^{+} + 4\,OH^{-} \longrightarrow 2\,H_2\uparrow + O_2\uparrow + 2\,H_2O$$

Faraday's Law of Electrolysis states that the weight of a substance produced by a cathode or anode reaction in electrolysis is directly proportional to the quantity of electricity passed through the cell and is proportional to the equivalent weight of the substance. Using the heat of formation of water, Faraday's Law, and the definition of a faraday (magnitude of the charge of one mole of electrons) as being equal to 96,500 ampere-seconds, the energy absorbed at the electrodes due to electrolysis is found to be equal to 5.05 BTU/amp-hr. The resistance of the loop external to the test section was calculated to be at least 200 times that of the test-section, so that essentially no energy generation occurred externally. Considering electrolysis and resistance heating, the energy generation taking place in the test-section fluid is given by

$$q'' = \frac{3.413\ E\ I - 5.05\ I}{\pi\ R_i^2\ L} \qquad (5.2)$$

5. Instrumentation

Instrumentation was required to measure and record fluid and wall temperatures, voltage and current, and fluid flow rate.

Transient measurement of thermocouple emf and test section voltage were recorded on a four channel Sanborn 150 series recorder which had a maximum sensitivity of 10μv/mm. The resolution of the line on the recording paper was estimated to be better than $\pm$ 0.5 millimeters.

A Leeds and Northrup model 8662 precision potentiometer was used to record the steady state thermocouple emfs. The resolution of the instrument was estimated to be 0.005 millivolts.

Volume flow rate was determined by a calibrated 1100 cm^3 vessel, accurate to 5 cm^3, and a stop watch.

The voltmeter and ammeter used to measure test-section energy generation were calibrated against Weston laboratory standard instruments. The resolution of the voltmeter was 0.2 volts and that of the ammeter was 0.02 amperes.

6. Bingham-plastic fluids

As described in Chapter II, colloidal slurries of solids in liquids behave like Bingham-plastic fluids when the solid particles are sufficiently small or sufficiently close together.

Slurries of titanium dioxide and Kaolin with 25 per cent sulfuric acid were found to be unsatisfactory because of rapid settling rates resulting from large particle size. Finally, aluminum oxide was adopted as a solid phase. After grinding the Al_2O_3 with water in a rotating ball mill for 10 days, the particle size was reduced to about 3 microns. On a microscope slide the particles formed flocs in concentrated areas, although independent particles were present as well.

B. Test Procedure

Major experimental programs conducted were velocity and heat transfer measurements for both Newtonian and Bingham plastic fluids, and the measurement of some rheological properties of Bingham-plastic fluids. Tube pressure drops and laminar velocity profiles were found with pitot-tube probes, while transient and steady-state temperatures were sensed by fine-wire thermocouples. Determination of viscosity and yield stress of Al_2O_3 slurries in H_2SO_4 was done with a Brookfield rotational viscometer.

1. Velocity measurements

Attempts to measure velocity profiles and wall shearing stresses in slurries with pitot-tube probes were not very successful. Static pressure probes 0.10 I.D., spaced 50 diameters apart, were located in the tube wall. In addition, the radial position of a total pressure probe 0.030 in I.D. was controlled by a micrometer screw. A Chattock gage[33], precision manometer, was modified to allow measurement of differential water pressures by replacing the usual water phase of the gage with an oil of specific gravity equal to 1.2. This replacement increased the sensitivity of the instrument by a factor of 5, so that the resolution of the gage was 0.0013 inches of water.

Prior to making tests with slurries, wall friction factor and pitot tube efficiency tests were conducted. The results are shown in Figure 28 where h_f represents the velocity head. The measured friction factor agrees quite well with the usual Moody diagram while the total-static pitot tube probes are seen to be about 95 per cent efficient.

Measurement of the velocity profile in distilled water yielded the expected results for a Newtonian fluid as given by Figure 29. The solid lines corresponding to the velocity head of a parabolic velocity profile were calculated from flow rate data. The tendency of the experimental points to lie above the calculated line could have resulted from the tendency of the observer to read the Chattock gage a little high.

A slurry of Al_2O_3, 1.3 per cent by volume with a particle size of about 1 micron, was prepared and circulated in the test apparatus. After 20 hours of operation, a hard cake had formed on the bottom of the

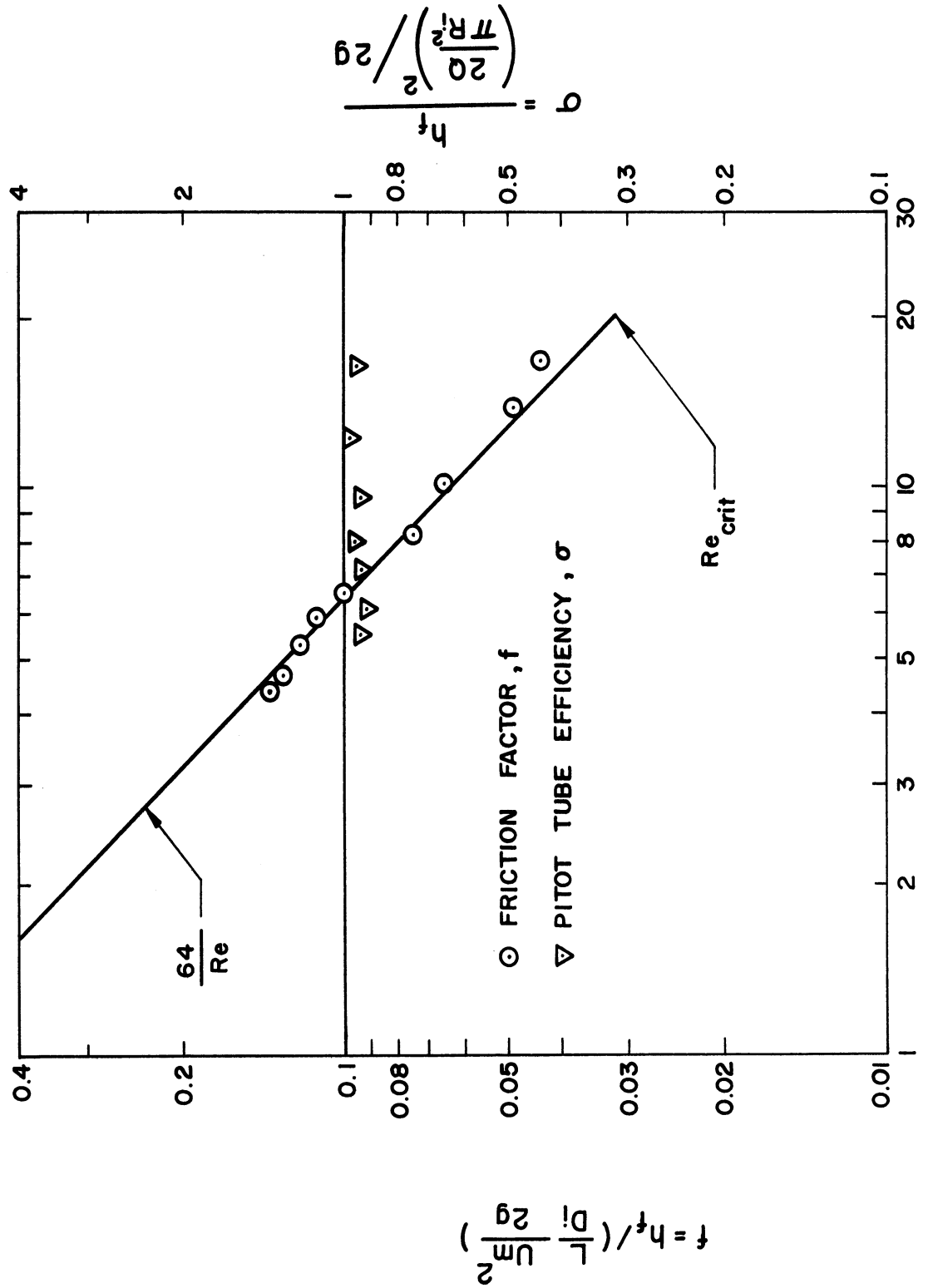

Figure 28. Friction Factor and Total-Static Pitot Tube Efficiency as Function of Reynolds Number.

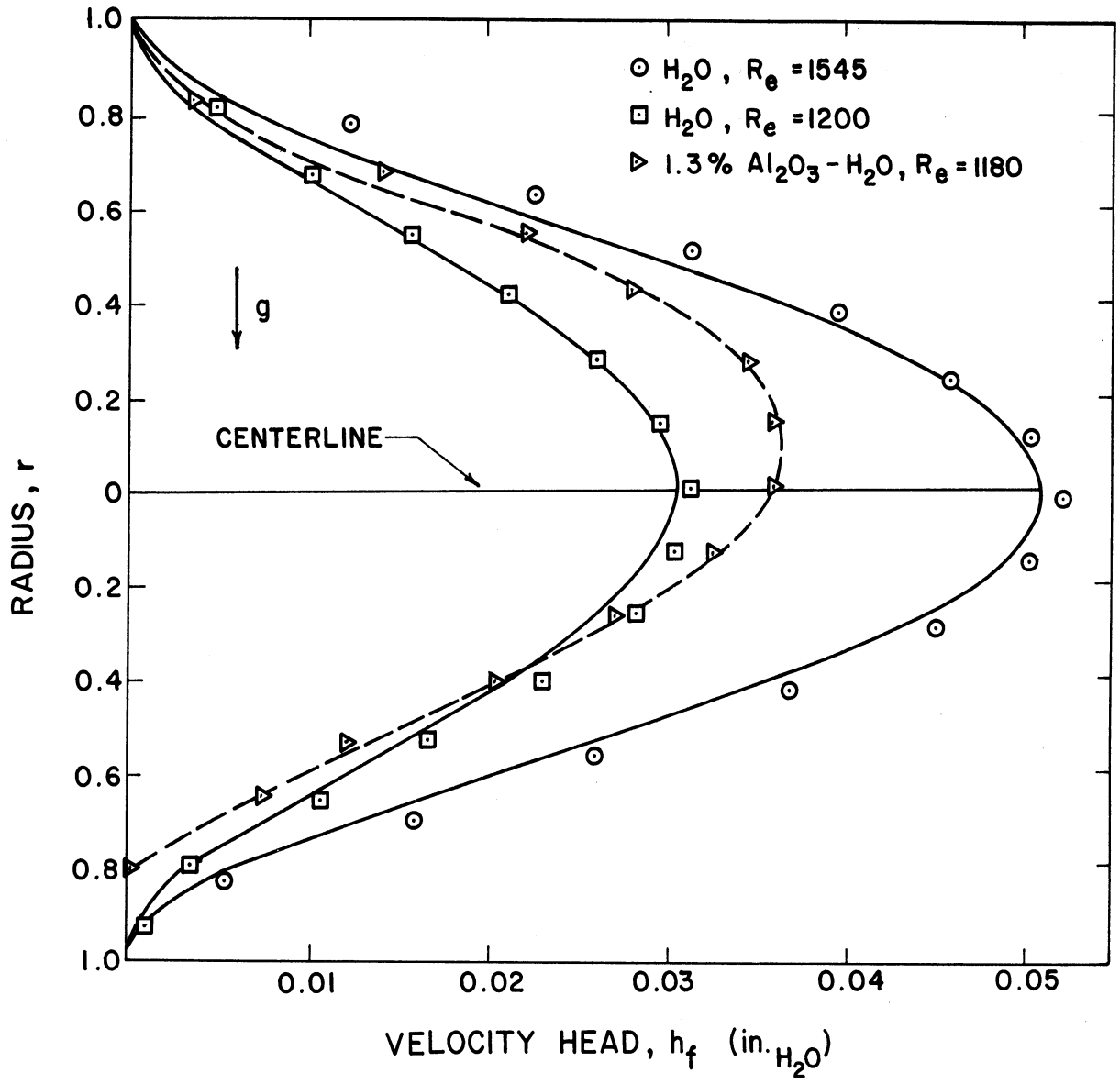

Figure 29. Radial Profiles of the Velocity Head in a Horizontal Tube.

tube which fractured when deformed (a report has been made of a 1/4 to 3/8 inch layer of ThO_2 cake being built up on all parts of a 3 inch 200 gallon per minute circulating system[25]). Attempts to measure the velocity profile in the slurry were frustrated by the plugging of the pitot tubes with solid particles and time variant density changes of the fluid in the pitot tubes. The pitot tubes were down-flushed with water to clean out the Al_2O_3 particles and to remove any density gradient in the probes. However diffusion, small disturbances in the fluid flow rate, and radial movement of the total pressure probe caused particles to enter the pitot probes, cause density changes, and seriously disrupt the measurement of pressures. One velocity profile of uncertain accuracy is presented in Figure 29. The zero velocity at the bottom of the tube was known to be present by the inability of the pitot tube to penetrate to the tube wall. The velocity profile shifts upward, but does not exhibit the characteristic plug of a Bingham plastic and appears to be Newtonian in nature.

2. Measurements and evaluation of physical properties of Bingham-plastic fluids

Increasing the concentration of the slurry to reduce settling and increase yield stress worsened the plugging of pitot tubes and inaccuracies of pressure measurements due to changing vertical density gradients in the probes. Finally a Brookfield LVT rotational viscometer with a UL adapter was used to rheologically define the properties of denser slurries. The UL adapter consisted of a rotating bob contained in an open cylinder with a ratio of cylinder to bob diameter, s , of 1.0983. By a method given by Metzner[19] the torque versus rotational

speed data in Figure 30 were converted into the conventional fluid-flow curves shown in Figure 31. The shearing stress is expressed as

$$\tau = \frac{2\ Torque}{\pi d^2 \ell} \tag{5.3}$$

The shearing rate was evaluated from the following equation:

$$-\frac{du}{dr} = \frac{4\pi N}{1 - 1/S^2}\left[1 + K_1\left(\frac{1}{n''} - 1\right) + K_2\left(\frac{1}{n''} - 1\right)^2\right] \tag{5.4}$$

where $K_1 = \frac{S^2 - 1}{2S^2}\left(1 + \frac{2}{3}\ln S\right)$

$$K_2 = \frac{S^2 - 1}{6S^2}\ln S$$

and n'' is the slope of the corresponding curve in Figure 30.

The slurries used were relatively dense (13% by volume, Al_2O_3) and 95 per cent of the particles were less than 3 microns. Other investigations[34] of yield stresses and viscosities for slurries of Al_2O_3 in water are given in Figure 32. These results show rough agreement with the slurries of Al_2O_3 in 25 per cent H_2SO_4 which were tested here.

Experiments have shown that the evaluation of the thermal conductivity of a slurry by averaging the conductivities of the solids and liquid according to the volume fraction of each phase present gave predicted thermal conductivities which were erroneous by an order of magnitude[19]. Orr and Dalla Valle[35] recommend the following equation for the evaluation of k of a suspension.

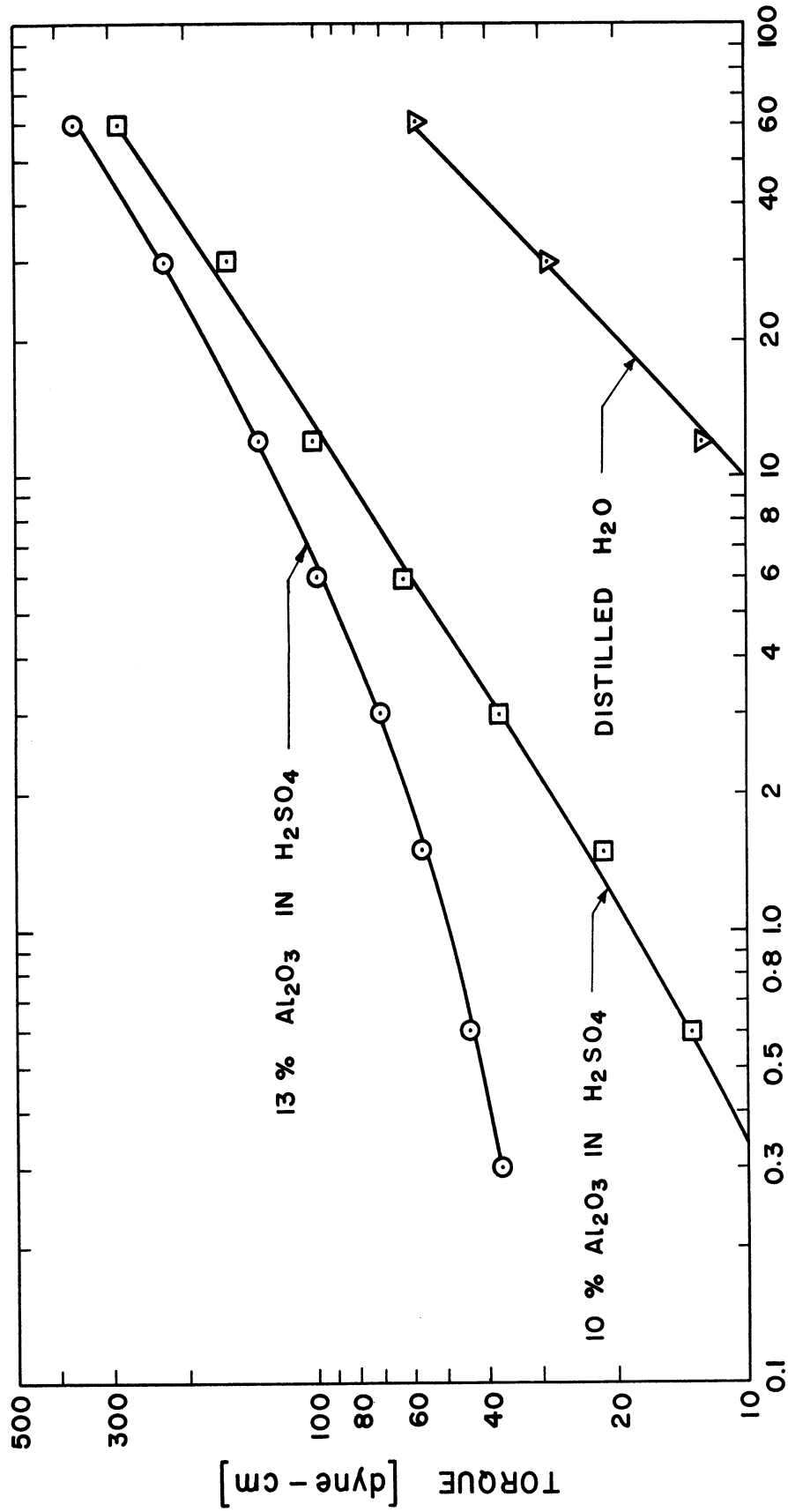

Figure 30. Relationship of Torque and Rotational Speed Obtained with Brookfield Rotational Viscometer for Various Bingham Plastics.

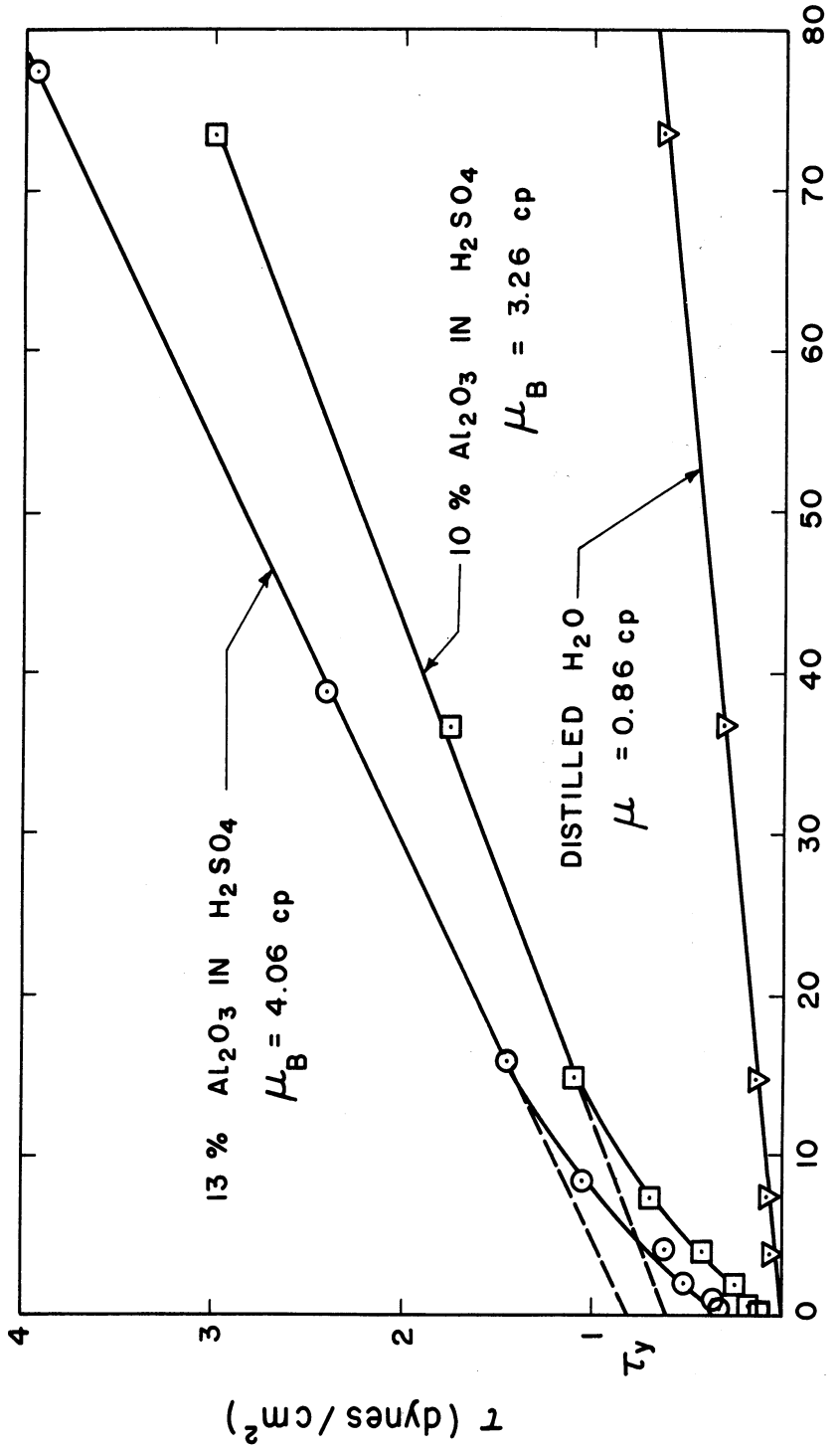

Figure 31. Flow Diagram for Various Bingham Plastics.

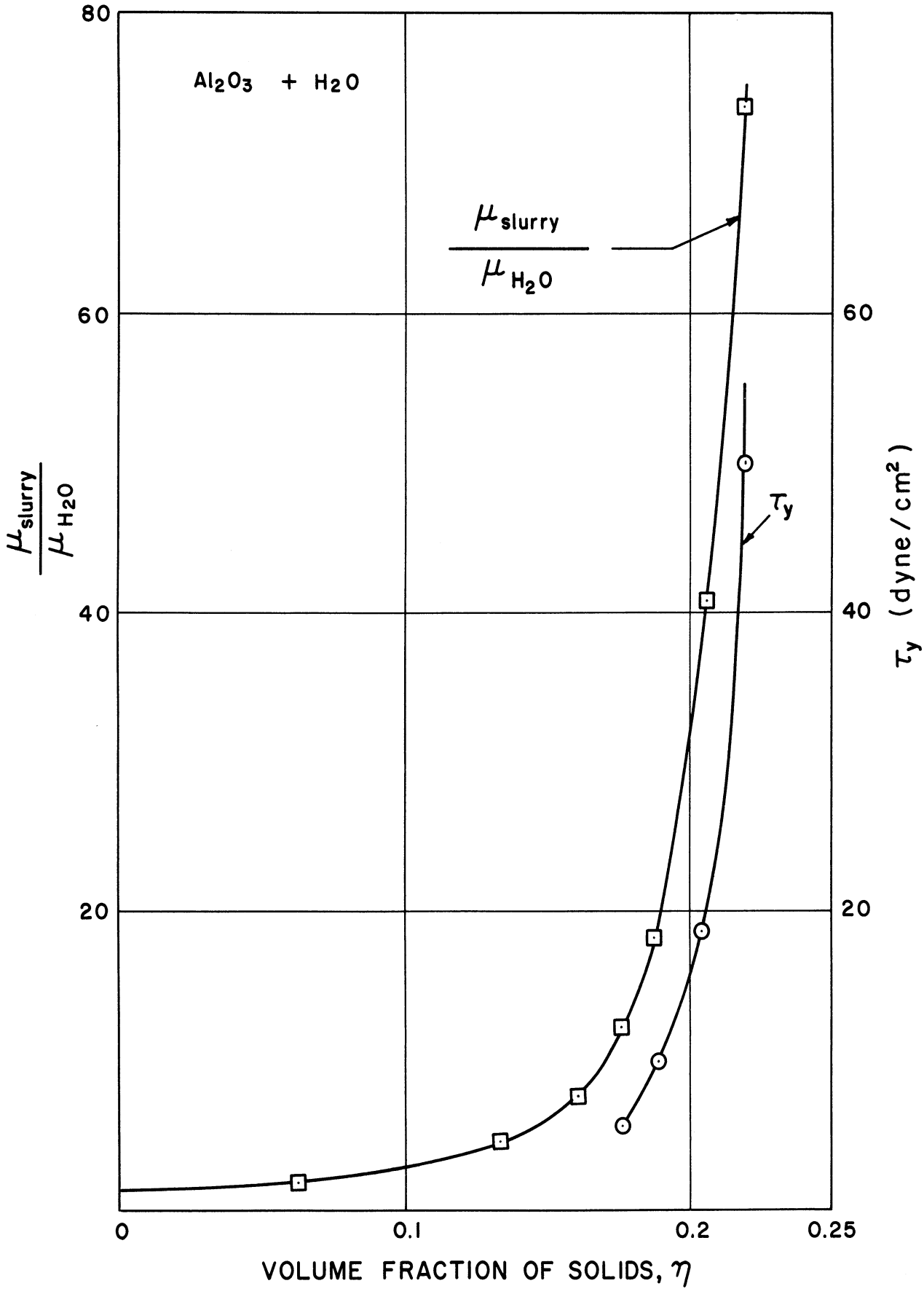

Figure 32. Rheological Data for Slurries of Alumina and Water.[34]

$$K_f = K_\ell \left[\frac{2K_\ell + K_s - 2\eta(K_\ell - K_s)}{2K_\ell + K_s + \eta(K_\ell - K_s)} \right] \tag{5.5}$$

where K_1 and K_s represent the conductivities of the liquid and solid particles, respectively, and η represents the volume fraction of solids in the suspension. Whenever possible, experimentally obtained values for thermal conductivity should be used. Tachibana and Morishita[5] measured the thermal conductivity of Al_2O_3 and H_2O slurries. The results shown in Figure 33 were extended to slurries of Al_2O_3 and 25 per cent H_2SO_4 as given by the broken line. For a 13 per cent by volume slurry of Al_2O_3 in H_2SO_4, the thermal conductivity was taken as $k = 0.52$ BTU/hr-ft-F.

The heat capacity of the slurry was taken as[5]

$$C_f = \frac{0.19\ \text{Weight}_{Al_2O_3} + 0.81\ \text{Weight}_{H_2SO_4}}{\text{Weight}_{Al_2O_3} + \text{Weight}_{H_2SO_4}} \tag{5.6}$$

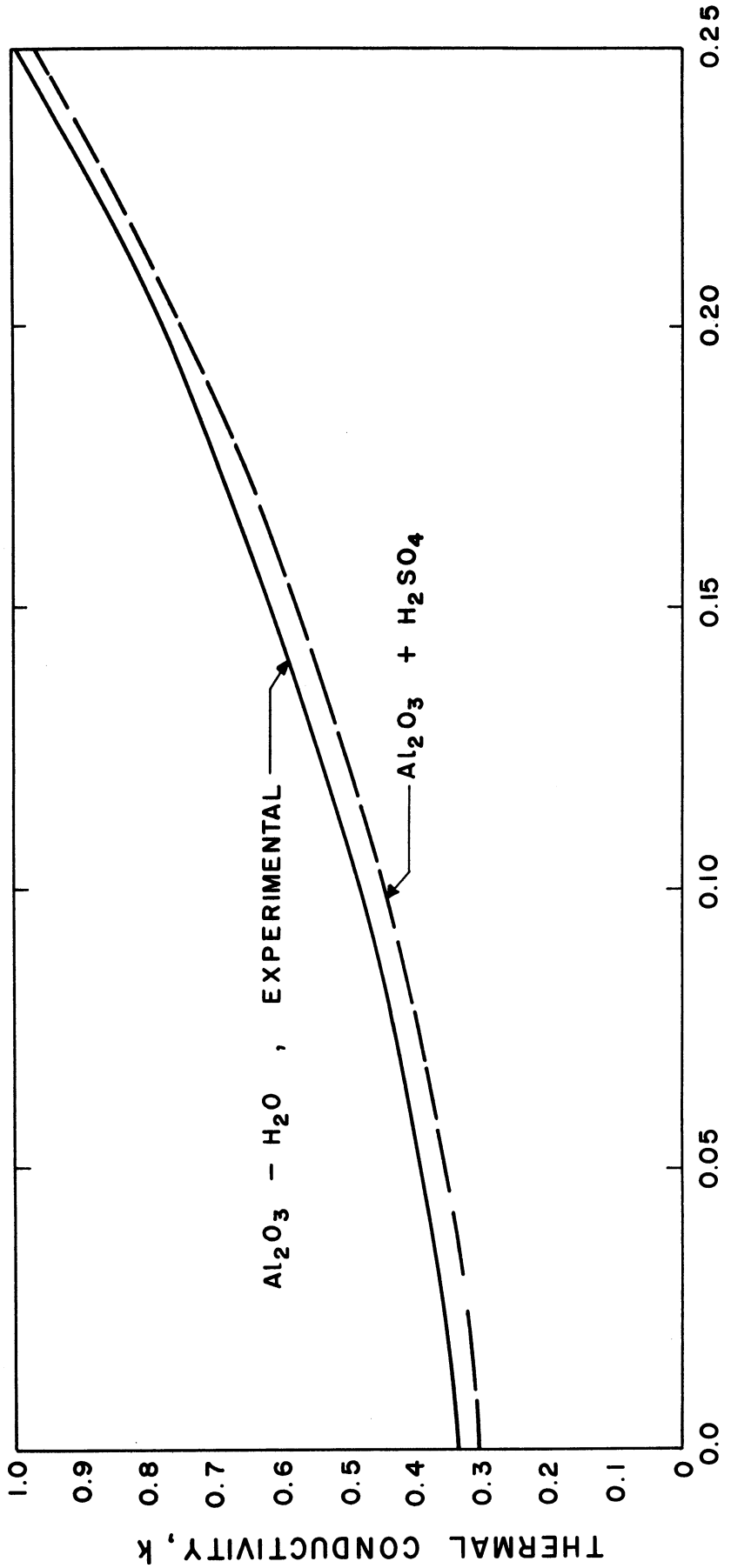

Figure 33. Thermal Conductivity of Alumina Suspensions.[5]

3. Transient and steady-state heat transfer measurements

The transient response of the fluid and tube temperatures was studied when subjected to a step change in the internal energy generation. A 25 per cent by weight H_2SO_2 solution with and without fine suspended alumina particles, 95 per cent less than 3 microns in diameter, was circulated through the test loop. Without the suspended alumina, the fluid corresponded to the limiting case of a Bingham plastic (a = 0.0), a Newtonian fluid. For 13 per cent by volume of Al_2O_3 suspended in the H_2SO_4 solution the Bingham plastic constant, 'a', was calculated from rheological and flow rate data. Equation (3.4) can be put in the following form:

$$\frac{u_m^*}{R_i \tau_y / \mu_B} = \frac{a^4 - 4a + 3}{12\,a} \qquad (5.7)$$

Since the factor 'a' cannot be solved for explicitly, a trial and error procedure was necessary using the rheological data from Figure 31 and the flow rate data corresponding to a given test condition.

Test section voltages ranged between 24 and 48 volts, while the Reynolds number was varied from 368 to 1333 for the H_2SO_4 and from 417 to 685 for the Al_2O_3 - H_2SO_4 slurry. A typical value of internal energy generation, 80,000 BTU/ft^{3}hr, resulted in a bulk fluid temperature rise of about 2°F.

All tests were conducted with the inlet fluid temperature at room temperature to reduce any heat transfer to the test section. The inlet temperature was adjusted by varying the heat exchanger coolant temperature and waiting whatever time necessary for thermal equilibrium to be established. Three flow measurements were made before each test. Once the desired flow rate was achieved, all thermocouple emfs were recorded with a precision potentiometer. The test section power was then turned on and transient centerline and wall temperatures recorded on the Sanborn recorder. Once steady state had been reached, the temperatures were again recorded with a precision potentiometer and three additional flow measurements made.

C. Results and Discussion

Experimental results obtained for a 25 per cent by weight H_2SO_4 electrolyte are presented in Table IV. These results correspond to a Newtonian fluid or Bingham plastic with constant a = 0.0. Similar results for a slurry of 13 per cent by volume of Al_2O_3 in H_2SO_4 are presented in Table V. The Bingham plastic constant, 'a', ranged between 0.30 and 0.39 for the slurry data. While the internal energy generation calculated from the rise in bulk fluid temperature agreed to within 5 per cent of that calculated from test-section voltage and current for the H_2SO_4, a disagreement was noted in the slurry data. Measured bulk fluid temperatures would indicate a greater energy generation than that given by the test-section electrical power measurements. Since this is physically impossible, the disagreement is attributed to the

TABLE IV

EXPERIMENTAL RESULTS FOR 25% H_2SO_4

Temperature (^oF)							
T_o(inlet)	71.5	71.5	71.5	71.5	71.0	71.2	71
T_{top}-To	4.44	7.77	5.55	5.69	6.09	5.16	6.89
T_{center}-To	7.55	1.33	0.49	0.62	0.80	0.40	0.755
T_{bottom}-To	1.38	2.76	2.13	2.00	2.98	2.13	2.62
T^*_{side}-To	1.51	3.33	2.27	2.09	2.40	1.91	2.93
T_{side}-To	1.51	3.20	2.58	1.96	2.89	2.31	3.02
T_{exit}-To	1.56	2.80	1.33	1.11	1.78	0.977	2.04
Volts	23.4	33.9	33.0	34.0	34.0	34.0	34.0
Amperes	1.24	1.95	1.95	1.96	1.99	1.97	1.98
Re	368	471	963	1190	790	1333	634
Pr	10.8	10.8	10.8	10.8	10.8	10.8	10.8
$X \times 10^3$	5.27	4.12	2.02	1.63	2.44	1.46	3.06
q''_{temp}(BTU/hr-ft^3)	34,400	79,400	77,000	79,300	83,600	78,200	77,500
q''_{elec}(BTU/hr-ft^3)	35,140	81,730	79,460	82,400	83,660	82,820	83,240
$\psi_{steady\ aver.wall} \times 10^2$	2.19	1.78	1.34	1.24	1.47	1.19	1.58
$\psi_{steady\ centrln} \times 10^2$	0.678	0.513	0.195	0.237	0.302	0.152	0.286
$GrPr \frac{D}{L} \times 10^{-4}$	0.4	0.8	0.8	0.8	0.8	0.8	0.8

* Wall temperature on same side that electrodes are located.

TABLE V

EXPERIMENTAL RESULTS FOR 13% Al_2O_3 in H_2SO_4

Temperature (^oF)					
To (inlet)	78.4	78.4	78.6	78.6	78.7
T_{top}-To	2.22	2.66	5.11	1.55	1.60
$T_{above\ center}$-To	0.222	0.355	0.666	0.222	0.311
T_{center} -To	0.400	0.444	0.89	0.311	0.800
$T_{below\ center}$-To	1.55	5.50	16.0	3.77	10.09
T_{bottom}-To	4.66	10.2	24.9	5.11	15.40
T^*_{side}-To	1.33	3.33	8.56	2.00	5.55
T_{side}-To	0.89	2.99	5.04	2.22	4.12
T_{exit}-To	0.579	0.890	2.04	0.489	0.756
Volts	24.2	36.2	48.3	24.3	36.2
Amperes	0.98	1.49	2.00	1.0	1.50
Re	417	540	533	530	685
Pr	7.22	7.22	7.22	7.22	7.22
X x 10^3	7.00	5.40	5.46	5.58	4.25
q''_{temp} (BTU/hr-ft^3)	38,600	76,600	174,000	41,500	82,600
q''_{elec} (BTU/hr-ft^3)	28,784	66,867	124,467	29,881	67,320
ψ steady aver. wall x 10^2	5.00	4.32	5.33	5.29	5.84
ψ steady centrln x 10^2	0.752	0.359	0.387	0.563	0.643
a	0.39	0.34	0.34	0.34	0.30

* Wall temperature on same side that electrodes are located.

filling of the cavities between the mixing baffles with solid particles resulting in inefficient mixing of the fluid.

For each test the transient response of the centerline fluid temperature was recorded as shown in Figure 34. For 25 per cent H_2SO_4 the experimental measurements give a faster response than predicted at the initial state, and then fall below as the system approaches its steady state. However, the discrepancy between the theory and experiment is within an acceptable range. For the Al_2O_3 suspension the measured response falls below the theoretical prediction but approaches the predicted steady state at large values of time. This deviation is thought to be due to a slower centerline fluid velocity than expected, resulting from settling of the solid phase or adhering of solid particles to the thermocouple probe. The 95 per cent confidence limits obtained by the method outlined in Appendix D are presented in Figures 34 and 35.

The steady-state temperatures for the fluid and wall are shown in Figure 35. For 25 per cent H_2SO_4, a Newtonian fluid, the experimental data of the centerline fluid temperature agree fairly well with the theoretical curve. However, a vertical assymmetry is noted in the wall temperature. This deviation is thought to result from free convection which was neglected in the analysis. The buoyant forces due to temperature differences in the fluid could cause a secondary flow which results in a radial mixing of the fluid, raising the centerline fluid temperature and lowering the average wall temperature.

This conclusion is supported by Metais and Eckert's study[27] of forced, free, and mixed convection regimes for horizontal tubes.

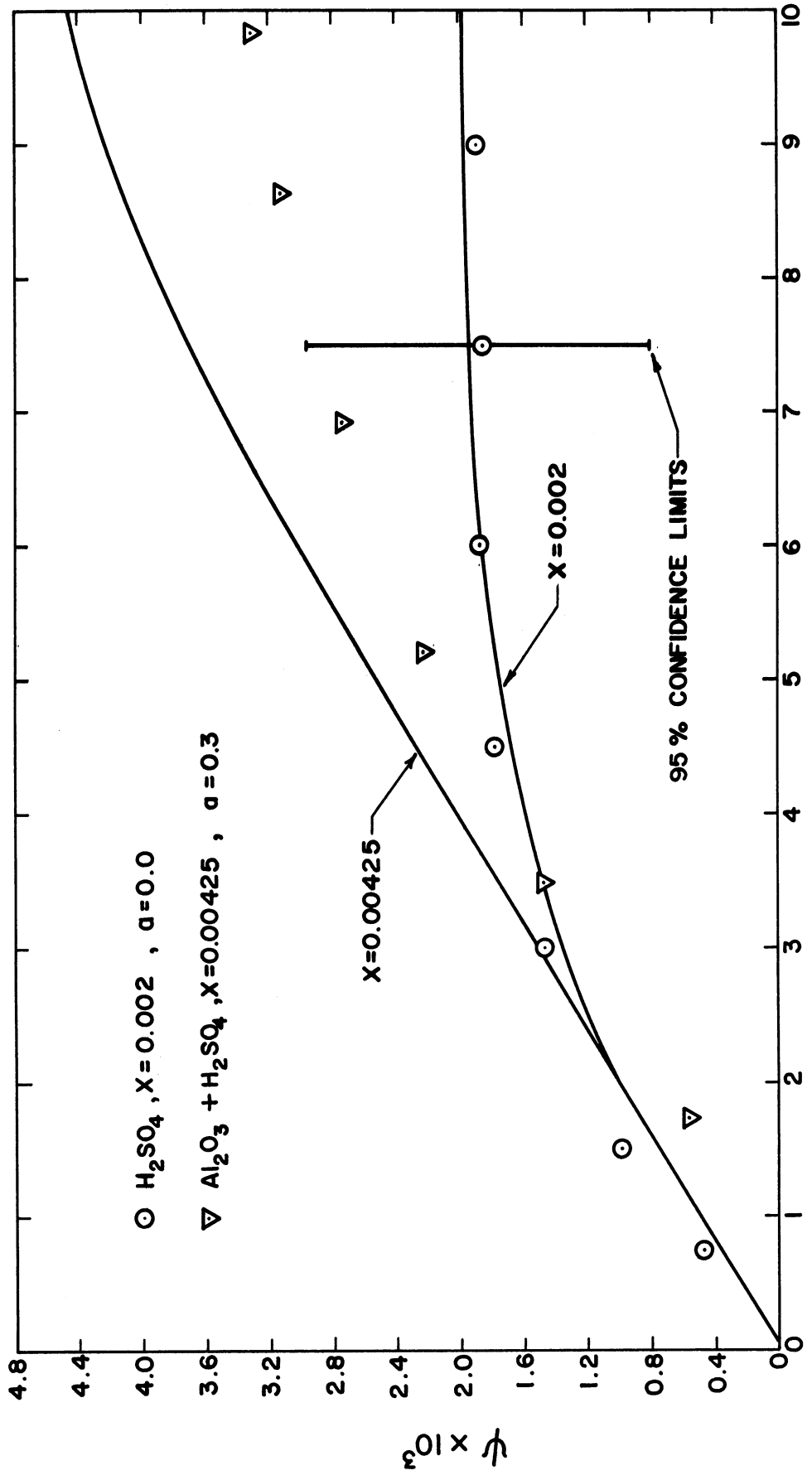

Figure 34. Step Response of Centerline Fluid Temperature.

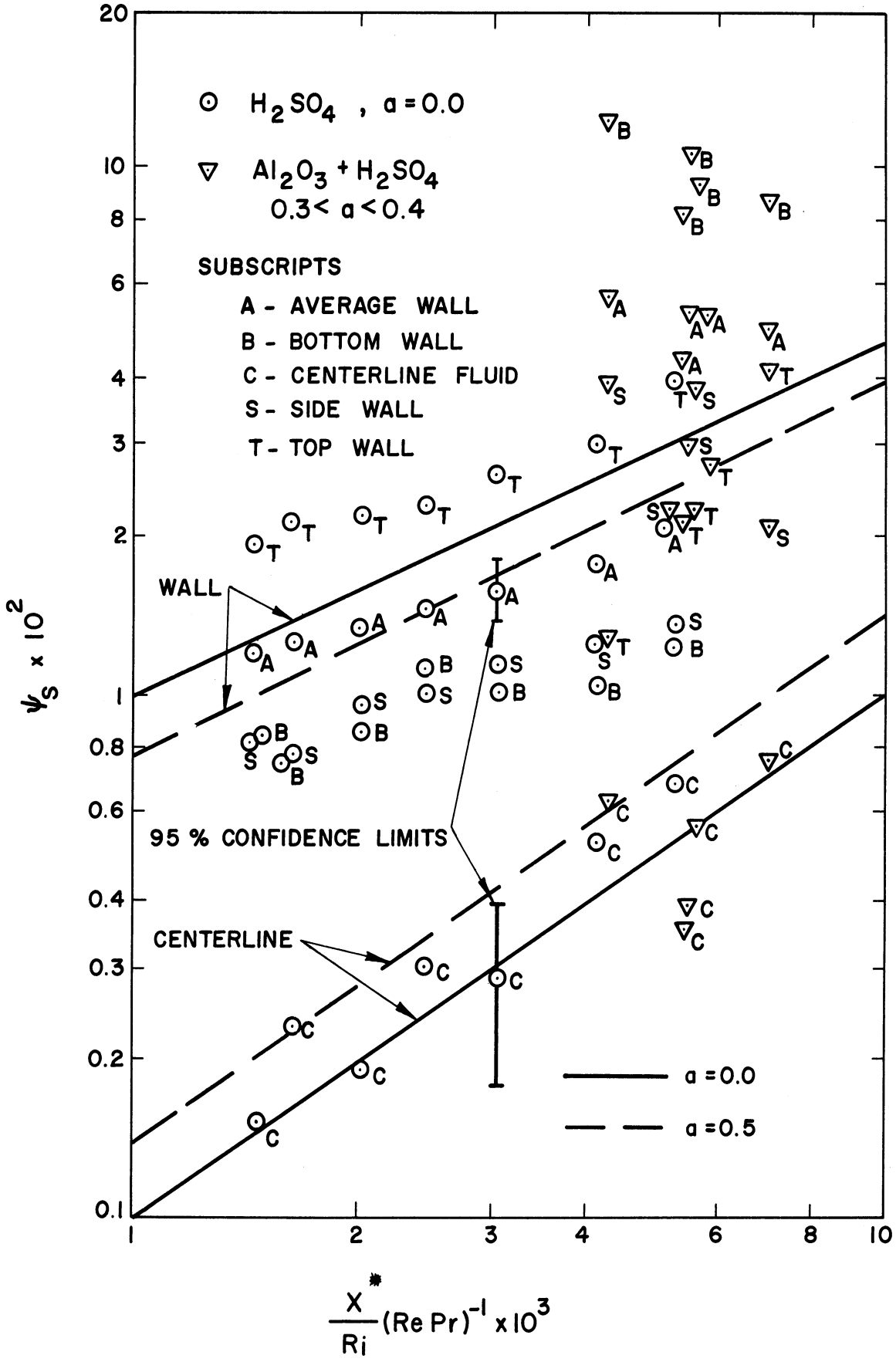

Figure 35. Steady Fluid and Wall Temperatures as a Function of Axial Distance.

Their findings for the case of constant wall temperature are shown in Figure 36, where the Grashof number, Gr, is based on the tube diameter and the difference between wall and fluid bulk temperatures. These results can be compared to the case under study here: internal energy generation in the fluid with insulated tube wall. As the quantity $\frac{X^*}{Ri}(RePr)^{-1}$ is decreased, the average wall temperature in Figure 35 is seen to approach the predicted value. The quantity $GrPr\frac{D}{L}$ associated with each test is nearly constant and equal to 8×10^3. Since $\frac{X^*}{Ri}(Pr)^{-1}$ is nearly constant, as Reynolds number is increased and $GrPr\frac{D}{L}$ held constant the effect of free convection is diminished. This would correspond to approaching the forced convection region in Figure 36 from the mixed convection region along the line $GrPr\frac{D}{L} = 8 \times 10^3$. This apparent agreement between Metais and Eckert's results and those presented here might have been anticipated because of the similarity of fluid temperature profiles resulting from either a heated tube wall or internal energy generation in the fluid and an insulated tube wall.

For 13 per cent by volume alumina in 25 per cent H_2SO_4, the centerline temperature agrees with the theoretical prediction. However, the bottom tube wall temperature is significantly higher than expected, causing the measured average wall temperature to fall above the predicted value. This disagreement was due to settling of the solid particles to the bottom of the tube. A non-symmetric vertical velocity gradient was established which greatly affected the temperature profiles. The denser, slower moving fluid at the bottom of the tube lost less heat due to the enthalpy flux, and became warmer.

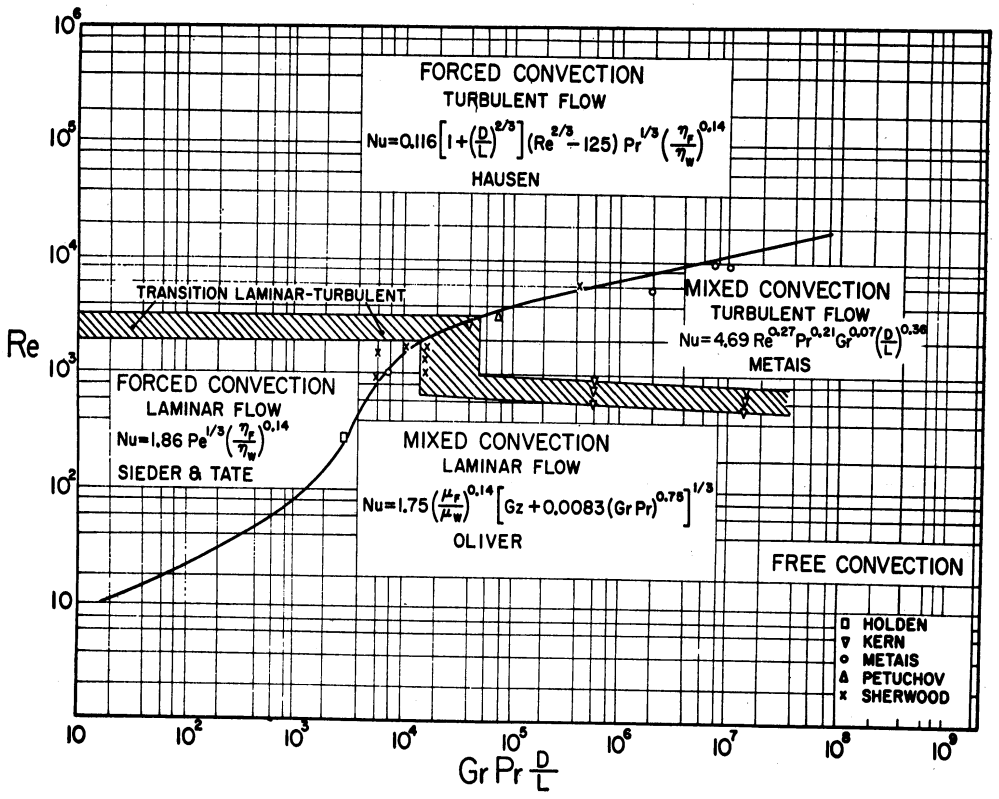

Figure 36. Regimes of Free, Forced, and Mixed Convection for Flow through Horizontal Tubes.(27)

Further illustration of the vertical temperature profile can be seen in Figures 37 and 38. One curve in Figure 37 corresponds to the Newtonian fluid, H_2SO_4, and exhibits the increased upper tube wall temperature thought to be due to free convection. All the other curves for the Al_2O_3 slurry exhibit an increased lower wall temperature which is attributed to settling of the solid phase. A time dependent effect is disclosed by Figure 37, resulting from the continued settling of the solid phase. The test conditions corresponding to the triangles and hexagons are nearly the same. However, the asymmetry of the temperature profile is becoming more pronounced as slurry-circulating-time increases. The tests as listed in Table V were separated by approximately one-half hour intervals from left to right. Thus, the test corresponding to the hexagons in Figure 37 took place about 2 hours later than that corresponding to the triangles. From the vertical temperature profiles it appears that the solid phase is slowly continuing to settle and increasing the fluid temperature assymmetry.

Examples have been cited where the solid phase of a slurry has continued to settle until the flow was entirely choked off[25]. Even in turbulent flow, a laminar sublayer exists in which particles can settle[20]. The settled particles may act as the effective tube wall, so that settling can continue until an equilibrium thickness is reached, or the tube is completely blocked. The rigidity of a settled bed appears to be inversely proportional to the particle size. Therefore, slurries utilizing large particles may form a vertical density gradient, but the thick mud at the bottom of the tube will continue to move rather than forming a hard cake and eventually plugging the tube.

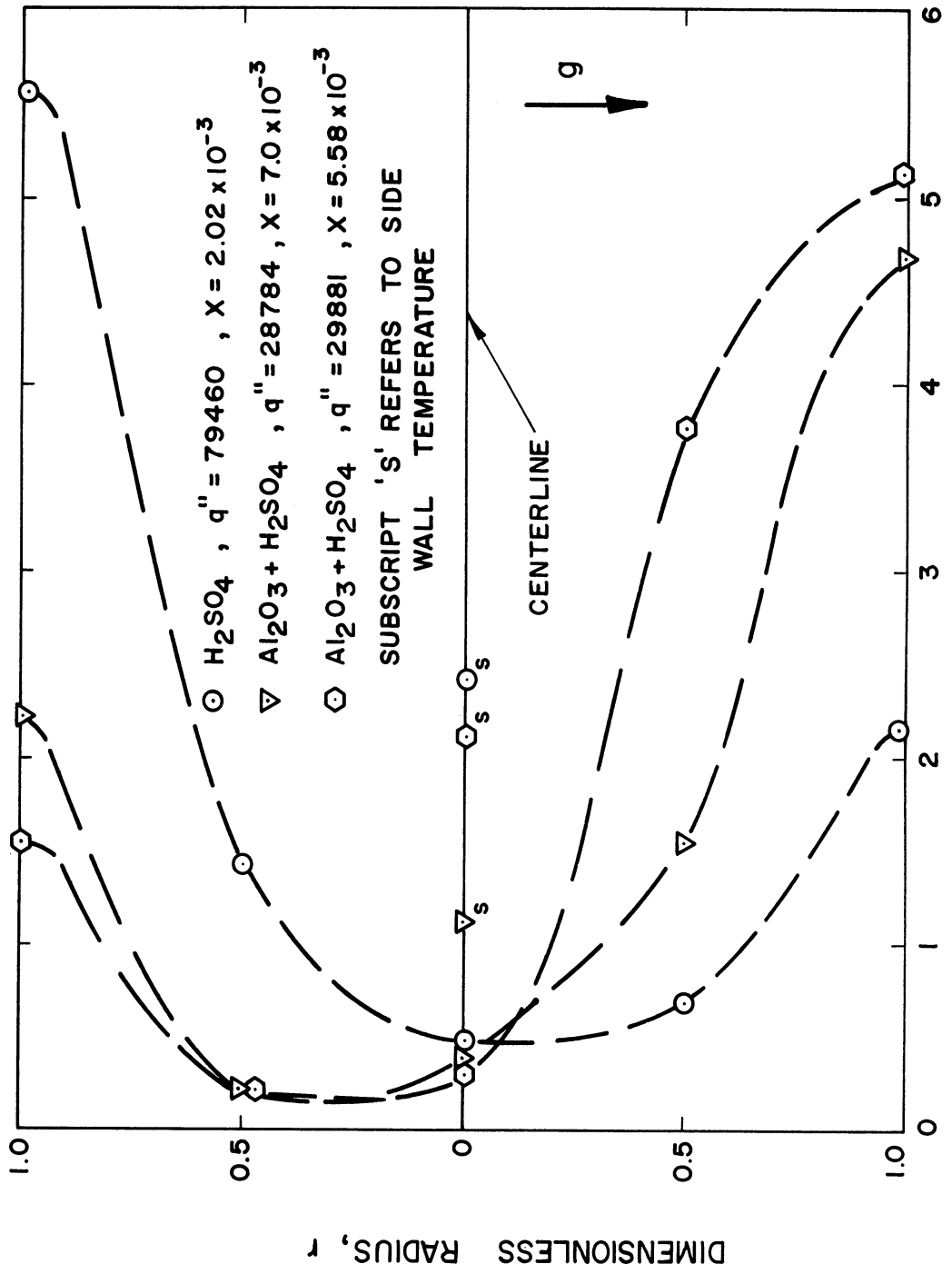

Figure 37. Vertical Temperature Profiles in a Horizontal Tube.

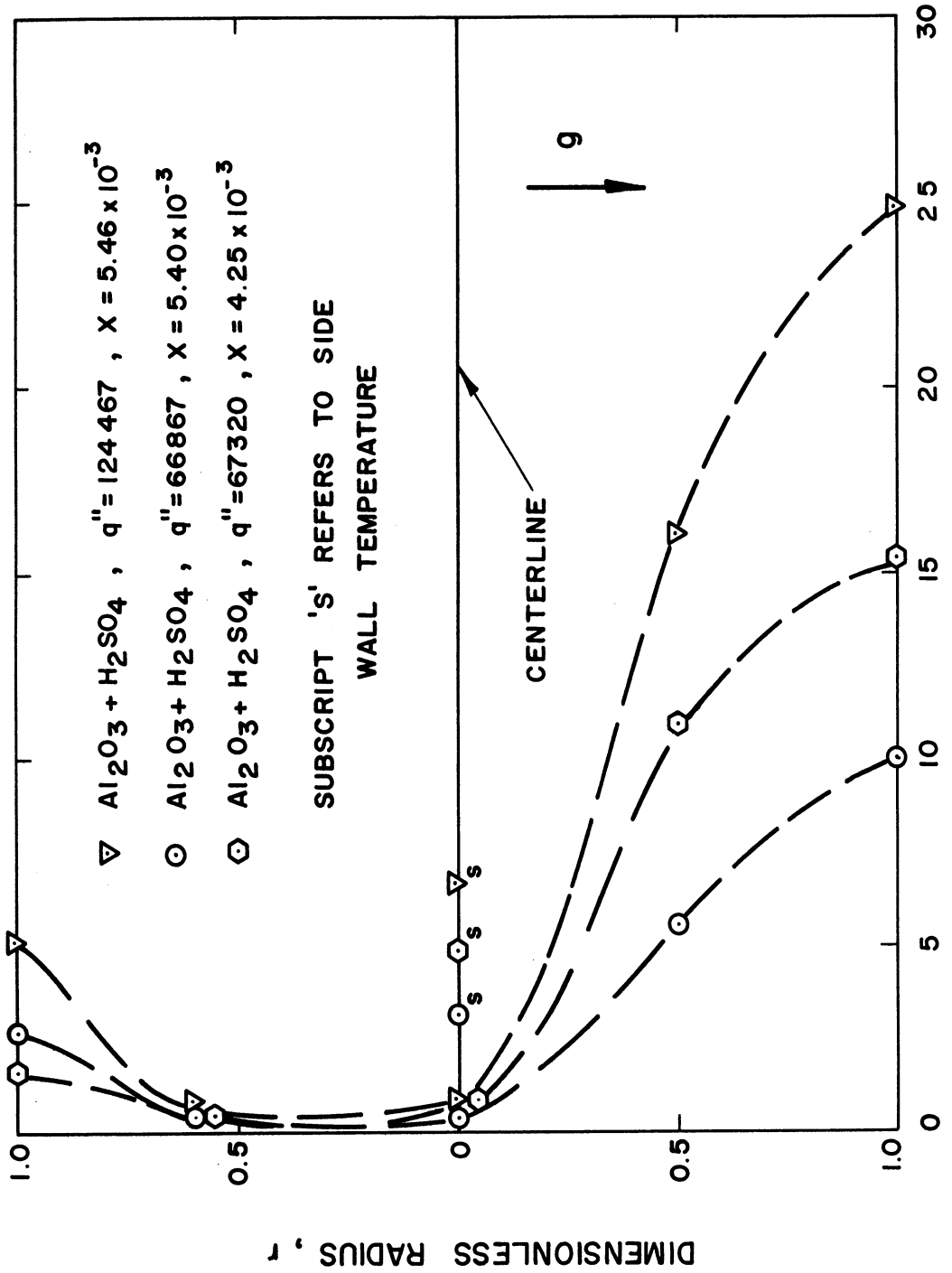

Figure 38. Vertical Temperature Profiles in a Horizontal Tube.

CHAPTER VI

CONCLUSIONS

1. The largest steady centerline-to-wall temperature difference exists for a Newtonian fluid, (a = 0.0). As the Bingham plastic constant 'a' is increased, the centerline-to-wall temperature difference decreases until at a = 1.0 (plug flow) it is equal to zero. This is due to the uniform velocity and insulated outer tube wall.

2. The response time necessary for the fluid-tube system to reach equilibrium is decreased by an increase in the Bingham plastic constant 'a'. A resonance phenomenon is observed in the steady-periodic temperature response. The period of resonance equals 2π for a Newtonian fluid (a = 0.0) and equals π for plug flow (a = 1.0). The heat capacity of the wall dampens the temperature fluctuations of the fluid near the wall.

3. The wall heat capacity has a large effect on the transient temperature response. This effect is one of increasing the length of time required to reach steady state and is intensified as the ratio of wall to fluid heat capacity is increased.

4. The regimes of forced, mixed, and free convection proposed by Metais and Eckert[27], for a horizontal tube with constant wall temperature, appear to be valid for the case of internal energy generation in a Newtonian fluid with an insulated tube wall.

5. Settling of suspended particles in a slurry distorts the velocity profile and produces a higher than expected temperature

at the bottom of a horizontal tube when energy is being generated in the fluid. Experimentally, the centerline fluid temperature agrees with the predicted value, but the average wall temperature is higher than expected.

A P P E N D I C E S

APPENDIX A

DERIVATION OF THE GOVERNING DIFFERENTIAL EQUATIONS

Under the assumption listed in Chapter III, the first law of thermodynamics can be written for the model showin in Figure 2.

Fluid

$$\frac{\partial T_f}{\partial t} + u^*(r^*)\frac{\partial T_f}{\partial X^*} = \alpha_f\left(\frac{\partial T_f}{\partial r^{*2}} + \frac{1}{r}\frac{\partial T_f}{\partial r^*}\right) + \frac{q''}{\rho_f C_f} \qquad (A.1)$$

Wall

$$\frac{\partial T_w}{\partial t} = \alpha_w\left(\frac{\partial^2 T_w}{\partial r^{*2}} + \frac{1}{r}\frac{\partial T_w}{\partial r^*}\right) \qquad (A.2)$$

For the three types of problems considered, steady-periodic, internal energy generation step response, and inlet temperature step response, the term q" in Equation (A.1) takes the following forms

energy generation step: $q'' = q_o$

inlet temperature step: $q'' = 0$ $\qquad t > 0$

steady periodic: $q'' = q_o \epsilon \sin\omega t$

The boundary conditions for the general problem are

$$T_f(X^*, 0, r^*) = T_w(X^*, 0, r^*) = T_i \qquad \text{(initial)}$$

$$T_f(0, t, r^*) = T_o \qquad \text{(entrance)}$$

$$\frac{\partial T_f}{\partial r}(X^*, t, 0) = 0 \qquad \text{(symmetry)}$$

$$T_f(X^*, t, R_i) = T_w(X^*, t, R_i) \qquad \text{(fluid-wall interface)}$$

$$\frac{\partial T_w}{\partial r}(X^*, t, R_o) = 0 \qquad \text{(adiabatic wall)}$$

By defining the following dimensionless variables

$$\psi = \frac{(T - T_o) k_f}{q_o R_i^2}$$:for disturbances due to internal heat generation

$$\xi = \frac{T - T_i}{T_o - T_i}$$:for step disturbance in inlet fluid temperature

$$r = \frac{r^*}{R_i} \qquad X = \frac{X^* \alpha_f}{2 u_m^* R_i^2} = \frac{X^*}{R_i} (Re\ Pr)^{-1} \qquad (A.3)$$

$$\theta = \frac{t\ \alpha_f}{R_i^2} \qquad \Gamma = \frac{\omega R_i^2}{\alpha_f} \qquad u(r) = \frac{u^*(r^*)}{2 u_m^*}$$

Equations (A.1) and (A.2) may be written in dimensionless form as

Fluid

$$\frac{\partial \psi_f}{\partial \theta} + u(r) \frac{\partial \psi_f}{\partial X} = \frac{\partial^2 \psi_f}{\partial r^2} + \frac{1}{r} \frac{\partial \psi_f}{\partial r} + Q'' \qquad (A.4)$$

Wall

$$\frac{\partial \psi_w}{\partial \theta} = \Lambda \left(\frac{\partial^2 \psi_w}{\partial r^2} + \frac{1}{r} \frac{\partial \psi_w}{\partial r} \right) \qquad (A.5)$$

where $Q'' = 1$:for step disturbance in internal heat generation

$Q'' = \epsilon \sin \Gamma\theta$:for sinusoidal disturbance in internal heat generation

and $\psi = \xi$, $Q'' = 0$:for step disturbance in inlet fluid temperature.

The boundary conditions are

$$\psi_f(X, 0, r) = \psi_w(X, 0, r) = 0$$

$$= \begin{cases} 0 & \text{:for disturbances due to internal heat generation} \\ 1 & \text{:for step disturbance in inlet fluid temperature only.} \end{cases}$$

$$\frac{\partial \Psi_f}{\partial r}\Big|_{X,\theta,0} = 0$$

$$\Psi_f(X,\theta,1) = \Psi_w(X,\theta,1)$$

$$\frac{\partial \Psi_w}{\partial r}\Big|_{X,\theta,R_o/R_i} = 0$$

APPENDIX B

FINITE DIFFERENCE EQUATIONS

1. Notation

As shown in Figure 4, the physical model in Figure 2 is divided radially and axially to form a grid, and a system of notation used by Ayers[8] adopted. The center of each element is referred to as a nodal point whose temperature is the average temperature of the element. Any nodal point in the fluid can be described by using a double subscript notation (I, J) , where I is the radial counter and J is the axial counter. For a wall nodal point the radial subscript is K , so a point in the wall is referred to by the subscript (K, J).

Radially, there are N + 1 fluid elements and M wall elements. It follows that the radial grid dimension in the fluid is 1/N , while in the wall the radial grid dimension is

$$\frac{R_o/R_i - 1}{M} = \frac{\delta}{M}$$

The radius of any fluid nodal point is given as I/N, (I = 0, 1, 2, ... N), and the radius of any wall nodal point is $1 + \frac{K\delta}{M}$,(K = 0, 1, 2, ... N).

Axially, there are P divisions of the tube length L , so the axial grid dimension is L/P. The axial distance is JL/P , which is measured from the point where energy generation begins, X = 0 .

2. Finite Difference Approximation of Derivatives

If a function u = u(x, y) is assumed to have enough partial derivatives, the value of the function at the two points (x, y) and

$(x + \Delta x, y)$ can be evaluated by the Taylor's series.

$$u_{i+1,j} = u_{i,j} + \Delta x \frac{\partial u}{\partial x} + \frac{\Delta x^2}{2!} \frac{\partial^2 u}{\partial x^2} + \cdots \tag{B.1}$$

The above equation can be solved for the first derivative

$$\frac{\partial u}{\partial x} = \frac{u_{i+1,j} - u_{i,j}}{\Delta x} + O(\Delta x) \tag{B.2}$$

Equation (B.2) is known as the forward difference approximation to the first derivative. The truncation error involved is of the order Δx .

A more accurate approximation to the first derivative can be had by writing Equation (B.1) for the point $u_{i-1,\,j}$.

$$u_{i-1} = u_{i,j} - \Delta x \frac{\partial u}{\partial x} + \frac{\Delta x^2}{2!} \frac{\partial^2 u}{\partial x^2} - \cdots \tag{B.3}$$

Then, subtracting Equation (B.3) from (B.1) and rearranging the result yields

$$\frac{\partial u}{\partial x} = \frac{u_{i+1} - u_{i-1}}{2\ \Delta x} + O(\Delta x)^2 \tag{B.4}$$

Equation (B.4) is the central difference approximation to the first derivative. It has a truncation error of order of magnitude Δx^2 .

The central difference approximation to the second derivative of $u(x, y)$ can be obtained by adding Equations (B.1) and (B.3) and eliminating unwanted derivatives.

$$\frac{\partial^2 u}{\partial X^2} = \frac{u_{i+1,j} + u_{i-1,j} - 2u_{i,j}}{\Delta X^2} + O(\Delta X)^2 \qquad (B.5)$$

Whenever possible, the central difference approximation to derivatives should be used because of the smaller truncation error involved.

3. Steady Finite Difference Equations

The partial differential equation for the steady temperature distribution in the fluid may be obtained from Appendix A as

$$u(r)\frac{\partial \psi_{sf}}{\partial X} = \frac{\partial^2 \psi_{sf}}{\partial r^2} + \frac{1}{r}\frac{\partial \psi_{sf}}{\partial r} + 1 \qquad (B.6)$$

Note that the wall need not be considered, because at steady state it has a uniform temperature equal to the fluid-wall interface temperature.

When writing the finite difference approximations to Equation (B.6), the axial counter need not be used since the resulting equations are only solved at one axial location at a time. This makes the designation of the nodal points more simple.

Fluid

$$\psi_{sf}(I,J) = S(I)$$
$$\psi_{sf}(I+1,J) = S(I+1)$$
$$\psi_{sf}(I-1,J) = S(I-1)$$
$$\psi_{sf}(I,J-1) = U(I)$$

Wall

$$\psi_{sw}(K,J) = V(K)$$
$$\psi_{sw}(K+1,J) = V(K+1)$$
$$\psi_{sw}(K-1,J) = V(K-1)$$

Using the above notation, the finite difference approximation for the terms in Equation (B.6) can be written

$$\frac{\partial \psi_{sf}}{\partial X} = \frac{S(I) - U(I)}{L/P} \tag{B.7}$$

$$\frac{1}{r}\frac{\partial \psi_{sf}}{\partial r} = \frac{1}{I/N}\left(\frac{S(I+1) - S(I-1)}{2/N}\right) \tag{B.8}$$

$$\frac{\partial^2 \psi_{sf}}{\partial r^2} = \frac{S(I+1) + S(I-1) - 2\,S(I)}{1/N^2} \tag{B.9}$$

Note that a central difference approximation is used radially, but axially a forward difference approximation is used. This is made necessary by the explicit method used in the axial direction.

Substitution of Equations (B.7), (B.8), and (B.9) into (B.6) gives the finite difference equation for a general point in the fluid.

Fluid

$$S(I) = \frac{N^2\left(1+\frac{1}{2I}\right)S(I+1) + N^2\left(1-\frac{1}{2I}\right)S(I-1) + \frac{P}{L}VEL(I)\,U(I) + 1}{2N^2 + \frac{P}{L}VEL(I)} \tag{B.10}$$

A special equation must be written for the centerline and fluid-wall interface elements, as special conditions exist at such limiting nodal points. At the centerline, the term in Equation (B.6) $\frac{1}{r}\frac{\partial \psi_{sf}}{\partial r}$ is not defined at $r = 0$. By l'Hospital's rule it is found that

$$\lim_{r \to 0} \frac{1}{r} \frac{\partial \psi_{sf}}{\partial r} = \frac{\partial^2 \psi_{sf}}{\partial r^2}$$

Therefore, the governing equation for the fluid at the centerline of the tube is

$$u_{max} \frac{\partial \psi_{sf}}{\partial X} = 2 \frac{\partial^2 \psi_{sf}}{\partial r^2} + 1 \qquad \text{(B.11)}$$

Using finite differences, Equation (B.11) becomes

$$S|0| = \frac{4N^2 S|1| + \frac{P}{L} VMAX \; U|0| + 1}{\frac{P}{L} VMAX + 4N^2} \qquad \text{(B.12)}$$

The fluid-wall interface element, whose fluid subscript is (N, J) , has a thickness equal to one-half of a general fluid element. The governing equation becomes

$$0 = - K_f \left. \frac{\partial T_{sf}}{\partial r} \right|_{r=1} + q_o V_f \qquad \text{(B.13)}$$

In terms of dimensionless parameters, the preceeding equation becomes

$$0 = - \frac{R_f}{R_i} \left. \frac{\partial \psi_{sf}}{\partial r} \right|_{r=1} + \frac{\delta_f}{R_i} \qquad \text{(B.14)}$$

where $\frac{R_f}{R_i} = 1 - \frac{1}{2N}$; $\frac{\delta_f}{R_i} = \frac{1}{2N}$

Application of finite differences then yields the following equation

$$S(N) = \frac{1}{2N(N-1/2)} + S(N-1) \tag{B.15}$$

4. Steady-Periodic Finite Difference Equations

The partial differential equations governing the steady-periodic temperatures in the fluid and wall have been found to be

Fluid

$$\frac{\partial \psi_{Pf}}{\partial \theta} + u(r)\frac{\partial \psi_{Pf}}{\partial X} = \frac{\partial^2 \psi_{Pf}}{\partial r^2} + \frac{1}{r}\frac{\partial \psi_{Pf}}{\partial r} + \epsilon \sin \Gamma\theta \tag{B.16}$$

Wall

$$\frac{\partial \psi_{Pw}}{\partial \theta} = \Lambda\left(\frac{\partial^2 \psi_{Pw}}{\partial r^2} + \frac{1}{r}\frac{\partial \psi_{Pw}}{\partial r}\right) \tag{B.17}$$

Let the periodic temperatures be written as follows

$$\psi_{Pf} = A(X,r)\sin \Gamma\theta + B(X,r)\cos \Gamma\theta \tag{B.18}$$

$$\psi_{Pw} = C(X,r)\sin \Gamma\theta + D(X,r)\cos \Gamma\theta \tag{B.19}$$

Substituting Equation (B.18) into (B.16) gives the following result for the fluid.

$$A\Gamma \cos \Gamma\theta - B\Gamma \sin \Gamma\theta + u(r)\left(\frac{\partial A}{\partial X} \sin \Gamma\theta + \frac{\partial B}{\partial X} \cos \Gamma\theta\right)$$

$$= \left(\frac{\partial^2 A}{\partial r^2} + \frac{1}{r}\frac{\partial A}{\partial r}\right) \sin \Gamma\theta + \left(\frac{\partial^2 B}{\partial r^2} + \frac{1}{r}\frac{\partial B}{\partial r}\right) \cos \Gamma\theta + \epsilon \sin \Gamma\theta \qquad \text{(B.20)}$$

Because Equation (B.20) is an identity, it can be separated into its Sin $\Gamma\theta$ and Cos $\Gamma\theta$ components.

$$A\Gamma + u(r)\frac{\partial B}{\partial X} = \frac{\partial^2 B}{\partial r^2} + \frac{1}{r}\frac{\partial B}{\partial r} \qquad \text{(B.21)}$$

$$-B\Gamma + u(r)\frac{\partial A}{\partial X} = \frac{\partial^2 A}{\partial r^2} + \frac{1}{r}\frac{\partial A}{\partial r} + \epsilon \qquad \text{(B.22)}$$

Again the notation can be simplified.

$$A(I,J) = A(I) \qquad B(I,J) = B(I)$$

$$A(I+1,J) = A(I+1) \qquad B(I+1,J) = B(I+1)$$

$$A(I-1,J) = A(I-1) \qquad B(I-1,J) = B(I-1)$$

$$A(I,J-1) = E(I) \qquad B(I,J-1) = F(I)$$

Employing finite differences with the above notation results in the following two equations for the fluid.

$$A(I) = \frac{N^2}{\Gamma}\left(1+\frac{1}{2I}\right)B(I+1) + \frac{N^2}{\Gamma}\left(1-\frac{1}{2I}\right)B(I-1)$$

$$-\left(\frac{2N^2}{\Gamma} + \frac{P}{L\Gamma}VEL(I)\right)B(I) + \frac{P}{L\Gamma}VEL(I)\,F(I) \qquad \text{(B.23)}$$

$$B(I) = \frac{-N^2}{\Gamma}\left(1+\frac{1}{2I}\right)A(I+1) - \frac{N^2}{\Gamma}\left(1-\frac{1}{2I}\right)A(I-1)$$

$$+\left(\frac{2N^2}{\Gamma} + \frac{P}{L\Gamma}VEL(I)\right)A(I) + \frac{P}{L\Gamma}VEL(I) - \frac{\epsilon}{\Gamma} \qquad \text{(B.24)}$$

By the same procedure given in Equations (B.18) through (B.24), the following result can be obtained for the wall.

$$C(K) = \frac{\Lambda}{\beta}\left(\frac{M^2}{\delta^2} + \frac{M}{2\delta\left(1+\frac{K\delta}{M}\right)}\right)D(K+1)$$

$$+\frac{\Lambda}{\Gamma}\left(\frac{M^2}{\delta^2} - \frac{M}{2\delta\left(1+\frac{K\delta}{M}\right)}\right)D(K-1) - \frac{2\Lambda M^2}{\Gamma\,\delta^2}D(K) \qquad \text{(B.25)}$$

$$D(K) = \frac{-\Lambda}{\Gamma}\left(\frac{M^2}{\delta^2} + \frac{M}{2\delta\left(1+\frac{K\delta}{M}\right)}\right)C(K+1)$$

$$-\frac{\Lambda}{\Gamma}\left(\frac{M^2}{\delta^2} - \frac{M}{2\delta\left(1+\frac{K\delta}{M}\right)}\right)C(K-1) + \frac{2\Lambda M^2}{\Gamma\,\delta^2}C(K) \qquad \text{(B.26)}$$

The equation for the centerline element takes on a special form because a term in Equation (B.16) is changed.

$$\lim_{r \to 0} \frac{1}{r} \frac{\partial \psi_{pf}}{\partial r} = \frac{\partial^2 \psi_{pf}}{\partial r^2}$$

Applying Equations (B.18) and (B.19) and finite differences to the modified form of Equation (B.16) yields the following result for the centerline element.

$$A|0| = \frac{4N^2}{\Gamma} B|1| - \left| \frac{4N^2 + \frac{P}{L} VMAX}{\Gamma} \right| B|0| + \frac{P}{L\Gamma} VMAX \; F|0| \qquad (B.27)$$

$$B|0| = \frac{-4N^2}{\Gamma} A|1| + \left| \frac{4N^2 + \frac{P}{L} VMAX}{\Gamma} \right| A|0| - \frac{P}{L\Gamma} VMAX \; E|0| - \frac{\epsilon}{\Gamma} \qquad (B.28)$$

The fluid-wall interface element is a composite of both fluid and wall materials. The energy equation for this element can be written

$$\left| \rho_w V_w C_w + \rho_f V_f C_f \right| \frac{\partial T}{\partial t} = q_{IN} A_{IN} - q_{out} A_{out} + V_f q_o \epsilon \sin \omega t \qquad (B.29)$$

where

$$V_w = 2\pi R_i \frac{\delta}{2M} \qquad q_{out} = -K_w \left. \frac{\partial T_w}{\partial r^*} \right|_{r^* = R_i}$$

$$V_f = 2\pi R_i \frac{R_i}{2N}$$

$$A_{out} = 2\pi R_i \left| 1 + \frac{\delta}{2M} \right| \qquad q_{IN} = -K_f \left. \frac{\partial T_f}{\partial r^*} \right|_{r^* = R_i}$$

$$A_{IN} = 2\pi R_i \left| 1 - \frac{1}{2N} \right|$$

A combination of dimensionless parameters, the above quantities, Equations (B.18) and (B.19), and finite differences, results in Equation (B.29) becoming the following two equations.

$$A(N) = \frac{-(N-1/2)\left|B(N)-B(N-1)\right| + \frac{\Lambda}{\beta}\left(\frac{M}{\delta}+\frac{1}{2}\right)\left|D(1)-D(0)\right|}{\Gamma\left(\frac{\delta}{2\beta M}+\frac{1}{2N}\right)} \tag{B.30}$$

$$B(N) = \frac{(N-1/2)\left|A(N)-A(N-1)\right| - \frac{\Lambda}{\beta}\left(\frac{M}{\delta}+\frac{1}{2}\right)\left|C(1)-C(0)\right| - \frac{\epsilon}{2N}}{\Gamma\left(\frac{\delta}{2\beta M}+\frac{1}{2N}\right)} \tag{B.31}$$

The element at the outside of the wall (M, J) has a thickness of one-half that of a general wall element. The energy equation is found to be

$$\rho_W C_W V_W \frac{\partial T_W}{\partial t} = q_{IN} A_{IN} \tag{B.32}$$

where

$$V_W = 2\pi R_o \frac{\delta}{2M}$$

$$A_{IN} = 2\pi R_i\left|1+\delta-\frac{\delta}{2M}\right|$$

$$q_{IN} = -K_W \frac{\partial T_W}{\partial r^*}\bigg|_{r^*=R_o}$$

Using the above quantities, dimensionless parameters, Equation (B.19), and finite differences, Equation (B.32) is transformed into the following two equations.

$$C(M) = \frac{-\Lambda\left(\frac{M}{\delta} + M - \frac{1}{2}\right)\left(D(M) - D(M-1)\right)}{\Gamma\frac{\delta}{2M}(1+\delta)} \tag{B.33}$$

$$D(M) = \frac{\Lambda\left(\frac{M}{\delta} + M - \frac{1}{2}\right)\left(C(M) - C(M-1)\right)}{\Gamma\frac{\delta}{2M}(1+\delta)} \tag{B.34}$$

5. Step Response Finite Difference Equations

Both the inlet temperature step response and internal energy step response are so similar that only the latter case will be considered. The only difference separating the two cases is the energy generation term in the fluid equation which is not present for the first case.

The energy equations for the fluid and wall were given in Chapter II. They are repeated here.

$$\frac{\partial \psi_f}{\partial \theta} + U(r)\frac{\partial \psi_f}{\partial X} = \frac{\partial^2 \psi_f}{\partial r^2} + \frac{1}{r}\frac{\partial \psi_f}{\partial r} + 1 \tag{B.35}$$

$$\frac{\partial \psi_w}{\partial \theta} = \Lambda\left(\frac{\partial^2 \psi_w}{\partial r^2} + \frac{1}{r}\frac{\partial \psi_w}{\partial r}\right) \tag{B.36}$$

Notation used in the finite difference equations can be simplified by eliminating the axial subscript and the superscript relating to time increments. This is possible because the variables are solved for at one axial location and for one time increment during any phase of the solution.

Fluid	Wall
$\psi_f^{n+1}(I,J) = S(I)$	$\psi_w^{n+1}(K,J) = V(K)$
$\psi_f^{n+1}(I+1,J) = S(I+1)$	$\psi_w^{n+1}(K+1,J) = V(K+1)$
$\psi_f^{n+1}(I-1,J) = S(I-1)$	$\psi_w^{n+1}(K-1,J) = V(K-1)$
$\psi_f^{n+1}(I,J-1) = U(I)$	$\psi_w^{n}(K,J) = W(K)$
$\psi_f^{n}(I,J) = F(I)$	

Central finite difference approximations to the derivatives are used in the radial direction, but forward differences are necessary in the axial and time directions due to the method of solution. The terms in Equation (B.35) can be written as follows

$$\frac{\partial \psi_f}{\partial \theta} = \frac{S(I) - F(I)}{\Delta \theta}$$

$$\frac{\partial \psi_f}{\partial X} = \frac{S(I) - U(I)}{L/P}$$

$$\frac{1}{r}\frac{\partial \psi_f}{\partial r} = \frac{1}{I/N}\left(\frac{S(I+1) - S(I-1)}{2/N}\right)$$

$$\frac{\partial^2 \psi_{sf}}{\partial r^2} = \frac{S(I+1) + S(I-1) - 2\,S(I)}{1/N^2}$$

Substitution of the above quantities into Equation (B.35) gives

$$-N^2\left(1 + \frac{1}{2I}\right) S(I+1) + \left(\frac{1}{\Delta\theta} + \frac{P}{L}\,VEL(I) + 2N^2\right) S(I)$$

$$-N^2\left(1 - \frac{1}{2I}\right) S(I-1) = \frac{U(I)}{\Delta\theta} + \frac{P}{L}\,VEL(I)\,U(I) + 1 \qquad \text{(B.37)}$$

The equation for a general point in the wall can similarly be found.

$$-\Lambda\left(\frac{M^2}{\delta^2} + \frac{M}{2\delta\left(1 + \frac{K\delta}{M}\right)}\right) V(K+1) + \left(\frac{1}{\Delta\theta} + 2\,\frac{\Lambda M^2}{\delta^2}\right) V(K)$$

$$-\Lambda\left(\frac{M^2}{\delta^2} - \frac{M}{2\delta\left(1 + \frac{K\delta}{M}\right)}\right) V(K-1) = \frac{W(K)}{\Delta\theta} \qquad \text{(B.38)}$$

Equation (B.36), changed to apply to a centerline element, takes the following form.

$$\frac{\partial \psi_f}{\partial \theta} + U_{MAX}\frac{\partial \psi_f}{\partial X} = 2\,\frac{\partial^2 \psi_f}{\partial r^2} + 1 \qquad \text{(B.39)}$$

In terms of finite differences, the centerline equation becomes

$$\left(\frac{1}{\Delta\theta} + \frac{P}{L}VMAX + 4N^2\right)S(0) - 4N^2 S(1)$$

$$= \frac{F(0)}{\Delta\theta} + \frac{P}{L}VMAX\ U(0) + 1 \qquad \text{(B.40)}$$

The composite fluid-wall interface equation appears as

$$\left(\frac{\delta}{2\beta M} + \frac{1}{2N}\right)\frac{\partial\psi}{\partial\theta} = -\left(1 - \frac{1}{2N}\right)\left.\frac{\partial\psi_f}{\partial r}\right|_{r=1}$$

$$+ \frac{\Lambda}{\beta}\left(1 + \frac{\delta}{2M}\right)\left.\frac{\partial\psi_w}{\partial r}\right|_{r=1} + \frac{1}{2N} \qquad \text{(B.41)}$$

If it is noted that $S(N) = V(0)$, Equation (B.41) takes the following form when written as a finite difference equation.

$$-\left(N - \tfrac{1}{2}\right)S(N-1) + \left(\frac{1}{2\Delta\theta}\left(\frac{\delta}{\beta M} + \frac{1}{N}\right) + \frac{\Lambda}{\beta}\left(\frac{M}{\beta} + \frac{1}{2}\right) + N - \tfrac{1}{2}\right)S(N)$$

$$-\frac{\Lambda}{\beta}\left(\frac{M}{\delta} + \tfrac{1}{2}\right)V(1) = \frac{1}{2\Delta\theta}\left(\frac{\delta}{\beta M} + \frac{1}{N}\right)F(N) + \frac{1}{2N} \qquad \text{(B.42)}$$

The energy equation for the half element at the outside of the wall can be written

$$\frac{\delta}{2M}(1+\delta)\frac{\partial\psi_w}{\partial\theta} = -\Lambda\left(1 + \delta - \frac{\delta}{2M}\right)\left.\frac{\partial\psi_w}{\partial r}\right|_{r=1} \qquad \text{(B.43)}$$

Applying finite differences results in the following equation for the element located at the outside of the wall.

$$-\Lambda\left(\frac{M}{\delta}+M-1/2\right)V(M-1)+\left(\frac{\delta(1+\delta)}{2\,\Delta\theta\,M}+\Lambda\left(\frac{M}{\delta}+M-1/2\right)\right)V(M)$$

$$=\frac{\delta(1+\delta)}{2\,\Delta\theta\,M}\,W(M) \qquad \text{(B.44)}$$

6. Truncation Error

Because the finite difference approximation to a derivative is found from a truncated Taylor series, an error of the order $(\Delta x)^2$ is introduced. This truncation error is directly dependent upon the grid size used in the numerical solution. Too few radial or axial divisions in the fluid or tube will cause a considerable deviation between the true solution and the numerical result. However, too many divisions will require more computations and increase the computer time.

Figure 39 shows the comparison between the exact solution by Michiyoshi, et al.[7] and the numerical solution with 20 radial grid divisions.

Figure 40 shows the effect of axial grid size. It can be seen that convergence to the correct solution is quite rapid as P/L is increased.

Evaluation of temperature gradients near the fluid-wall interface is difficult because of the large temperature changes which occur there. In the step response solution as many as 100 fluid and wall divisions were used to accurately evaluate the temperature gradients.

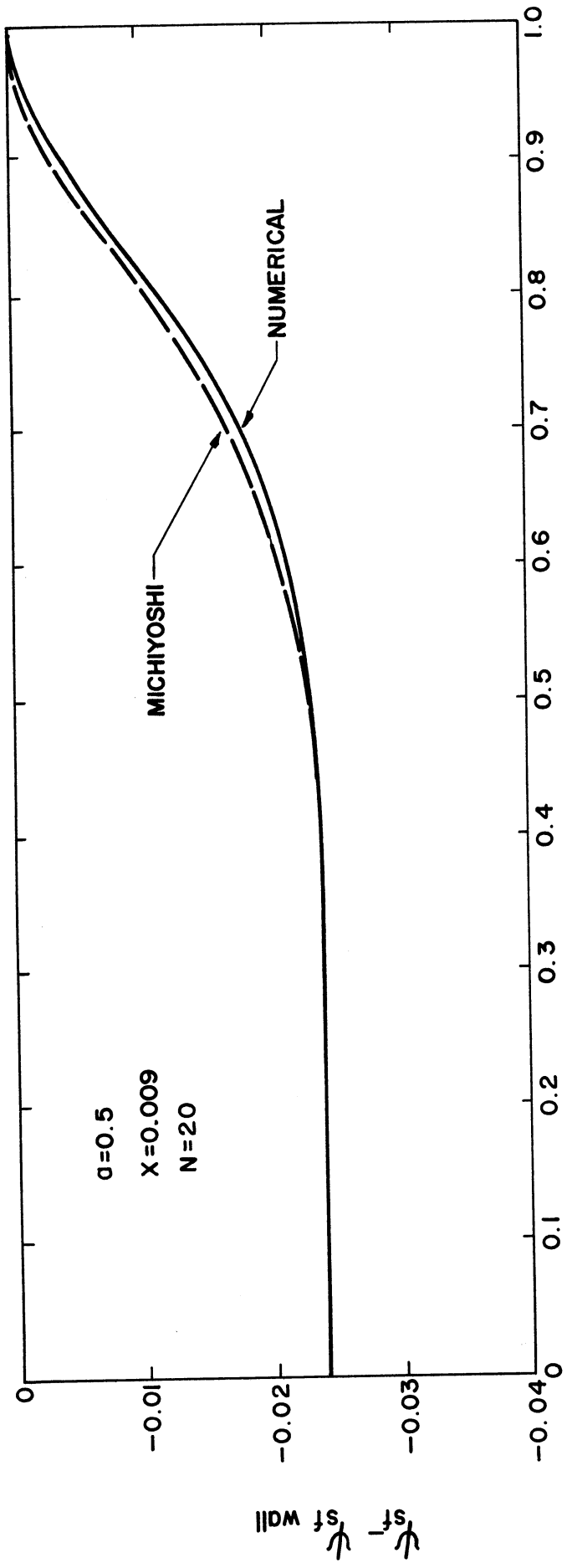

Figure 39. Comparison of Numerical Results with Exact Solution by Michiyoshi, et al.(7)

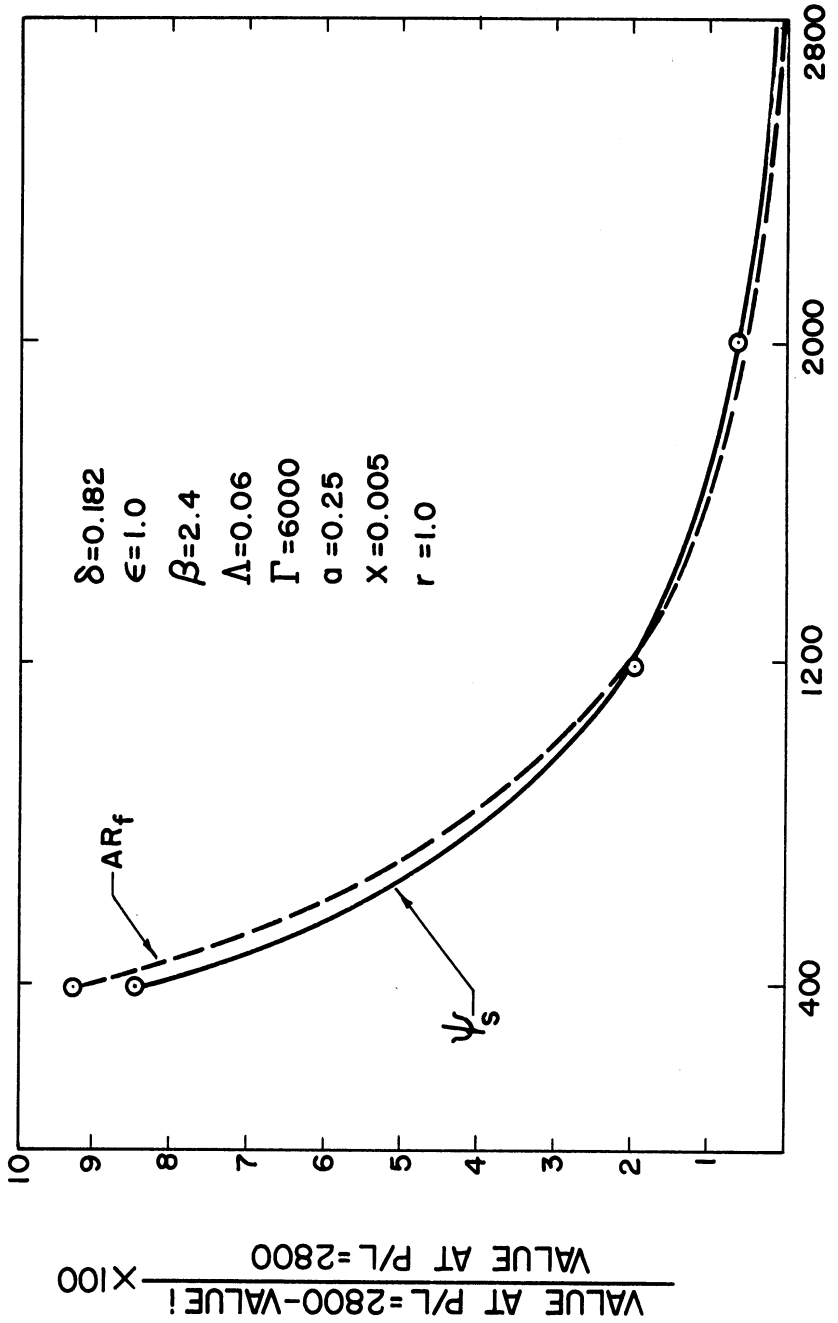

Figure 40. Test of Truncation Error Due to Axial Grid Dimension.

APPENDIX C

ELECTRICAL ENTRANCE LENGTH ASSOCIATED WITH ELECTRODES

A non-uniform energy generation across the tube section in the region of the test-section electrodes results from their non-symmetrical location at the side of the tube. An estimate of the entrance length required before the electrical potential is uniform across the tube can be obtained by considering a two-dimensional infinite channel of width D_i which has a source at the origin and a sink at $+\infty$ (see Figure 41). The potential for this configuration can be obtained by adding the potential which causes a uniform flow of $\pi M/2D_i$ along the positive real axis to the potential resulting from an infinite number of equi-distant sources of strength $2\pi M$ separated by a distance $2D_i$ along the imagninary axis[36]. The resulting potential, ϕ_e, is given by

$$\phi_e = -\frac{M}{2} \ln \frac{1}{2}\left| \cosh \frac{\pi Z}{D_i} - \cos \frac{\pi Y}{D_i} \right| - \frac{\pi M}{2 D_i} Z \qquad (C.1)$$

Numerical substitution reveals that at $Z = 1.3D_i$ there is only a one per cent variation of the potential across the channel section.

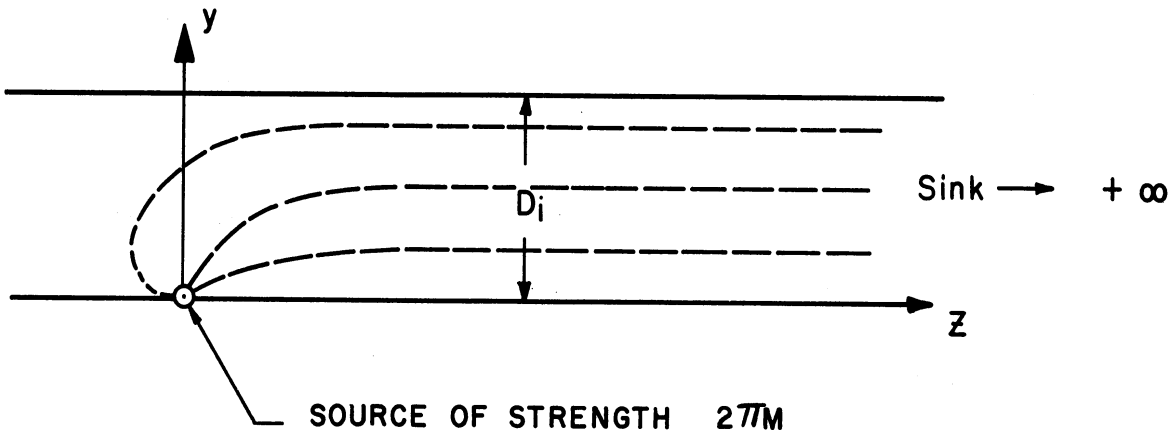

Figure 41. Two-dimensional Infinite Channel with Source at Origin and Sink at $+\infty$.

APPENDIX D

CONFIDENCE LIMITS

By a method outlined by Kline and McClintock[37], an uncertainty interval or confidence limit can be placed on an experimental result which is a function of several variables that possess an uncertainty themselves. The uncertainty interval is specified as that interval about the mean into which a certain percentage of the values of a variable or result would have fallen if the experiment had been repeated an infinite number of times. When the result R is a function of n independent variables, then the uncertainty interval is given by

$$W_R = \left[\left(\frac{\partial R}{\partial V_1} W_1 \right)^2 + \left(\frac{\partial R}{\partial V_2} W_2 \right)^2 + \cdots + \left(\frac{\partial R}{\partial V_n} W_n \right)^2 \right]^{1/2} \qquad \text{(D.1)}$$

where: V_n = independent variables

W_R = uncertainty interval of the result

W_n = uncertainty interval of the independent variable

Table VI contains typical mean values of important variables with an uncertainty of which the author is 95 per cent confident. These values will be used to determine the confidence limits for typical results in order to illustrate the method employed and the factors considered.

Energy generation in the test-section fluid is seen from Equation (5.2) to be a function of test-section voltage, amperage, radius, and length between the electrodes. The uncertainty interval

TABLE VI

UNCERTAINTIES IN VARIABLES

Description	Mean Value	Uncertainty (±)
r*	0.371 in.	0.002 in.
Length between electrodes, L	10.5 in.	0.5 in.
x*	7.8 in.	0.3 in.
Test-Section Voltage	36 volts	0.2 volts
Test-Section Current	2 amps	0.02 amps
Position of fluid thermocouples		0.050 in.
Absolute thermocouple reading	75°F	1°F
Wall thermocouple error due to heat loss to ambient	10°F	0.47°F
Wall thermocouple temperature disturbance	10°F	0.25°F
Resolution of Sanborn Recorder and Potentiometer		0.2°F
q"	88,915 $\frac{BTU}{hr\text{-}ft^3}$	4489 $\frac{BTU}{hr\text{-}ft^3}$
Wall temperature	10°F	0.84°F
Centerline fluid temperature	0.5°F	0.284°F

of this result is given by

$$W_{q''} = \left[\left(\frac{\partial q''}{\partial E} W_E\right)^2 + \left(\frac{\partial q''}{\partial I} W_I\right)^2 + \left(\frac{\partial q''}{\partial R_i} W_{R_i}\right)^2 + \left(\frac{\partial q''}{\partial L} W_L\right)^2\right]^{1/2} \qquad (D.2)$$

By taking the appropriate derivatives and using the values given in Table IV, the uncertainty in energy generation is found to be $W_{q''} = 4480$ BTU/hr-ft^3. The mean value of energy generation is 88,915 BTU/hr-ft^3. Thus, the uncertainty is about 5 per cent of the total.

The centerline fluid temperature uncertainty is a function of the resolution of the recording instruments and radial and axial location of the thermocouple

$$W_T = \left[\left(\frac{\partial T}{\partial R} W_R\right)^2 + \left(\frac{\partial T}{\partial r^*} W_{r^*}\right)^2 + \left(\frac{\partial T}{\partial X^*} W_{X^*}\right)^2\right]^{1/2} \qquad (D.3)$$

Assuming the mean value of the centerline temperature rise to be 0.5°F, the uncertainty may be evaluated

$$W_T = \left[\left((0.1)(0.2)\right)^2 + \left(\frac{1.5}{0.371}\, 0.05\right)^2 + \left(\frac{0.5}{7.8}\, 0.2\right)^2\right]^{1/2} \qquad (D.4)$$

This uncertainty equals 56.8 per cent of the total centerline fluid temperature.

The uncertainty in the wall temperature measurement is a function of the resolution of the recorder, axial location, heat loss from the tube wall, and the disturbance due to the presence of the thermocouple itself. For a 10°F wall temperature rise, the uncertainty interval is 0.84°F, which amounts to 8.4 per cent of the total.

The uncertainty interval or confidence limit on the result can be expressed in a dimensionless form

$$\Psi = \frac{T k_f}{q'' R_i^2} \tag{D.5}$$

$$\frac{W\Psi}{\Psi} = \left[\left(\frac{W_T}{T}\right)^2 + \left(\frac{Wq''}{q''}\right)^2 + \left(\frac{2 W_{Ri}}{R_i}\right)^2\right]^{1/2} \tag{D.6}$$

For the dimensionless centerline temperature

$$\frac{W\Psi_f}{\Psi_f} = \left[\left(\frac{0.284}{0.5}\right)^2 + \left(\frac{4,480}{88,915}\right)^2 + \left(\frac{2(0.002)}{0.371}\right)^2\right]^{1/2} = 0.571 \tag{D.7}$$

and for the dimensionless wall temperature

$$\frac{W\Psi_w}{\Psi_w} = \left[\left(\frac{0.84}{10}\right)^2 + \left(\frac{4,480}{88,915}\right)^2 + \left(\frac{2(0.002)}{0.371}\right)^2\right]^{1/2} = 0.0985 \tag{D.8}$$

The 95 per cent confidence limit placed on the dimensionless centerline and wall temperatures would be 57.1 and 9.85 per cent, respectively, of the total, based on the typical mean values considered.

APPENDIX E

COMPUTER PROGRAMS

The Computer Programs A and B were used to solve the finite difference equations listed in Tables I and III for the step response and steady-periodic temperature distribution, respectively. The steady-periodic computer program and nomenclature are based on those developed by Ayers[8].

A flow diagram preceeds each program to schematically show the order of computations.

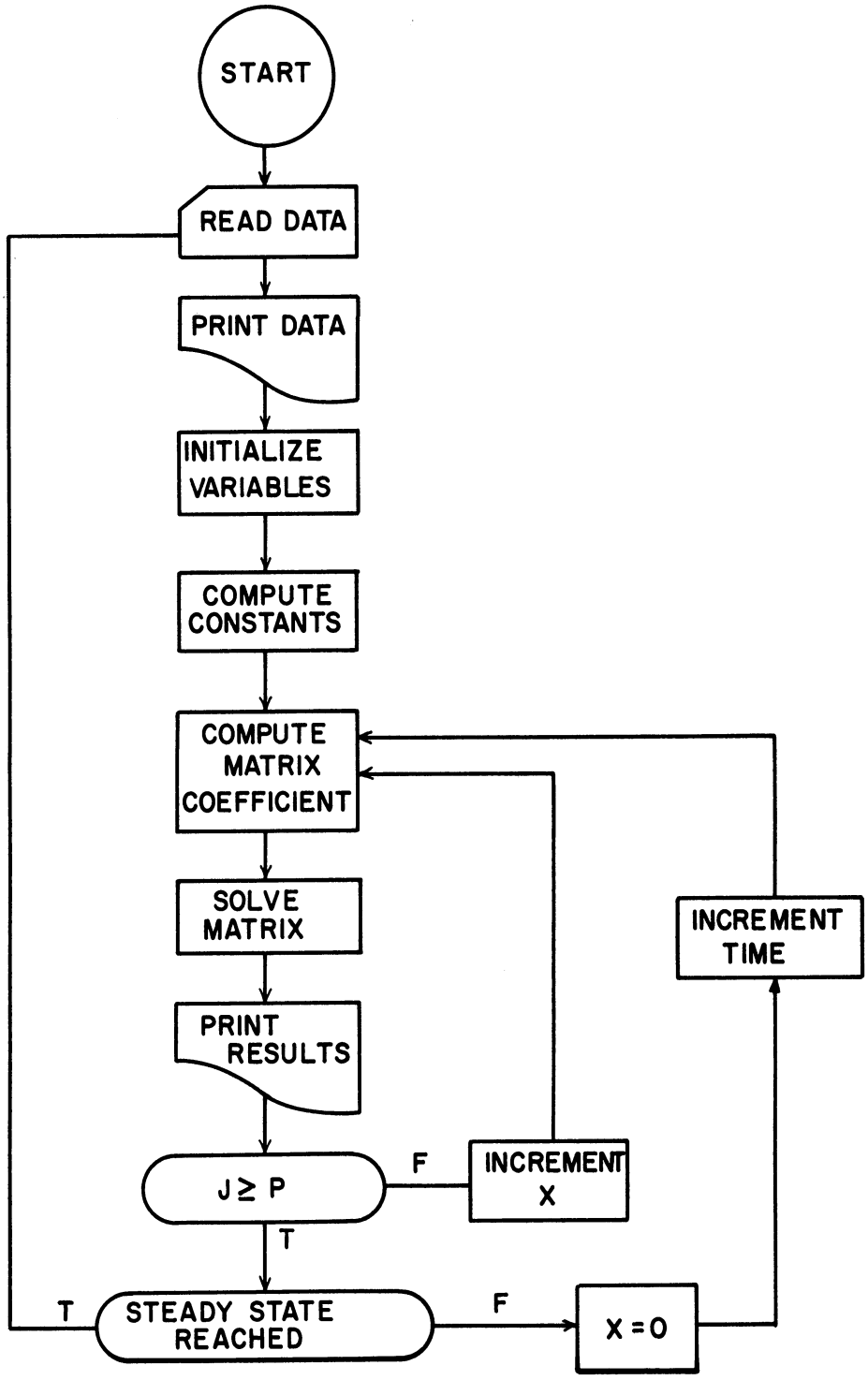

Figure 42. Computer Program A Flow Diagram, Step Response.

COMPUTER PROGRAM NOMENCLATURE

STEP RESPONSE

A(I)	Coefficient of first independent variable in Equation I
ALPHA	Convergence limit
B(I)	Coefficient of second independent variable in Equation I
BETA	$\rho_f C_f / \rho_w C_w$
C(I)	Coefficient of third independent variable in Equation I
CMPARE	WGRAD(Λ/B)
COUNT	Time step counter
DELT	Time increment
DELTA	Dimensionless wall thickness, δ
D(I)	Constant terms in Equation I
FGRAD	Temperature gradient in fluid at fluid-wall interface
F(I, J)	Storage matrix for ψ_f(I, J)
FREQ	Time frequency of solution printout
I	Radial counter in the fluid, (I = 0, 1, 2...N)
INLET	Inlet fluid temperature
J	Axial counter, (J = 0, 1, 2...P)
K	Radial counter in wall, (K = 0, 1, 2...M)
L	Length of grid network in the axial direction
LAM	Λ
M	Number of radial elements in the wall
MIXEDT	Mixed mean temperature of fluid
N	Number of radial elements in the fluid

P	Number of axial elements in the fluid and wall
Q	Internal energy generation switch, (Q = 1.0, there is energy generation; Q = 0.0, there is no energy generation)
RATIO	Bingham plastic constant, a
S(I)	Fluid temperature , ψ_f
T	Time , Θ
U(I)	S(I, J-1)
V(I)	Wall temperature , ψ_w
VEL(I)	Fluid velocity , VEL(I) = u(r)
VMAX	Maximum fluid velocity , VMAX = $u^*_{max}/2u^*_m$
WGRAD	Temperature gradient in wall at fluid-wall interface
W(I,J)	Storage matrix for $\psi_w(K, J)$, $x = (x^*/R_i)(R_eP_r)^{-1}$
X	Axial distance

COMPUTER PROGRAM A - STEP RESPONSE

```
          DIMENSION A(200),B(200),C(200),D(200),S(200),EPS(200),GAMMA(200),
        1 F(6000,AC),W(4000,AD),V(100),VEL(100),U(100)
          VECTOR VALUES AC= 2,20,20
          VECTOR VALUES AD= 2,20,20
          INTEGER COUNT,FREQ,N,M,I,K,J
          PRINT COMMENT $2HEAT TRANSFER TO BINGHAM PLASTIC IN LAMINAR
        1 FLOW WITH INTERNAL HEAT GENERATION  *** STEP RESPONSE ***$
START     READ DATA
          PRINT COMMENT $1 NEW DATA$
          PRINT RESULTS N,M,RATIO,FREQ,DELT,BETA,LAM,DELTA,L,P,ALPHA,Q,INLET
          WHENEVER (P*N.G.6000).OR.(P*M.G.4000).OR.N.G.100.OR.M.G.100
          PRINT COMMENT $DIMENSION OF ARRAY EXCEEDED. DATA REJECTED$
          END OF CONDITIONAL
          VMAX =(3.*(1.-RATIO).P.2.)/(RATIO.P.4.-4.*RATIO+3.)
          WHENEVER RATIO.E.1.
          THROUGH LOOPA, FOR I=0,1,I.E.N
LOOPA     VEL(I)=0.5
          TRANSFER TO ENTRYA
          END OF CONDITIONAL
          THROUGH LOOPB, FOR I=0,1,I.E.N
          IF=I
          NF=N
          VEL(I)=3.*(1.-2.*RATIO+2.*RATIO*IF/NF-IF*IF/NF/NF)/(
        1 RATIO.P.4.-4.*RATIO+3.)
LOOPB     WHENEVER IF/NF.LE.RATIO, VEL(I)=VMAX
ENTRYA    CA = N*N
          CB = P/L
          CC = N-0.5
          CD = 0.5/DELT*(DELTA/BETA/M+1./N)
          CE = LAM/BETA*(M/BETA+0.5)
          CF = LAM*M*M/DELTA/DELTA
          CG = 0.5*LAM*M/DELTA
          CH = DELTA/M
          CI = LAM*(M/DELTA+M-0.5)
          CJ = 0.5*DELTA*(1.+DELTA)/DELT/M
          PRINT COMMENT $THE CONSTANTS GENERATED BY THIS DATA ARE$
          PRINT RESULTS CA,CB,CC,CD,CE,CF,CG,CH,CI,CJ,VEL(0)...VEL(N-1)
          COUNT = 0
          T = DELT
          THROUGH LOOPD, FOR J=0,1,J.G.P
          THROUGH LOOPC, FOR I=0,1,I.G.N
LOOPC     F(I,J) = 0.
          THROUGH LOOPD, FOR K=1,1,K.G.M
LOOPD     W(K,J) = 0.
          B(0) = 1./DELT+VMAX*CB+4.*CA
          C(0) = -4.*CA
          THROUGH LOOPE, FOR I=1,1,I.G.N-1
          A(I) = -CA*(1.-0.5/I)
          B(I) = 1./DELT+VEL(I)*CB+2.*CA
LOOPE     C(I) = -CA*(1.+0.5/I)
          A(N) = -CC
          B(N) = CD+CC+CE
          C(N) = -CE
```

```
          THROUGH LOOPF, FOR K=1,1,K.G.M-1                                                    *051
          A(N+K) = -CF+CG/(1.+K*CH)                                                           *052                01
          B(N+K) = 1./DELT+2.*CF                                                              *053                01
LOOPF     C(N+K) = -CF-CG/(1.+K*CH)                                                           *054                01
          A(N+M) = -CI                                                                        *055
          B(N+M) = CJ+CI                                                                      *056
ENTRYB    THROUGH LCOPFA, FOR I=0,1,I.G.N                                                     *057
LOOPFA    U(I) = INLET                                                                        *058                01
          THROUGH LOOPP, FOR J=1,1,J.G.P                                                      *059
          THROUGH LOOPG, FOR I=0,1,I.G.N-1                                                    *060                01
          D(I) = F(I,J)/DELT+VEL(I)*CB*U(I)+Q                                                 *061                02
LOOPG     CONTINUE                                                                            *062                02
          D(N) = CD*F(N,J)+0.5*Q/N                                                            *063                01
          THROUGH LOOPH, FOR K=1,1,K.G.M-1                                                    *064                01
LOOPH     D(N+K) = W(K,J)/DELT                                                                *065                02
          D(N+M) = CJ*W(M,J)                                                                  *066                01
          EPS(0) = B(0)                                                                       *067                01
          GAMMA(0) = D(0)/EPS(0)                                                              *068                01
          THROUGH LOOPK, FOR I=1,1,I.G.M+N                                                    *069                01
          EPS(I) = B(I)-A(I)*C(I-1)/EPS(I-1)                                                  *070                02
LOOPK     GAMMA(I) = (D(I)-A(I)*GAMMA(I-1))/EPS(I)                                            *071                02
          S(M+N) = GAMMA(M+N)                                                                 *072                01
          THROUGH LOOPL, FOR I= M+N-1,-1,I.L.0                                                *073                01
LOOPL     S(I) = GAMMA(I)-C(I)*S(I+1)/EPS(I)                                                  *074                02
          THROUGH LOOPM, FOR K=0,1,K.G.M                                                      *075                01
LOOPM     V(K) = S(N+K)                                                                       *076                02
          THROUGH LOOPN, FOR I=0,1,I.G.N                                                      *077                01
          U(I) = F(I,J)                                                                       *078                02
LOOPN     F(I,J)= S(I)                                                                        *079                02
          THROUGH LOOPO, FOR K=1,1,K.G.M                                                      *080                01
LOOPO     W(K,J)= V(K)                                                                        *081                02
          WHENEVER (COUNT+1)/FREQ.E.(COUNT+1.)/FREQ                                           *082                01
          PRINT COMMENT$**********************************************$                     *083          01    01
          X = J/CB                                                                            *084          01    01
          PRINT RESULTS T,X                                                                   *085          01    01
          PRINT RESULTS S(0)...S(N),V(0)...V(M)                                               *086          01    01
          FGRAD= N*(S(N)-S(N-1))                                                              *087          01    01
          PRINT RESULTS FGRAD                                                                 *088          01    01
          WGRAD= M*(V(1)-V(0))/DELTA                                                          *089          01    01
          PRINT RESULTS WGRAD                                                                 *090          01    01
          CMPARE= WGRAD*LAM/BETA                                                              *091          01    01
          PRINT RESULTS CMPARE                                                                *092          01    01
          FAC= 12.*(1.-RATIO).P.2./(RATIO.P.4.-4.*RATIO+3.)                                   *093          01    01
          SUMS= FAC*S(0)/8./CA                                                                *094          01    01
          THROUGH LOOPS, FOR I=1,1,I.G.RATIO*N                                                *095          01    01
LOOPS     SUMS = SUMS+S(I)*FAC*I/CA                                                           *096          01    02
          THROUGH LOOPT, FOR I=I,1,I.G.N-1                                                    *097          01    01
          FAC= 12./(RATIO.P.4.-4.*RATIO+3.)*((1.-2.*RATIO)*I/CA+                              *098          01    02
        1  2.*RATIO*I*I/(N.P.3.)-I.P.3./(N.P.4.))                                            *098
LOOPT     SUMS= SUMS+FAC*S(I)                                                                 *099          01    02
          MIXEDT= SUMS                                                                        *100          01    01
          PRINT COMMENT $THE MIXED MEAN TEMPERATURE IS$                                       *101          01    01
          PRINT RESULTS MIXEDT                                                                *102          01    01
          END OF CONDITIONAL                                                                  *103          01    01
LOOPP     CONTINUE                                                                            *104                01
          COUNT = COUNT+1                                                                     *105
          T = T+DELT                                                                          *106
          WHENEVER COUNT/FREQ.E.(COUNT+0.0)/FREQ                                              *107
          WHENEVER .ABS.((V(1)-V(0))*M/DELTA).G.ALPHA.OR.T.L.5.*X/U(0)                        *108          01
          TRANSFER TO ENTRYB                                                                  *109          02
          END OF CONDITIONAL                                                                  *110          02
          TRANSFER TO START                                                                   *111          01
          END OF CONDITIONAL                                                                  *112          01
          TRANSFER TO ENTRYB                                                                  *113
          END OF PROGRAM                                                                      *114
```

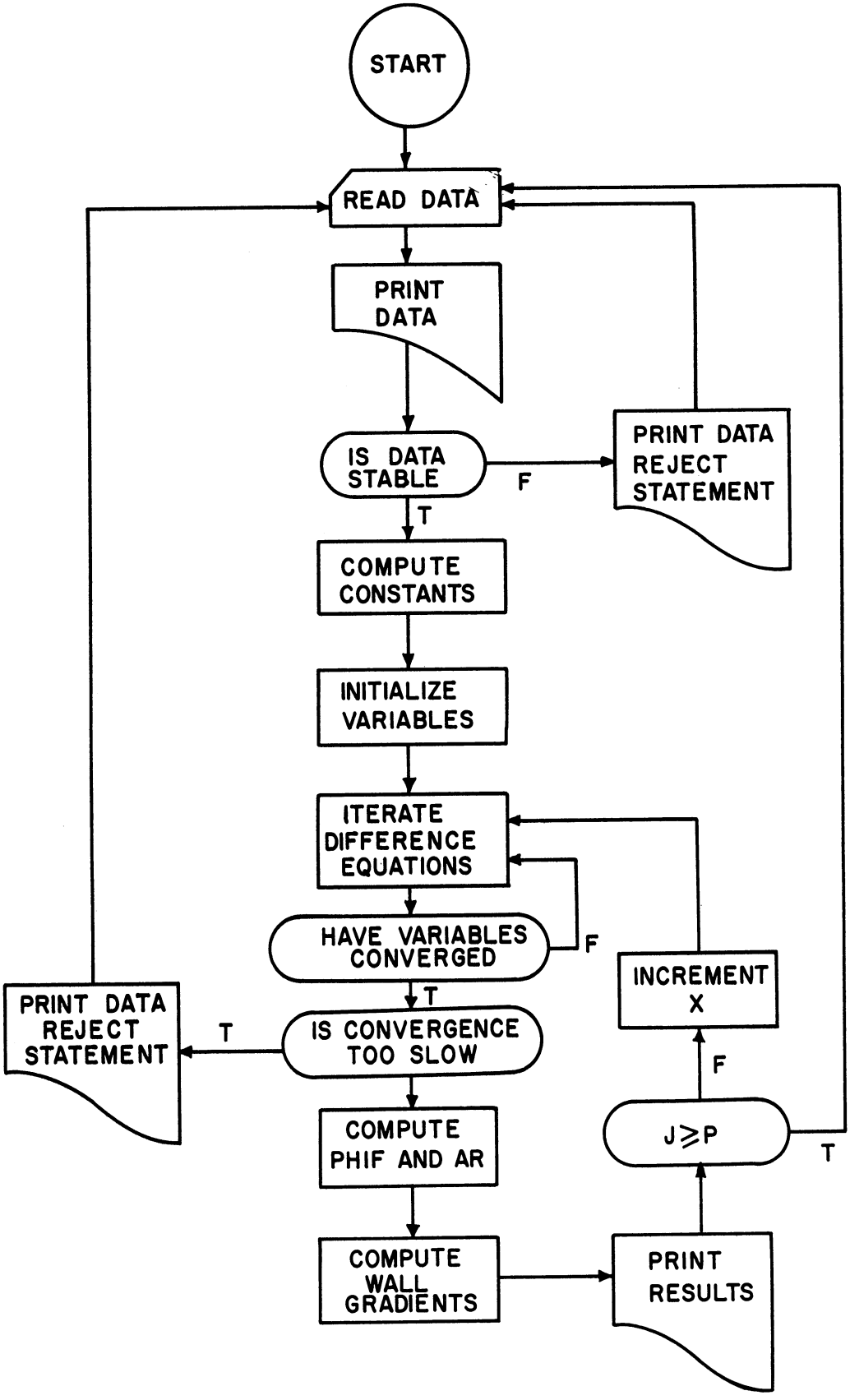

Figure 43. Computer Program B Flow Diagram, Steady-Periodic.

COMPUTER PROGRAM 3 NOMENCLATURE

STEADY-PERIODIC

A(I)	Sin $\Gamma\theta$ coefficient in ψ_{pf} at the point (I, J) in the fluid; A(I, J)
ALPHA	Convergence limit
AMPRAF(I)	Periodic amplitude ratio at the point (I, J) in the fluid, $\sqrt{A(I)^2 + B(I)^2}$ /ϵ S(I)
AMPRAW(K)	Periodic amplitude ratio at the point (K, J) in the wall, $\sqrt{C(K)^2 + D(K)^2}$ /ϵ V(K)
ATN1.	Arctangent subroutine
B(I)	Cos $\Gamma\theta$ coefficient in ψ_{pf} at the point (I, J) in the fluid; B(I, J)
BETA	$\rho_f C_f/\rho_w C_w$
C(K)	Sin $\Gamma\theta$ coefficient in ψ_{pw} at the point (K, J) in the wall; C(K, J)
COUNT	Iteration counter
D(K)	Cos $\Gamma\theta$ coefficient in ψ_{pw} at the point (K, J) in the wall; D(K, J)
DELTA	Dimensionless wall thickness, δ
E(I)	A(I, J-1)
EPS	ϵ
FGRAD	Periodic fluid temperature gradient at wall
FREQ	Axial frequency of solution printout
F(I)	B(I, J-1)
G(I)	A(I, J) after the previous iteration. Used in the convergence inequality for A(I, J)
GAM	Γ

H(I)	B(I, J) after the previous iteration. Used in the convergence inequality for B(I, J)
I	Radial counter in the fluid, (I = 0, 1, 2...N)
J	Axial counter, (J = 0, 1, 2...P)
K	Radial counter in the wall, (K = 0, 1, 2...M)
L	Length of grid network in the axial direction
LAM	Λ
M	Number of radial elements in the wall
MIXEDT	Mixed mean temperature of fluid
N	Number of radial elements in the fluid
P	Number of axial elements in the wall and fluid
PHIF(I)	ϕ_f = Arc tan - B(I)/A(I)
PHIW(K)	ϕ_w = Arc tan - D(K)/C(K)
PERCOF(I)	Periodic coefficient in the fluid, $\sqrt{A(I)^2 + B(I)^2}$
PERCOW(K)	Periodic coefficient in the wall, $\sqrt{C(K)^2 + D(K)^2}$
Q(K)	C(K, J) after the previous iteration
RATIO	Bingham plastic constant, a
R(K)	D(K, J) after the previous iteration
S(I)	ψ_{sf} at the point (I, J), in the fluid, S(I, J)
SQRT.	Square root subroutine
TIMEAV	Time Average of periodic fluid temperature gradient, $\overline{FGRAD}$
U(I)	S(I, J-1)
VEL(I)	Fluid velocity, VEL(I) = u(r)
VMAX	Maximum fluid velocity, VMAX = $u^*_{max}/2\ u^*_m$
V(K)	ψ_{sw} at the point (K, J) in the wall; V(K, J)
W(I)	S(I, J) after the previous iteration
Y(K)	V(K, J) after the previous iteration

COMPUTER PROGRAM B - STEADY-PERIODIC

```
          DIMENSION A(50),B(50),C(50),D(50),F(50),G(50),H(50),Q(50),R(50),
         1 S(50),U(50),E(50),W(50),Y(50),PHIW(50),PHIF(50),PERCOF(50),
         2 VEL(50),EPSW(50),OPPF(50),CPPW(50),ADJF(50),ADJW(50),
         3 AMPRAF(50),AMPRAW(50),PERCCW(50)
          INTEGER I,J,K,M,N,P,COUNT,FREQ
          PRINT COMMENT $2 HEAT TRANSFER TO BINGHAM PLASTIC IN CIRCULAR
         1  TUBES IN LAMINAR FLOW WITH INTERNAL HEAT GENERATION$
START     READ DATA
          PRINT COMMENT $1NEW DATA$
          PRINT RESULTS EPS,BETA,LAM,GAM,DELTA,L,P,RATIO,N,M,FREQ
          PRINT COMMENT $ THE NUMBER OF RADIAL POINTS IN THE FLUID IS$
          PRINT RESULTS N
          DELT= 10.0E-37
          ALPHA = .001
          PI = 3.14159
          WHENEVER RATIO.E.1.
          THROUGH LCOPW, FOR I=0,1,I.E.N
LCOPW     VEL(I)=0.5
          VMAX=0.5
          TRANSFER TO ENTRY
          END OF CONDITIONAL
          VMAX =(3.*(1.-RATIO).P.2.)/(RATIO.P.4.-4.*RATIO+3.)
          THROUGH LCOPX, FOR I=0,1,I.E.N
          IF=I
          NF=N
          VEL(I)=3.*(1.-2.*RATIO+2.*RATIO*IF/NF-IF*IF/NF/NF)/(
         1 RATIO.P.4.-4.*RATIO+3.)
LCOPX     WHENEVER IF/NF.LE.RATIO, VEL(I)=VMAX
ENTRY     THROUGH LCOPT, FOR P=P,5,P/L.G.50000
          WHENEVER P/L.G.GAM/VEL(N-1)
          PRINT COMMENT $0THE NUMBER OF AXIAL NODAL POINTS IS$
          PRINT RESULTS P
          TRANSFER TO ENTRYA
          OTHERWISE
          CONTINUE
LCOPT     END OF CONDITIONAL
          PRINT COMMENT $0DIVERGENCE OCCURS IN THE FLUID EQUATIONS WHEN
         1  P IS INCREASED TO P/L = 50000. DATA REJECTED$
          TRANSFER TO START
ENTRYA    THROUGH LCOPL, FOR M=M,-1,M.L.2.
          WHENEVER GAM .G.(2.*N-1.+2.*LAM*M/BETA/DELTA+LAM/BETA)/(DELTA/
         1 BETA/2./M+0.5/N).AND.GAM.G.4.*LAM*M*M/DELTA/DELTA
          PRINT COMMENT $0 THE NUMBER OF NODAL POINTS IN THE WALL is
          PRINT RESULTS M
          TRANSFER TO ENTRYB
          OTHERWISE
          CONTINUE
LCOPL     END OF CONDITIONAL
          PRINT COMMENT$0 DIVERGENCE OCCURS IN THE WALL EQUATIONS WHEN
         1  M IS REDUCED TO 2.  DATA REJECTED$
          TRANSFER TO START
ENTRYB    CA = N.P.2.
          CB = 1.*P/L
```

```
            CC = CB/GAM                                                          *046
            CD = M/DELTA+2.5                                                     *047
            CE = LAM/GAM                                                         *048
            CF = M*M/DELTA/DELTA                                                 *049
            CG = GAM*DELTA/LAM/2./M                                              *050
            CH = LAM*(M/DELTA+M-3.5)                                             *051
            CI = GAM*DELTA*2.5/ M*(1.+DELTA)                                     *052
            PRINT COMMENT $THE CONSTANTS GENERATED BY THIS DATA ARE$             *053
            PRINT RESULTS CA,CB,CC,CD,CE,CF,CG,CH,CI,VMAX,VEL(C)...VEL(N-1)      *054
            THROUGH LCOPA, FOR I=0,1,I.G.N                                       *055
            A(I) = 0.                                                            *056                    01
            B(I) = 0.                                                            *057                    01
            S(I) = 0.                                                            *058                    01
            E(I) = 0.                                                            *059                    01
            F(I) = 0.                                                            *060                    01
LOOPA       U(I) = 0.                                                            *061                    01
            THROUGH LCOPV, FOR I=0,1,I.G.M                                       *062
            C(I) = 0.                                                            *063                    01
LCOPV       D(I) = 0.                                                            *064                    01
            THROUGH LCOPB, FOR J=1,1,J.G.P                                       *065
            THROUGH LCOPC, FOR I=0,1,I.G.N                                       *066                    01
            G(I) = 0.                                                            *067                    02
            H(I) = 0.                                                            *068                    02
LOOPC       W(I) = 0.                                                            *069                    02
            THROUGH LCOPD, FOR I=0,1,I.G.M                                       *070                    01
            C(I) = 0.                                                            *071                    02
LCOPD       R(I) = 0.                                                            *072                    02
            COUNT= 0                                                             *073                    01
ENTRYC      D(M)= CH*(C(M)-C(M-1))/CI                                            *074                    01
            C(M)= -CH*(D(M)-C(M-1))/CI                                           *075                    01
            THROUGH LCOPE, FOR K=M-1,-1,K.L.1                                    *076                    01
            FAC= 2.*DELTA*(K*DELTA/M+1.)                                         *077                    02
            C(K)= -CE*(CF+M/FAC)*C(K+1)-CE*(CF-M/FAC)*C(K-1)                     *078                    02
          1  +2.*CE*CF*C(K)                                                      *078
LCOPE       C(K)= CE*(CF+M/FAC)*D(K+1)+CE*(CF-M/FAC)*D(K-1)-2.*CE*CF*D(K)        *079                    02
            B(N)= (-LAM/BETA*CD*(C(1)-C(0))+(N-0.5)*(A(N)-A(N-1))-EPS            *080                    01
          1 /2./N)/(GAM*(DELTA/BETA/2./M+0.5/N))                                 *080
            A(N)= ((LAM/BETA*CD*(D(1)-D(0))-(N-0.5)*(B(N)-B(N-1)))/              *081                    01
          1 (GAM*(DELTA/BETA/2./M+0.5/N))                                        *081
            S(N)= 0.5/(N*N-0.5*N) +S(N-1)                                        *082                    01
            C(0)= A(N)                                                           *083                    01
            D(0)= B(N)                                                           *084                    01
            THROUGH LCOPF, FOR I=N-1,-1,I.L.1                                    *085                    01
            A(I)= (CA*(1.+0.5/I)*A(I+1)+CA*(1.-0.5/I)*A(I-1)+CB*VEL(I)*          *086                    02
          1 E(I)+GAM*B(I)+EPS)/(2.*CA+CB*VEL(I))                                 *086
            B(I)= (CA*(1.+0.5/I)*B(I+1)+CA*(1.-0.5/I)*B(I-1)+CB*VEL(I)           *087                    02
          1 *F(I)-GAM*A(I))/(2.*CA+CB*VEL(I))                                    *087
LOOPF       S(I)= (CA*(1.+0.5/I)*S(I+1)+CA*(1.-0.5/I)*S(I-1)+CB*U(I)             *088                    02
          1  *VEL(I+1.))/(2.*CA+CB*VEL(I))                                       *088
            A(0)= (4.*CA*A(1)+CB*VMAX*E(0)+GAM*B(0)+EPS)/                        *089                    01
          1 (4.*CA+CB*VMAX)                                                      *089
            B(0)= (4.*CA*B(1)+CB*VMAX*F(0)-GAM*A(0))/                            *090                    01
          1 (4.*CA+CB*VMAX)                                                      *090
            S(0)= (4.*CA*S(1)+CB*VMAX*U(0)+1.)/(CB*VMAX+4.*CA)                   *091                    01
            THROUGH LCOPG, FOR I=0,1,I.G.M                                       *092                    01
            WHENEVER .ABS.(C(I)).L.DELT.OR..ABS.(D(I))LL.DELT                    *093                    02
            TRANSFER TO ENTRYE                                                   *094          01        02
            OTHERWISE                                                            *095          01        02
            WHENEVER .ABS.(C(0)/C(I)).G.1000000.AND..ABS.(C(0)/D(I)).G.1000000   *096          01        02
            TRANSFER TO LOOPG                                                    *097          02        02
```

```
      END OF CONDITIONAL                                                    *098          02    02
      WHENEVER .APS.((C(I)-G(I))/C(I)).L.ALPHA*10..AND.                     *099          01    02
     1 .ABS.((D(I)-R(I))/D(I)).L.ALPHA*10.                                  *099
      CONTINUE                                                              *100          02    02
      OTHERWISE                                                             *101          02    02
      COUNT=COUNT+1                                                         *102          02    02
      WHENEVER COUNT.G.100                                                  *103          02    02
      PRINT COMMENT $*********************************************$         *104          03    02
      PRINT COMMENT$ CONVERGENCE IS TOO SLOW.  DATA REJECTED$               *105          03    02
      PRINT COMMENT$ SLOW CONVERGENCE IN THE WALL EQUATIONS.$               *106          03    02
      PRINT RESULTS S(0)...S(N),W(0)...W(N),A(0)...A(N),G(0)...G(N),        *107          03    02
     1 B(0)...B(N),H(0)...H(N),C(0)...C(M),C(0)...C(M),D(0)...D(M),         *107
     2 R(0)...R(M)                                                          *107
      PRINT COMMENT $*********************************************$         *108          03    02
      TRANSFER TO START                                                     *109          03    02
      OTHERWISE                                                             *110          03    02
      CONTINUE                                                              *111          03    02
      END OF CONDITIONAL                                                    *112          03    02
      THROUGH LCOPF, FOR K=0,1,K.G.M                                        *113          02    02
      C(K) = C(K)                                                           *114          02    03
LCOPF R(K) = D(K)                                                           *115          02    03
      THROUGH LCOPI, FOR K=0,1,K.G.N                                        *116          02    02
      G(K) = A(K)                                                           *117          02    03
      H(K) = B(K)                                                           *118          02    03
LCOPI W(K) = S(K)                                                           *119          02    03
      TRANSFER TO ENTRYC                                                    *120          02    02
      END OF CONDITIONAL                                                    *121          02    02
      END OF CONDITIONAL                                                    *122          01    02
LCOPG CONTINUE                                                              *123                02
      THROUGH LCOPJ, FOR I=0,1,I.G.N                                        *124                01
      WHENEVER .ABS.(A(I)).L.DELT.OR..ABS.(B(I)).L.DELT.OR..ABS.            *125                02
     1 (S(I)).L.DELT                                                        *125
      TRANSFER TO ENTRYE                                                    *126          01    02
      OTHERWISE                                                             *127          01    02
      WHENEVER .ABS.((A(I)-G(I))/A(I)).L.ALPHA.AND..ABS.((B(I)-H(I))/       *128          01    02
     1 B(I)).L.ALPHA.AND..ABS.((S(I)-W(I))/S(I)).L.ALPHA                    *128
      CONTINUE                                                              *129          02    02
      OTHERWISE                                                             *130          02    02
      COUNT=COUNT+1                                                         *131          02    02
      WHENEVER COUNT.G.25.AND..ABS.(B(I)).G..ABS.(1.0E 05*A(I))             *132          02    02
      PRINT COMMENT $*********************************************$         *133          03    02
      PRINT COMMENT $SLOW CONVERGENCE IN FLUID EQUATIONS BECAUSE  A         *134          03    02
     1   TENDS TOWARD ZERO$                                                 *134
      PRINT RESULTS W(0)...W(N),G(0)...G(N),H(0)...H(N)                     *135          03    02
      TRANSFER TO ENTRYD                                                    *136          03    02
      END OF CONDITIONAL                                                    *137          03    02
      WHENEVER COUNT.G.100                                                  *138          02    02
      PRINT COMMENT $ *********************************************$        *139          03    02
      PRINT COMMENT$ CONVERGENCE IS TOO SLOW.  DATA REJECTED$               *140          03    02
      PRINT COMMENT$ SLOW CONVERGENCE IN FLUID EQUATIONS.$                  *141          03    02
      PRINT RESULTS S(0)...S(N),W(0)...W(N),A(0)...A(N),G(0)...G(N),        *142          03    02
     1 B(0)...B(N),H(0)...H(N),C(0)...C(M),C(0)...C(M),D(0)...D(M),         *142
     2 R(0)...R(M)                                                          *142
      PRINT COMMENT $*********************************************$         *143          03    02
      TRANSFER TO START                                                     *144          03    02
      OTHERWISE                                                             *145          03    02
      CONTINUE                                                              *146          03    02
      END OF CONDITIONAL                                                    *147          03    02
      THROUGH LCOPK, FOR K=0,1,K.G.M                                        *148          02    02
      C(K) = C(K)                                                           *149          02    03
```

```
LCCRK       R(K) = D(K)                                                          *150        02    03
            THROUGH LCCPL, FOR K=0,1,K.G.N                                       *151        02    02
            G(K) = A(K)                                                          *152        02    03
            H(K) = B(K)                                                          *153        02    03
LCCPL       W(K) = S(K)                                                          *154        02    03
            TRANSFER TO ENTRYC                                                   *155        02    02
            END OF CONDITIONAL                                                   *156        02    02
ENTRYE      END OF CONDITIONAL                                                   *157        01    02
LCCPJ       CONTINUE                                                             *158                    02
ENTRYD      THROUGH LCCPM, FOR I=0,1,I.G.N                                       *159                    01
            E(I) = A(I)                                                          *160                    02
            F(I) = B(I)                                                          *161                    02
LCCPM       U(I) = S(I)                                                          *162                    02
            WHENEVER J/FREQ.E.(0.0+J)/(0.0+FREQ)                                 *163                    01
            X =J/CB                                                              *164        01          01
            PRINT COMMENT $0$                                                    *165        01          01
            PRINT RESULTS X,COUNT                                                *166        01          01
            THROUGH LCCPN, FOR I=0,1,I.G.N                                       *167        01          01
            NORMF = 1./(.ABS.(B(I)))                                             *168        01          02
            CPPF(I) = -B(I)*NORMF                                                *169        01          02
            ADJF(I) = A(I)*NORMF                                                 *170        01          02
            PHIF(I) = ATN1.(CPPF(I)/ADJF(I))                                     *171        01          02
LCCPN       PERCOF(I) = (SQRT.((CPPF(I).P.2.)+(ADJF(I).P.2.)))/NORMF             *172        01          02
            THROUGH LCCPC, FOR K=0,1,K.G.M                                       *173        01          01
            NORMW = 1./(.ABS.(D(K)))                                             *174        01          02
            CPPW(K) = -D(K)*NORMW                                                *175        01          02
            ADJW = C(K)*NORMW                                                    *176        01          02
            PHIW(K) = ATN1.(CPPW(K)/ADJW(K))                                     *177        01          02
LCCPC       PERCOW(K) = (SQRT.((CPPW(K).P.2.)+(ADJW(K).P.2.)))/NORMW             *178        01          02
            THROUGH LCCPC, FOR I=0,1,I.G.N                                       *179        01          01
LCCPC       AMPRAF(I) = PERCOF(I)/(S(I)*EPS)                                     *180        01          02
            THROUGH LCCPR, FOR I=0,1,I.G.M                                       *181        01          01
LCCPR       AMPRAW(I) = PERCOW(I)/(S(N)*EPS)                                     *182        01          02
            FAC= 12.*(1.-RATIO).P.2./(RATIO.P.4.-4.*RATIO+3.)                    *183        01    01
            SUMS= FAC*S(0)/8./CA                                                 *184        01    01
            SUMA= FAC*A(0)/8./CA                                                 *185        01    01
            SUMB= FAC*B(0)/8./CA                                                 *186        01    01
            THROUGH LCCPP, FOR I=1,1,I.G.RATIO*N                                 *187        01    01
            SUMS = SUMS+S(I)*FAC*I/CA                                            *188        01    02
            SUMA = SUMA+A(I)*FAC*I/CA                                            *189        01    02
LCCPP       SUMB = SUMB+B(I)*FAC*I/CA                                            *190        01    02
            THROUGH LCCPZ, FOR I=I,1,I.G.N-1                                     *191        01    01
            FAC= 12./(RATIO.P.4.-4.*RATIO+3.)*(1.-2.*RATIO)*I/CA+                *192        01    02
          1  2.*RATIO*I*I/(N.P.3.)-I.P.3./(N.P.4.))                             *192
            SUMS= SUMS+FAC*S(I)                                                  *193        01    02
            SUMA= SUMA+FAC*A(I)                                                  *194        01    02
LCCPZ       SUMB= SUMB+FAC*B(I)                                                  *195        01    02
            NUMA= N*(A(N)-A(N-1))                                                *196        01    01
            NUMB= N*(B(N)-B(N-1))                                                *197        01    01
            PRINT COMMENT $0THE STEADY PERIODIC WALL TEMPERATURE                 *198        01    01
          1 GRADIENT IN PI/6 INCREMENTS IS$                                      *198
            SUM= 0.                                                              *199        01    01
            THROUGH LCCPS, FOR ARG=PI/6.,PI/6.,ARG.G.2.*PI                       *200        01    01
            FGRAD= NUMA*SIN.(ARG)+NUMB*COS.(ARG)                                 *201        01    02
            SUM= SUM+FGRAD                                                       *202        01    02
            MIXEDT= SUMS+SUMA*SIN.(ARG)+SUMB*COS.(ARG)                           *203        01    02
LCCPS       PRINT RESULTS ARG,FGRAD,MIXEDT                                       *204        01    02
            TIMEAV= SUM/12.                                                      *205        01    01
            PRINT COMMENT $0THE TIME AVERAGE OF THE WALL TEMPERATURE             *206        01    01
          1 GRADIENT IS$                                                         *206
            PRINT RESULTS TIMEAV                                                 *207        01    01
            PRINT RESULTS S(0)...S(N),PHIF(0)...PHIF(N),AMPRAF(0)...AMPRAF(N),   *208        01    01
          1 A(0)...A(N),B(0)...B(N),PHIW(0)...PHIW(M),                           *208
          2 AMPRAW(0)...AMPRAW(M),C(0)...C(M),D(0)...D(M)                        *208
            END OF CONDITIONAL                                                   *209        01    01
LCCPB       CONTINUE                                                             *210                    01
            TRANSFER TO START                                                    *211
            END OF PROGRAM                                                       *212
```

BIBLIOGRAPHY

1. Schechter, R. S., and E. H. Wissler, "Heat Transfer to Bingham Plastics in Laminar Flow through Circular Tubes with Internal Heat Generation," Nucl. Sci. and Eng. 6 (1959) 371-375.

2. Poppendiek, H. F., "Forced-Convection Heat Transfer in Pipes with Volume-Heat Sources within the Fluids," Chem. Eng. Sympos. Ser., 50 (1954) 93-104.

3. Grigull, U. "Warmeubergang an nicht-Newtonsche Flussigkeiten bei laminarer Rohrstromung," Chemie-Ing. Techn. 28 (1956) 553-556.

4. Sparrow, E. M., and R. Siegel, "Laminar Tube Flow with Arbitrary Internal Heat Sources and Wall Heat Transfer," Nucl. Sci. and Eng., 4 (1958) 239-245.

5. Tachibana, F., and T. Morishita, Heat Transfer of Inside Tube Flow of Slurry, Industrial Research, Tokyo Univ., 11 (1959) 45-46.

6. Michiyoshi, I., Heat Transfer of Slurry Flow with Internal Heat Generation - Part I. Bulletin of Japan Soc. Mech Mech. Eng. 5 (1962) 315-319.

7. Michiyoshi, I., et al., "Heat Transfer of Slurry Flow with Internal Heat Generation - Part II," Trans., Japan Soc. Mech. Eng., 28 (1962).

8. Ayers, D. L., The Asymptotic Behavior of Periodic Heat Transfer to Laminar Flow in Tubes, Ph.D. thesis, Department of Mechanical Engineering, University of Michigan, (1963).

9. Clark, J. A., V. S. Arpaci and K. M. Treadwell, "Dynamic Response of Heat Exchangers Having Internal Heat Sources - Part I", Trans. ASME, 80 (1958) 612-624.

10. Arpaci, V. S., and J. A. Clark, "Dynamic Response of Heat Exchangers Having Internal Heat Sources - Part II," Trans. ASME, J. 80 (1958) 625-634.

11. Arpaci, V. S., and J. A. Clark, "Dynamic Response of Heat Exchangers Having Internal Heat Sources - Part III," Trans. ASME, J. of Heat Transfer, 81 (1959), 253-266.

12. Yang, W. J., J. A. Clark, and V. S. Arpaci, "Dynamic Response of Heat Exchangers Having Internal Heat Sources - Part IV," Trans. ASME, J. of Heat Transfer, 83 (1961), 321-323.

13. Yang, W. J., "Dynamic Response and Resonance Phenomenon of a Single-Solid, Single-Fluid Heat Exchanger - Part I," Trans. Japan Soc. Mech. Engrs. 27 (1961), 1276-1285.

14. Yang, W. J. "Dynamic Response and Resonance Phenomenon of a Single-Solid, Single-Fluid Heat Exchanger - Part II," Trans. Japan Soc. Mech. Engrs., 27 (1961), 1892-1907.

15. Yang, W. J. "Dynamic Response and Resonance Phenomenon of a Single-Solid, Single-Fluid Heat Exchanger - Part III," Trans. Japan Soc. Mech. Engrs. 28 (1962), 551-558.

16. Keller, R. B., The Dynamic Response of a Heat Exchanger with Constant Internal Heat Generation to Several Types of Fluid Velocity Transients," Ph.D. thesis, Department of Mechanical Engineering, University of Michigan, (1961).

17. Yang, W. J., "Frequency Response of Heat Exchangers Having Sinusoidal Internal Heat Generation," ASME paper 62-H-21 presented at the 5th National Heat Transfer Conference, ASME-AIChE, Houston, Texas, (1962).

18. Yang, W. J. "Temperature Response of Nuclear Reactors Having Sinusoidal Space-Dependent Internal Heat Generation," 1961 National Nuclear Congress, Abstract No. 48, Tokyo, Japan and Trans. Japan Soc. Mech. Engrs., 28 (1962).

19. Metzner, A. B., "Non-Newtonian Technology: Fluid Mechanics, Mixing, and Heat Transfer," Advances in Chemical Engineering, Volume 1, Academic Press Inc., New York (1956).

20. Bird, R. B., et al., Transport Phenomena. John Wiley and Sons, Inc., New York (1960).

21. Yang, W. J., Transient Heat Transfer in Heat Exchangers Having Arbitrary Time- and Space-Dependent Internal Heat Generation, Publication of the Industry Program, College of Engineering, the University of Michigan, IP 582 (1962).

22. Harnett, J. P., "Experimental Determination of the Thermal Entrance Length for the Flow of Water and of Oil in Circular Pipes," Trans. ASME, 77 (1955), 1211-1220.

23. Eckert, R. G., and A. J. Diaguila, "Convective Heat Transfer for Mixed, Free, and Forced Flow through Tubes," Trans. ASME, 76 (1954) 497-504.

24. Schneider, P. J., "Effect of Axial Fluid Conduction on Heat Transfer in the Entrance Regions of Parallel Plates and Tubes," Trans. ASME, 79 (1957), 765.

25. Lane, J. A., H. G. MacPherson, and Frank Maslon, Fluid Fuel Reactors, Addison-Wesley Publishing Co., Inc., Reading, Massachusetts, (1958).

26. Carnahan, B., H. A. Luther, and J. O. Wilkes, Applied Numerical Methods, John Wiley and Sons, Inc., New York, (1964).

27. Metais, B., and E. R. G. Eckert, "Forced, Mixed and Free Convection Regimes," Trans. ASME, J. of Heat Transfer 86 (1964), 295-296.

28. Thomas, D. G., E. L. Compere, and J. P. McBride, "Thorium Oxide Suspensions," Nucleonics, 18 (1960), 104-110.

29. Thomas, D. G., "Homogeneous Reactor Project Quarterly Progress Report for the Period Ending July 31, 1954," USAEC Report ORNL-1813 (Del.), Oak Ridge National Laboratory, (1954), 125.

30. Beck, J. V., "Thermocouple Temperature Disturbance in Low Conductivity Materials," Trans. ASME, J. of Heat Transfer, 84 (1962), 124-132.

31. Inman, R. M., "Experimental Study of Temperature Distribution in Laminar Tube Flow of a Fluid with Internal Heat Generation," International Journal of Heat and Mass Transfer, 5 (1962), 1053-1058.

32. Pauling, L., College Chemistry, W. H. Freeman and Co., San Francisco, (1956).

33. Pannell, J. R., "Experiments with a Tilting Manometer for Measurement of Small Pressure Differences," Engineering (Sept. 12, 1963) 343-344.

34. Tachibana, F., T. Morishita, T. Naito and M. Okubo, "Pool Boiling Heat Transfer in Slurries," Paper no. 28 presented at the Heat Transfer and Thermodynamics Conference, Japan Society of Mechanical Engineers, (Nov. 28, 1963), Nagasaki, Japan.

35. Orr, C. Jr., and J. M. Dalla Valle, "Heat-Transfer Properties of Liquid-Solid Suspensions," Chem. Eng. Progr. Symposium Series no. 9, (1954), 29.

36. Streeter, V. L., Fluid Mechanics, Third edition, McGraw-Hill Book Co., Inc., New York (1962).

37. Kline, S. J., and F. A. McClintock, "Describing Uncertainties in Single-Sample Experiments," Mechanical Engineering, 75 (1953), 3-8.